MECHANICS OF MOLECULAR COLLISIONS

A Thesis submitted for the Degree of Doctor of Philosophy at Oxford University

by

Jonathan N L Connor B A B Sc

Physical Chemistry Laboratory
Wadham College
Christ Church

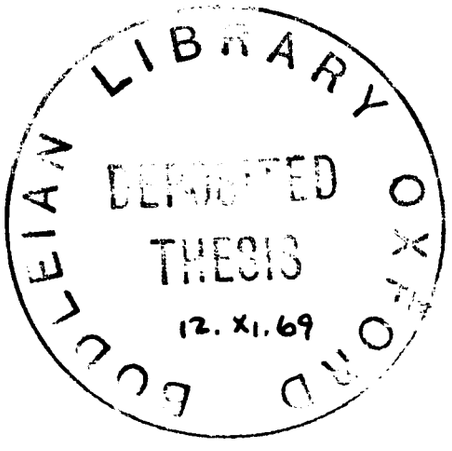

July 1969

ABSTRACT

This thesis presents a semiclassical development of the theory required for the interpretation of thermal energy molecular beam experiments in the study of molecular interactions, and for the prediction of new effects.

Chapter (1) provides a brief introduction to molecular scattering and describes the work in the following Chapters.

In Chapter (2), semiclassical connection formulae based on an exact solution of the Schrödinger equation for a parabolic well and a parabolic barrier are derived and their properties developed. These results are required in later Chapters. The connection formulae for a parabolic well (barrier) are valid for energies which lie either above or below the well minimum (barrier maximum) and provide a direct connection between one classically disallowed (allowed) region and another. These connection formulae contain important quantum correction functions which remove certain singularities from the semiclassical analysis.

Chapter (3) presents a semiclassical analysis of resonance effects in molecular orbiting collisions. The explicit introduction of a complex energy is

used to characterize the quasi-stationary states in the dip of the effective potential for the collision. Expressions for the resonance energies and widths of the quasi-stationary states are derived from the semiclassical wavefunction, obtained with the help of the connection formulae in Chapter (2), and a formula is given for the resonant contribution to the measurable total elastic cross section.

In Chapter (4), a quantum mechanical theory is developed for an electronically adiabatic bimolecular exchange reaction, with the restriction that the three atoms are constrained to move on a straight line but with the whole system free to rotate in three dimensions. An important feature of the analysis is the use of a set of coordinates which pass smoothly from those suited to reactants to those suited to products. A vibrationally adiabatic approximation is used to reduce the scattering problem to the solution of one dimensional Schrödinger equations. Semiclassical techniques are used to evaluate the partial wave summations that occur in the theory and elastic and reactive differential cross sections are calculated for three different kinds of potential surface. An interesting

feature of the calculations is the occurrence of a new kind of rainbow effect,which is named a 'cubic' rainbow since it arises when the deflection function varies cubically with impact parameter. The classical and semiclassical theory of cubic rainbows is developed.

Chapter (5) investigates the effect of a dip in the activation barrier for a chemical reaction using the model developed in Chapter (4). The complex energy techniques introduced in Chapter (3) are used to relate the resonance tunnelling through the barriers to Breit-Wigner theory. A novel feature of the theory is the use of a complex energy with an imaginary part that may be positive,negative or zero. Such a complex energy is the natural consequence of applying a 'forward moving waves only' boundary condition and the sign of the imaginary term has a straightforward interpretation in terms of the population of states within the dip.

Chapter (6) investigates the effect of the rotational motion of the reactants on the differential cross sections of a chemical reaction. In order to allow a tractable development of the theory,a model is adopted with the following restrictions: first the atoms are constrained to

move in a plane and secondly the central atom is given an infinite mass. The use of a set of natural collision coordinates and an adiabatic separation of variables is used to reduce the scattering problem to the solution of one dimensional Schrödinger equations. Partial wave expansions for the elastic and reactive scattering amplitudes are obtained.

Appendix (A) is devoted to various numerical aspects of the theory. The properties of the integral:

$$\int_{-\infty}^{\infty} \exp[i(x^4 + ax)]\,dx,$$

which characterizes the semiclassical description of the cubic rainbow effect are considered together with its numerical evaluation. Numerical methods for the evaluation of phase integrals and their derivatives are described when one of the integration limits is zero (existing methods break down for this case).

Appendix (B) presents a discussion of two dimensional elastic scattering from a central potential for use in conjunction with Chapter (6). The topics considered include the partial wave

expansion of the wavefunction,the semiclassical approximation for the phase shift and the correspondence with classical two dimensional scattering.

'Only connect...'

E M Forster

This emotive phrase occurs on the
title page of 'Howards End'

ACKNOWLEDGMENTS

It is a pleasure to thank Dr M S Child for his helpful suggestions, constructive criticisms and constant optimism throughout the course of this work.

I also gratefully acknowledge a Research Scholarship from the Salters' Institute of Industrial Chemistry of the Worshipful Company of Salters and a Senior Scholarship from Wadham College.

CONTENTS

CHAPTER ONE: INTRODUCTION

Molecular beam experiments provide direct information on the details of molecular collisions. The ultimate beam experiment is easy to describe: velocity and state selected atoms and molecules are made to collide at various angles and the identities, velocities, quantum states and angular distributions of the products are measured. Considerable progress towards this goal has been achieved and information on molecular interactions has been obtained that is inaccessible to conventional bulk experiments which involve measurements of average properties over a wide distribution of velocities and internal states. This thesis describes calculations that have been made in order to assist in the interpretation of molecular beam experiments and to predict new effects.

In general the scattering of an atom by another atom or molecule is a many body problem requiring consideration of both electrons and nuclei. However, for many systems the Born-Oppenheimer separation of nuclear and electronic motions is valid because the nuclear velocities are small relative to the velocities of the electrons at the collision energies of chemical interest.[1] This

decoupling of nuclear and electronic motions reduces the collision problem to one involving nuclear coordinates only. Thus many collision processes are adiabatic in the sense that the energy of a single electronic wavefunction defines the potential surface (or curve) which governs the motion of the nuclei. Only electronically adiabatic collisions are considered in this thesis.

The scattering of heavy particles (atoms and molecules) may often be described successfully by means of semiclassical mechanics. For example, the thermal energy elastic scattering of atoms and molecules exhibits specific quantum effects (rainbows, glories, etc.) whose semiclassical interpretation provides detailed information on the intermolecular potential.[2-4] In this case the semiclassical method provides a straightforward analytical treatment of the scattering, leads to a simple understanding of the physical situation and substantially reduces the labour of a full quantum mechanical treatment.

The semiclassical or WKBJ (Wentzel, Kramers, Brillouin, Jeffreys) method provides (approximate) asymptotic solutions of differential equations of the one dimensional Schrödinger type. The semiclassical

solutions may break down in certain regions and this requires the derivation of 'connection formulae' to bridge these regions. The connection formulae may be deduced from exact solutions of the Schrödinger equation with model potentials. For example, 'linear connection formulae' are derived from solutions of the Schrödinger equation with a linearly varying potential.[5] In Chapter (2) semiclassical connection formulae based on an exact solution of the Schrödinger equation for a parabolic well and a parabolic barrier are derived and their properties developed. These connection formulae are called 'parabolic connection formulae' and are deduced from the asymptotic representations of Weber parabolic cylinder functions,in an analogous manner to the derivation of linear connection formulae from the asymptotic representations of the Airy function.[5] The connection formulae for a parabolic barrier (well) are valid for energies which lie either above or below the barrier maximum (well minimum) and provide a direct connection between one classically allowed (disallowed) region and another. An important feature of the connection formulae is the existence of explicit expressions for the so-called quantum correction functions.[6] These play an important

role in removing an unacceptable singularity from the semiclassical analysis of orbiting collisions, as was first pointed out by Ford,Hill,Wakano and Wheeler.[6] The connection formulae are applied to a variety of problems in Chapters (3)-(6).

Chapter (3) presents a semiclassical analysis of resonance effects in molecular orbiting collisions. The simplest system to study with molecular beams is the elastic scattering of two atoms interacting via a single spherically symmetrical potential energy curve. High energy beam scatterings have yielded reliable values for the short range forces between atoms,[4,7] whilst thermal energy measurements provide information on the intermediate and long range nature of the potential.[2-4] Typically the interatomic potential has a long range attractive part and a short range repulsive part (for example,the Lennard-Jones (12,6) potential) so that the effective potential (= interatomic potential + centrifugal potential) may possess a maximum and a minimum. The presence of a dip in the effective potential implies the possibility of setting up quasi-stationary states. These states may produce a severe distortion in the radial wavefunction of the system which gives rise to orbiting-resonance effects. Such behaviour is under-

stood in Breit-Wigner theory in terms of complex energies whose real and imaginary parts determine the resonance energies and widths of the quasi-stationary states respectively.[8] Expressions for the resonance energies and widths of the quasi-stationary states are derived from the semiclassical wavefunctions. Using the boundary condition that the radial wavefunction is regular at the origin together with parabolic connection formulae, the asymptotic form of the wavefunction is found. This allows the phase shift to be determined. Imposing the further boundary condition that there be no incoming wave yields a complex Bohr-Sommerfeld quantization condition for the resonance energies and widths of the quasi-stationary states. It is shown that when the widths of the energy levels are small compared with their separation, explicit expressions may be deduced for the resonance energies and their widths. These expressions allow the phase shift, scattering amplitude, differential and total cross sections to be expressed in a Breit-Wigner resonance form. This procedure permits a simple discussion of the resonance effects and provides an additional insight into the molecular orbiting phenomenon.

The investigation of chemical reactions by molecular beam techniques is much more difficult than the study of pure elastic scattering. However, considerable progress has been made since the first successful detection of a chemical reaction in a crossed molecular beam experiment by Taylor and Datz in 1955.[9] Observations have been made on the differential and total reaction cross sections, internal excitation and velocity distribution of the products, and the influence of steric factors on the reaction.[10-12] Measurements of product angular distributions have revealed two possible reaction mechanisms. Anisotropic reactive differential cross sections are taken as evidence for direct collisions, in which the collision complex disintegrates before it can rotate through half a turn. Examples of direct reactions are: rebound reactions (e.g. $K + CH_3I = KI + CH_3$) in which most of the product KI recoils backwards relative to the direction of the incoming K atom, and stripping reactions (e.g. $K + Br_2 = KBr + Br$) in which the product KBr is mostly scattered in the forward direction relative to the incoming K atom.[10-12] Intermediate behaviour between the rebound and stripping mechanisms is also known.[13] Complex

collisions on the other hand (e.g. Cs + RbCl = CsCl + Rb) are characterized by reactive differential cross sections that are symmetrical about 90° in the centre of mass frame and this is taken to indicate that collision complexes with lifetimes long compared with a rotational period are formed.[14]

The theoretical approaches to reactive scattering fall into three main groups: classical dynamical calculations, statistical calculations and quantum mechanical calculations.

The classical mechanical approach calculates the trajectories of the reacting atoms on an assumed potential energy surface by numerical integration of the classical equations of motion from a given set of initial parameters.[15] Information on collision times, internal energy distributions, and differential and total reaction cross sections are obtained by Monte Carlo averaging of initial impact parameters, orientations and phases. Calculations have been performed for collisions on a line, in a plane and in three dimensions. Hybrid quasi-classical calculations have also been made wherein the initial vibration-rotation energies are selected according to quantum mechanically allowed values.[16,17] The

Monte Carlo approach has been the most successful to date, although the limitations of the method are difficult to assess at the present time. Mortensen[18,19] has compared the classical and quantum results for the reaction $H + H_2 = H_2 + H$ on a line and has concluded that a quantum mechanical treatment of this reaction is essential.

'Absolute' transition state theory is the best known example of a statistical approach. In this theory the dynamical aspects of the problem are replaced by a quasi-equilibrium assumption.[20] Marcus has shown how this approach may also be used to calculate reaction cross sections.[21,22] Another statistical theory is the phase space theory developed by Light and co-workers,[23] where it is assumed that in a strong coupling collision, energy is equilibrated in all degrees of freedom available to the system, subject to the constraints of the conservation laws. The probability of formation of a given product is then assumed to be proportional to some measure of the phase space available to that product.

Quantum mechanics provides the most rigorous approach to reactive scattering. The classical and

statistical theories described above require quantum mechanical theories in order to assess their validity, limitations and possible extensions. It is well known however that the quantum mechanics of three body systems interacting via strong forces and involving many states is a difficult problem and approximations must be introduced. In Chapters (4) and (5) a quantum mechanical theory is developed for the electronically adiabatic bimolecular exchange reaction:

$$A + BC = AB + C,$$

with the restriction that the three atoms are constrained to move on a straight line but with the system free to rotate in three dimensions in such a manner so as to conserve angular momentum.[24] In this way one can discuss collisions with all impact parameters and hence calculate differential and total cross sections. The restriction to the case of zero impact parameter (head-on collision) would allow only the calculation of a reaction probability.[18,19,25,26] The assumption of an infinitely heavy central mass that is present in an earlier model is removed.[24] An important feature of the

analysis is the use of a set of coordinates which pass smoothly from those suited to reactants to those suited to products. Such 'natural collision coordinates' were introduced independently by Child[27] and Marcus[28-30] in 1966. In the way the theory is developed, the reaction is characterized by the notion of a representative particle along a reaction coordinate s, which varies in value from $-\infty$ at the beginning of the reaction to $+\infty$ at the end. Initially s represents the relative translation of A with respect to BC, in the region $s \approx 0$ it represents the asymmetric stretching vibration of the ABC complex and finally s represents the relative translation of C with respect to AB . A vibrational coordinate v is also defined such that initially v corresponds with the BC vibration, for $s \approx 0$ it corresponds with the (non-reactive) symmetric stretch of the ABC complex and finally v corresponds with the vibration of the AB molecule.

In order to solve the Schrödinger equation that involves these coordinates a vibrationally adiabatic approximation is introduced.[27,28] In this, terms which couple together different vibrational states are neglected so that the system remains in the

same vibrational state throughout the course of the reaction. Vibrationally adiabatic reactions are of particular interest since they form the basis of the current justification of absolute transition state theory.[31-33] An adiabatic reactive collision is the analogue of an elastic collision in non-reactive scattering; in both cases there is no change in the quantum numbers associated with the collision. However large changes in the physical nature of the adiabatic degrees of freedom may occur during the course of the reaction and adiabatic correlation diagrams may be drawn for the changes in energy that take place as the reaction proceeds.

The adiabatic approximation allows the scattering problem to be reduced to the solution of one dimensional Schrödinger equations for the adiabatically separated coordinates. It is shown that for a given impact parameter and collision energy the effective barrier to reaction along the reaction coordinate s has contributions from three possible sources: (1) the potential energy barrier (if any) that belongs to the original potential surface, (2) the change in vibrational energy for a given vibrational state as the reaction proceeds,

(3) the centrifugal barrier associated with the conservation of angular momentum. The Schrödinger equation for motion along the reaction coordinate is solved semiclassically in Chapter (4) for the case that the effective barrier to reaction has a single maximum. Semiclassical techniques are also used to evaluate the partial wave summations that occur in the theory. The resulting equations are sufficiently straightforward for a calculation of the elastic and reactive differential cross sections to be undertaken and calculations are made for three different kinds of potential surface. An interesting feature of the calculations is the occurrence of a new kind of rainbow effect. This is called a 'cubic' rainbow because it arises when the deflection function varies cubically with impact parameter, as opposed to the more usual 'quadratic' rainbow in which the deflection function possesses a maximum or a minimum (that is varies quadratically with impact parameter). The integral that characterizes the semiclassical analysis of the cubic rainbow effect is:

$$C(a) = \int_{-\infty}^{\infty} \exp[i(x^4+ax)]\,dx\,,$$

and this integral plays an analogous role to the Airy integral in the semiclassical description of the quadratic rainbow effect.[3]

Chapter (5) considers the case when the activation barrier belonging to the potential energy surface for the reaction possesses two maxima along the reaction coordinate. The presence of a dip in the effective potential implies the possibility of setting up quasi-stationary states. Child[24] has shown that the existence of these states has an important effect on the reaction cross section and rate constant. At energies in the region of the dip, the reaction cross section shows a well resolved resonance structure whenever the energy available for reaction coincides with one of the asymmetric vibration-rotation states of the activated complex. This provides a powerful mechanism for tunnelling through the barrier even when the collision energy is far below the barrier maxima and the rate constant then shows a different behaviour from that expected for simple tunnelling through a single humped barrier. The name resonance tunnelling has been proposed for this phenomenon[24].

This system is investigated using the parabolic connection formulae of Chapter (2) to derive the semiclassical form of the wavefunction. The complex energy techniques introduced in Chapter (3) are used to relate the resonance tunnelling phenomenon to Breit-Wigner theory. The resonance features in the reactive scattering may be understood by imposing the usual 'outgoing waves' only boundary condition, which results in the usual complex energy:

$$E = E_{nL} - i\Gamma_{nL}/2,$$

where E_{nL} is the resonance energy and Γ_{nL} the level width which is a positive quantity. Terms involving Γ_{nL} also contribute to the elastic scattering but there is also another term, which is best understood by applying a 'forward moving wave' only boundary condition. This results in a novel form of complex energy:

$$E = E_{nL} + i\gamma_{nL}/2,$$

where γ_{nL} is positive if the second barrier is larger than the first barrier, negative if the first barrier is larger than the second one and zero if the two

barriers are of equal size. The sign of γ_{nL} has a natural interpretation in terms of the population of states within the dip. A positive sign corresponds with a building up and a negative sign with a decay. The calculations described in Chapter (5) complement those in reference (24) where a complex energy approach was not used and only the reaction cross section (and rate constant) was calculated.

The model adopted for reactive molecular collisions in Chapters (4) and (5) does not take into account the effect of the initial BC rotations on the reaction. This problem is considered in Chapter (6). In order to allow a tractable development of the theory a model is adopted with the following restrictions.[27] First the atoms are constrained to move in a plane in order to simplify the discussion of angular momentum and secondly B is given an infinite mass so that a set of natural collision coordinates may be defined for the reaction. An adiabatic separation of variables is again used to reduce the scattering problem to the solution of one dimensional Schrödinger equations. These correspond to motion along the reaction coordinate, the purely vibrational motion of the atoms and

the internal rotational motion of the atoms. The new feature of this model is the internal rotations of the system. At $s = -\infty$ and $+\infty$ these correspond with the free rotation of BC and AB respectively. For many systems the initially free rotation of the BC molecule is quenched as the reaction enters the transition state and the internal rotational motion then corresponds with the bending vibration of the ABC complex at $s \approx 0$. As the rotational energy of BC increases however, a situation may obtain where the rotational motion of BC remains essentially free in the transition state region.

A partial wave analysis allows the differential cross sections to be determined. It is shown that for free internal rotational motion in the transition state region, each partial wave has the same angular part which gives rise to an isotropic differential reactive cross section. On the other hand when the initial rotational motion of BC is quenched as the reaction proceeds, each partial wave has a different angular part and an anisotropic differential reactive cross section will (in general) result.

Appendix (A) is devoted to various numerical aspects of the theory developed in the preceding Chapters. The properties of the integral C(a) (defined above) are considered together with its numerical evaluation. Also numerical methods for the evaluation of semiclassical phase integrals and their derivatives are described which are valid when one of the limits of integration is zero (existing methods break down for this case).

Appendix (B) presents a discussion of two dimensional elastic scattering from a central potential, as there does not appear to be an account available in the literature. The results of this Appendix are required in Chapter (6). Among the topics considered are the partial wave expansion of the wavefunction, the semiclassical approximation for the phase shift and the correspondence with classical two dimensional scattering.

The work described in Chapters (2), (3) and a portion of Chapter (5) have formed the contents of two research papers[34,35] and a research note[36] in Molecular Physics.

CHAPTER TWO: PARABOLIC CONNECTION FORMULAE

2.1 INTRODUCTION

The semiclassical or WKBJ method provides asymptotic solutions of the one dimensional Schrödinger equation:[5]

$$\frac{d^2\psi(s)}{ds^2} + \frac{2\mu}{\hbar^2}\left[E - V(s)\right]\psi(s) = 0, \qquad (2.1)$$

where E is the total energy of the system, $\hbar$ is Planck's constant divided by 2π, μ and V(s) are (in general) an effective mass and an effective potential that characterize the system respectively, and $\psi(s)$ is the wavefunction for s motion. s takes values from $-\infty$ to $+\infty$; radial wave equations are not thereby excluded as the Langer transformation[37] may be used to map $[0,+\infty)$ onto $(-\infty,+\infty)$ - see Appendix (B) for a specific example of this technique in two dimensional elastic scattering. Semiclassical solutions of equation (2.1) are valid when the de Broglie wavelength is sufficiently small that the fractional change in V(s) over a wavelength is negligible:[5]

$$\left|\frac{d\lambda(s)}{ds}\right| \ll 1, \qquad (2.2)$$

where

$$\lambda(s) = 1/k(s),$$

and

$$k(s) = \left\{ \frac{2m}{\hbar^2}[E - V(s)] \right\}^{1/2}.$$

The semiclassical solutions of equation (2.1) satisfying condition (2.2) are of two types: oscillatory for $E \gg V(s)$ and exponentially increasing and decreasing for $E \ll V(s)$. Condition (2.2) clearly breaks down if $E \approx V(s)$, that is near the classical turning points of the motion and evidently the exact solution of equation (2.1) differs substantially from its asymptotic representations near these points. Moreover, the same asymptotic form cannot be used to represent an exact solution of equation (2.1) on either side of the turning point, but on the contrary different asymptotic forms are required. This is the Stoke's phenomenon.[38] When present it is necessary to associate these different asymptotic representations with each other and this requires the deduction of connection formulae.

There are two main approaches available for the calculation of connection formulae:

A. The real variable s in equation (2.1) is replaced by a complex variable s. A contour is then chosen in the complex s plane which avoids the turning point neighbourhood, yet connects either side of the turning point as required. This approach, which has been called the phase integral method (a terminology adopted in this thesis), has been described by Heading[39] and Fröman and Fröman.[40]

B. Equation (2.1) is replaced by an equation which approximates equation (2.1) in the turning point region and for which an exact solution is known. The asymptotic representations of this exact solution are then joined on to the semiclassical solutions of equation (2.1), from which the connection formulae are deduced.[5]

Method (B) is the one used in this thesis. Semiclassical connection formulae based on exact solutions of the Schrödinger equation for a parabolic barrier and a parabolic well are derived and their properties developed. The resulting connection formulae contain explicit expressions for the quantum correction functions, whose importance was first pointed out by Ford, Hill, Wakano and Wheeler.[6] These correction functions remove a singularity in

the semiclassical description of orbiting collisions (the 'orbiting singularity'). In contrast the magnitude of these quantum correction functions cannot be determined by method (A).[40,41] The derivation of the connection formulae is described below and in the following Chapters they are used in a simple and direct manner to solve various physical problems.

2.2 CONNECTION FORMULAE FOR A PARABOLIC BARRIER

In this section semiclassical connection formulae are derived from the properties of the asymptotic representations of the Schrödinger equation for a parabolic barrier and their properties are developed.

In the first instance the solutions of equation (2.1) are assumed to be subject to the boundary conditions that they represent incident, reflected and transmitted waves with the transmitted wave moving off to the right (see figure (1)).

The semiclassical solutions of equation (2.1) valid at large |s| are:

$$\psi(s) = \frac{A}{\sqrt{k(s)}} \exp\left\{ i\int^{s} k(s')ds' + i\alpha \right\}, \qquad (2.3)$$

for the transmitted wave and

$$\psi(s) = \frac{B}{\sqrt{k(s)}} \exp\left\{ i\int_{s} k(s')ds' + i\beta \right\} + \frac{C}{\sqrt{k(s)}} \exp\left\{ -i\int_{s} k(s')ds' + i\gamma \right\}, \qquad (2.4)$$

for the reflected wave (first term) and the incident wave (second term). Equations (2.3) and (2.4) need to be supplied with convenient phase reference points

Figure 1

The potential energy curve V(s). V(s) is assumed to be quadratic in s near its maximum. a and c denote the classical turning points and b is the position of the barrier maximum. E is the total energy of the system. The arrows indicate incident, reflected and transmitted waves.

E
S
a
b
c

(either the classical turning points or the top of the barrier - see below). In writing down phase integrals as in equations (2.3) and (2.4) the following conventions will be adopted: the integrand will be written in such a way as to make it positive definite and the integration limits will be arranged so that (upper limit)$\rangle$(lower limit). Other authors adopt different conventions and some care is necessary when comparing results in the literature.

The problem thus reduces to the determination of A,B,C which can always be chosen to be real, and of the phases α, β, γ which depend on the choice of phase reference points, such that the solution valid for $s \gg 0$ connects with that valid for $s \ll 0$.

The potential V(s) is assumed to be parabolic near its centre so that (in the notation of figure (1)):

$$V(s) = V(b) - \tfrac{1}{2}\mu\omega^2(s-b)^2, \qquad (2.5)$$

where ω is the classical angular frequency of oscillation in the upturned barrier. Equation (2.1), together with equation (2.5) may be simplified by the change of variable:

$$\varepsilon = \frac{E - V(b)}{\hbar\omega},$$

$$x = \left(\frac{2\mu\omega}{\hbar}\right)^{1/2}(s-b),$$

to give

$$\frac{d^2\psi(x)}{dx^2} + \left[\varepsilon + \frac{x^2}{4}\right]\psi(x) = 0. \tag{2.6}$$

Equation (2.6) is a form of Weber's equation.[42,43] The solution of equation (2.6) that satisfies the above boundary conditions is in terms of Weber parabolic cylinder functions:

$$\psi(x) = U(-i\varepsilon, xe^{-i\pi/4}), \tag{2.7}$$

where the symmetrical notation U(a,x) of Miller has been used rather than the older notation $D_{-a-\frac{1}{2}}(x)$ of Whittaker.[42,43] Equation (2.7) is related to the tabulated functions $W(-\varepsilon,\pm x)$ by:

$$U(-i\varepsilon, xe^{-i\pi/4}) = \frac{1}{\sqrt{2}}e^{\pi\varepsilon/4}\exp\left[-\frac{i\pi}{8} + \frac{i}{2}\arg\Gamma\left(\tfrac{1}{2}+i\varepsilon\right)\right]E(-\varepsilon,x), \tag{2.8}$$

and

$$E(-\varepsilon,x) = k^{-1/2}W(-\varepsilon,x) + ik^{1/2}W(-\varepsilon,-x), \qquad (2.9)$$

in which

$$k = [1 + e^{-2\pi\varepsilon}]^{1/2} - e^{-\pi\varepsilon}.$$

Equations (2.8) and (2.9) are convenient for the numerical evaluation of equation (2.7). Using the asymptotic representations of $W(-\varepsilon,\pm x)$ that are valid for $|x| \gg |\varepsilon|$, namely:[42,43]

$$W(-\varepsilon,x) \sim \left(\frac{2k}{x}\right)^{1/2}\left[S_1\cos\left\{\frac{x^2}{4} + \varepsilon\ln x - \tfrac{1}{2}\arg\Gamma(\tfrac{1}{2}+i\varepsilon) + \tfrac{\pi}{4}\right\}\right.$$

$$\left. - S_2\sin\left\{\frac{x^2}{4} + \varepsilon\ln x - \tfrac{1}{2}\arg\Gamma(\tfrac{1}{2}+i\varepsilon) + \tfrac{\pi}{4}\right\}\right],$$

and

$$W(-\varepsilon,-x) \sim \left(\frac{2}{kx}\right)^{1/2}\left[S_1\sin\left\{\frac{x^2}{4} + \varepsilon\ln x - \tfrac{1}{2}\arg\Gamma(\tfrac{1}{2}+i\varepsilon) + \tfrac{\pi}{4}\right\}\right.$$

$$\left. + S_2\cos\left\{\frac{x^2}{4} + \varepsilon\ln x - \tfrac{1}{2}\arg\Gamma(\tfrac{1}{2}+i\varepsilon) + \tfrac{\pi}{4}\right\}\right],$$

with

$$S = S_1 + iS_2,$$

$$S \sim \sum_{r=0}^{\infty}(-i)^r\,\frac{\Gamma(2r+\tfrac{1}{2}-i\varepsilon)}{\Gamma(\tfrac{1}{2}-i\varepsilon)}\,\frac{1}{2^r r!\,x^{2r}},$$

the asymptotic form for $\psi(x)$ in equation (2.7) becomes:

$$\psi(x) \sim \frac{1}{\sqrt{x}} e^{\pi\varepsilon/4} \exp\left\{ i\left[\frac{x^2}{4} + \varepsilon \ln x + \frac{\pi}{8} \right] \right\}, \qquad (2.10)$$

valid for $x \gg 0$ and

$$\psi(x) \sim \frac{1}{\sqrt{|x|}} e^{-3\pi\varepsilon/4} \exp\left\{ i\left[\frac{x^2}{4} + \varepsilon \ln|x| - \frac{3\pi}{8} \right] \right\} \qquad (2.11)$$

$$+ \frac{1}{\sqrt{|x|}} \left[1 + e^{-2\pi\varepsilon}\right]^{i/2} e^{\pi\varepsilon/4} \exp\left\{ i\left[-\frac{x^2}{4} - \varepsilon \ln|x| + \frac{\pi}{8} + \arg\Gamma\left(\tfrac{1}{2} + i\varepsilon\right) \right] \right\},$$

valid for $x \ll 0$; in deriving equations (2.10) and (2.11) terms in x^{-2} (which represent first order corrections to the asymptotic wavefunction) and higher have been neglected. In equation (2.11) the first term represents a reflected wave and the second term an incident wave (the direction of propagation of a wave is the direction in which its phase increases). Comparison of the semiclassical solutions of equation (2.6) with equations (2.10) and (2.11) then determines the constants in equations (2.3) and (2.4). As a concrete example consider the case of a transmitted wave in the energy region $\varepsilon < 0$ with the classical turning point ($x = 2\sqrt{|\varepsilon|}$) chosen as the phase reference point (this is the situation illustrated

in figure (1)). The semiclassical solution of equation (2.6) is in this case ($x \gg 0$):

$$\psi(x) = \left[\frac{x^2}{4} - |\varepsilon|\right]^{-1/4} \exp\left\{ i \int_{2\sqrt{|\varepsilon|}}^{x} \left[\frac{x'^2}{4} - |\varepsilon|\right]^{1/2} dx' \right\},$$

$$= \left[\frac{x^2}{4} - |\varepsilon|\right]^{-1/4} \exp\left\{ i \left[\frac{x}{4}(x^2 - 4|\varepsilon|)^{1/2} - |\varepsilon| \ln\left[x + (x^2 - 4|\varepsilon|)^{1/2}\right] \right.\right.$$

$$\left.\left. + |\varepsilon| \ln 2\sqrt{|\varepsilon|} \right] \right\},$$

$$\sim \left(\frac{2}{x}\right)^{1/2} \exp\left\{ i \left[\frac{x^2}{4} - |\varepsilon| \ln x - \frac{|\varepsilon|}{2} + \frac{|\varepsilon|}{2} \ln |\varepsilon| \right] \right\}. \qquad (2.12)$$

In deriving equation (2.12) terms of order x^{-2} and higher have again been neglected. Comparison of equation (2.12) with equation (2.10) gives for the constants A and α:

$$A = e^{-\pi|\varepsilon|/4} / \sqrt{2}, \qquad \alpha = \frac{\pi}{8} + \frac{|\varepsilon|}{2} - \frac{|\varepsilon|}{2} \ln |\varepsilon| .$$

A similar calculation may be carried out for the incident and reflected waves, from which the following connection formulae may be deduced. The functions:

$$\frac{1}{\sqrt{k(s)}} \exp\left\{ \pm i\int_c^s k(s')ds' \pm i\frac{\pi}{4} \right\}, \qquad (2.13)$$

valid for $s \gg c$ connect with

$$\frac{1}{\sqrt{k(s)}} \exp\left\{ \pm i\int_s^a k(s')ds' \mp i\frac{\pi}{4} \right\} e^{-\pi\varepsilon}$$

$$+ \frac{1}{\sqrt{k(s)}} \exp\left\{ \mp i\int_s^a k(s')ds' \pm i\frac{\pi}{4} \right\} e^{\pm i\phi(\varepsilon)} \left[1 + e^{-2\pi\varepsilon}\right]^{1/2}, \qquad (2.14)$$

valid for $s \ll a$. The quantum correction function $\phi(\varepsilon)$ is defined by:

$$\phi(\varepsilon) = \varepsilon + \arg\Gamma\left(\tfrac{1}{2} + i\varepsilon\right) - \varepsilon \ln|\varepsilon|. \qquad (2.15)$$

When the energy is incident above the barrier maximum, a convenient phase reference point is the top of the barrier s=b. On repeating the calculation described above, it is found that the connection formulae (2.13) and (2.14) remain valid provided the turning points a and c are replaced by b. The connection formulae are therefore valid for energies which lie either above or below the barrier maximum,

and they provide a direct connection between one classically allowed region and another. The factors $\pi/4$ have been included in the connection formulae (2.13) and (2.14) to facilitate their use in conjunction with connection formulae based on a linear turning point.[5] The lower set of signs in (2.13) and (2.14) arises by taking the complex conjugate of the semiclassical solutions (2.3) and (2.4). The formulae (2.13) and (2.14) provide one of the desired set of connection formulae. A similar analysis based on the solution:

$$\psi(x) = U\left(-i\varepsilon, -xe^{-i\pi/4}\right),$$

of equation (2.6) leads to the second set of connection formulae. The functions:

$$\frac{1}{\sqrt{k(s)}} \exp\left\{ \pm i\int_s^a k(s')ds' \pm i\frac{\pi}{4} \right\}, \qquad (2.16)$$

valid for $s \ll a$ connect with

$$\frac{1}{\sqrt{k(s)}} \exp\left\{ \pm i\int_c^s k(s')ds' \mp i\frac{\pi}{4} \right\} e^{-\pi\varepsilon}$$

$$+ \frac{1}{\sqrt{k(s)}} \exp\left\{ \mp i\int_c^s k(s')ds' \pm i\frac{\pi}{4} \right\} e^{\pm i\phi(\varepsilon)} \left[1 + e^{-2\pi\varepsilon}\right]^{1/2}, \qquad (2.17)$$

valid for $s \gg c$ and $\phi(\varepsilon)$ is again defined by equation (2.15).

Numerical values of $\phi(\varepsilon)$ are given in Table (1) whilst Figure (2) shows a plot of $\phi(\varepsilon)$ against ε ($\arg\Gamma(\frac{1}{2}+i\varepsilon)$ is tabulated in reference (42)). Since $\arg\Gamma(\frac{1}{2}+i\varepsilon) = -\arg\Gamma(\frac{1}{2}-i\varepsilon)$, $\phi(\varepsilon)$ is an odd function of ε :

$$\phi(\varepsilon) = -\phi(-\varepsilon),$$

so it is only necessary to plot $\phi(\varepsilon)$ for positive ε (say). The following properties are evident: $\phi(0) = 0$ and $\phi(\infty) = 0$ with $\phi(\varepsilon)$ rising to a maximum of ≈ 0.15 at $\varepsilon \approx 0.3$. Equation (2.15) shows that the slope of $\phi(\varepsilon)$ tends to $+\infty$ as $\varepsilon \rightarrow 0$ because of the presence of the logarithmic singularity at $\varepsilon = 0$. It will be seen in Chapters (3)-(6) that this logarithmic singularity exactly cancels another logarithmic singularity and thereby removes an unphysical singularity from the semiclassical analysis. Figure (2) also shows plots of:

$$\frac{\varepsilon}{2}\ln\left[\left(\frac{\varepsilon}{2}\right)^2 + \left(\frac{1}{4\gamma}\right)^2\right] + \varepsilon - \varepsilon\ln|\varepsilon|, \qquad (2.18)$$

where $\gamma = 1.78107$ and

Table 1

Numerical values of $\phi(\varepsilon) = \varepsilon + \arg\Gamma(\frac{1}{2}+i\varepsilon) - \varepsilon\ln\varepsilon$.

ε	$\phi(\varepsilon)$
0.00	0.0000**
0.05	0.1020
0.10	0.1367
0.15	0.1491
0.20	0.1498
0.25	0.1442
0.30	0.1354
0.40	0.1149
0.50	0.0958
0.60	0.0801
0.70	0.0678
0.80	0.0583
0.90	0.0508
1.00	0.0450
1.50	0.0287
2.00	0.0212
2.50	0.0168
3.00	0.0140
4.00	0.0105
5.00	0.0083

** Using $\lim_{\varepsilon\to 0} \varepsilon\ln\varepsilon = 0$

Figure 2

The quantum correction function $\phi(\varepsilon)$.
The full line is equation (2.15).
The dotted line is equation (2.19).
The dashed line is the first term of
the series (2.22).
The dash-dot line is equation (2.18).

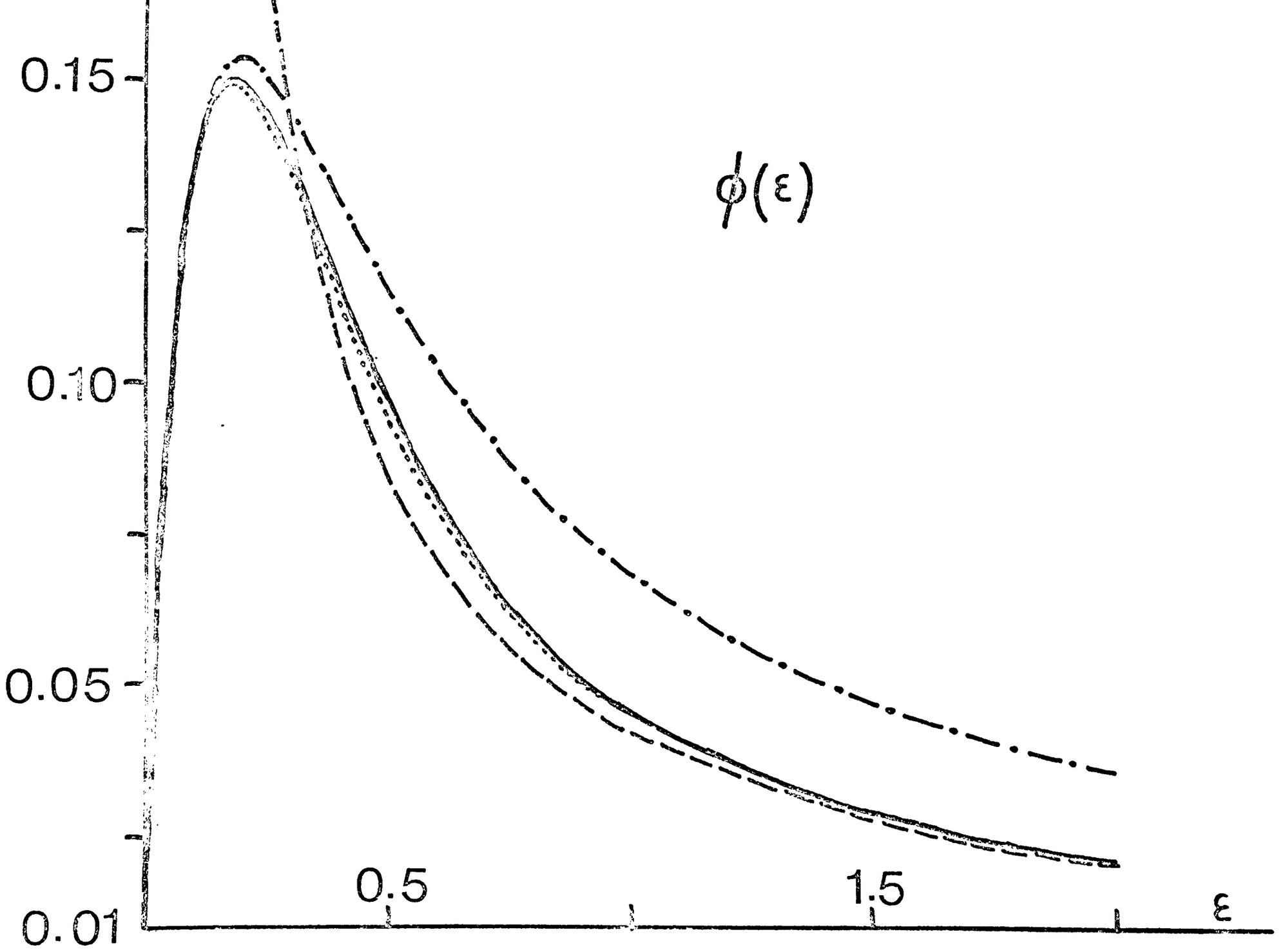
0.15
0.10
0.05
0.01
$\phi(\varepsilon)$
0.5
1.5
ε

$$\frac{\varepsilon}{2}\ln\left[1+\frac{1}{4\varepsilon^2}\right] - \frac{\varepsilon}{12(\varepsilon^2+\frac{1}{4})}\left[1+\frac{(\varepsilon^2-\frac{3}{4})}{60(\varepsilon^2+\frac{1}{4})^2}\right], \qquad (2.19)$$

which use analytical approximations that have been suggested for $\arg\Gamma(\frac{1}{2}+i\varepsilon)$.[6,41] The asymptotic behaviour of $\phi(\varepsilon)$ may be derived from the relation:

$$\arg\Gamma(\tfrac{1}{2}+i\varepsilon) = \arg\Gamma(i2\varepsilon) - \arg\Gamma(i\varepsilon) - 2\varepsilon\ln 2, \qquad (2.20)$$

which follows from the duplication formula:[43]

$$\Gamma(2z) = (2\pi)^{-1/2}\,2^{2z-1/2}\,\Gamma(z)\,\Gamma(\tfrac{1}{2}+z),$$

with $z = i\varepsilon$. In addition:[42]

$$\arg\Gamma(i\varepsilon/2) \sim \frac{\varepsilon}{2}\ln\left(\frac{\varepsilon}{2}\right) - \frac{\varepsilon}{2} - \frac{\pi}{4} - \sum_{r=1}^{\infty}\frac{2^{2r-2}}{r(2r-1)}\frac{B_r}{\varepsilon^{2r-1}}, \qquad (2.21)$$

where B_r are the Bernoulli numbers, the first three of which are:

$$B_1 = 1/6, \quad B_2 = 1/30, \quad B_3 = 1/42.$$

Inserting equations (2.20) and (2.21) into equation (2.15) leads to:

$$\phi(\varepsilon) \sim \sum_{r=1}^{\infty} \frac{B_r}{2r(2r-1)} \cdot \frac{1}{\varepsilon^{2r-1}} \cdot \left(1 - \frac{1}{2^{2r-1}}\right),$$

$$= \frac{1}{24\varepsilon} + \frac{7}{2880\,\varepsilon^3} + \frac{31}{40320\,\varepsilon^5} + \cdots \quad (2.22)$$

The first term of the series (2.22) is within 15% of the exact value of $\phi(\varepsilon)$ for $\varepsilon > 0.25$ and within 10% for $\varepsilon > 1.0$; $1/24\varepsilon$ is also plotted in Figure (2).

A guide to the regions where the semiclassical solutions of equation (2.6) are valid may be obtained from the first order correction terms to the asymptotic wavefunctions (2.10) and (2.11). In particular if $F_{\pm}$ is given by:

$$F_{\pm} = 1 - \frac{\varepsilon}{x^2} \pm i\frac{\left(\frac{3}{4} - \varepsilon^2\right)}{2x^2},$$

it is found that equation (2.10) and the first term of equation (2.11) are to be multiplied by F_- whilst the second term of equation (2.11) is to be multiplied by F_+. A comparison of the asymptotic representations (2.10) and (2.11) with the exact

solutions (2.8) and (2.9) indicates that the range of x values for which (2.10) and (2.11) are within an order of magnitude of the exact solution may be found from the inequalities $|\varepsilon|/x^2 < 0.05$ or $(\frac{3}{4} - |\varepsilon|^1)/2x^2 < 0.05$, with the larger value of x being taken each time. For $|\varepsilon| = 0{,}2$ this condition is satisfied at points one or two wavelengths outside the roots of the equation $(x^2 - 4|\varepsilon|) = 0$.

It is of interest to note that the transmission coefficient derived from equations (2.13) and (2.14), namely $(1+\exp(-2\pi\varepsilon))^{-1}$ has been proposed on intuitive grounds by Bell[44] (in 1959). His considerations were based on the known behaviour for $\varepsilon \gg 0$ (transmission coefficient of unity), $\varepsilon \ll 0$ (WKBJ result based on two linear turning points) and $\varepsilon = 0$ (transmission coefficient of approximately one half for an Eckart potential). Actually this result for a parabolic barrier was known much earlier[45] although apparently not noticed.

Child[27] has intuitively derived semiclassical connection formulae for a parabolic barrier from the ratios of the amplitudes of the incident and reflected waves and his formulae differ by the omission of the phase factor $\phi(\varepsilon)$. It was this

lack that prompted the above more detailed investigation. Phase integral methods have also been used to derive connection formulae for a barrier,[40,41] but in this approach the value of $\phi(\varepsilon)$ cannot be determined. On the other hand, the phase integral treatment does not require the barrier to be exactly parabolic but only approximately so. By comparison with the phase integral results, equations (2.13)-(2.17) may be generalized by the substitutions:

$$-\pi\varepsilon \longrightarrow \int_a^c |k(s)|\,ds \qquad \varepsilon<0, \tag{2.23a}$$

$$-\pi\varepsilon \longrightarrow \mathrm{Re}\, i\int_{ia}^{ic} k(s)\,ds \qquad \varepsilon>0, \tag{2.23b}$$

in which ia and ic represent the complex zeros of the integrand in the substitution (2.23b). The arrows become equality signs for an exactly parabolic barrier. For potentials which are even in s, the right hand side of the substitution (2.23b) contains no imaginary part and the operation Re is

superfluous. In the energy region $\xi \ll 0$, the substitution (2.23a) together with the parabolic connection formulae become equivalent to connection formulae based on two linear turning points.[5]

The principal results of this section are given by the formulae (2.13)-(2.17). They may be summarized in another way as follows. If the semiclassical solutions of equation (2.1) to the left and right of the barrier are written as:

$$\frac{c_1}{\sqrt{k(s)}} \exp\left\{-i\int_s^a k(s')ds'\right\} + \frac{c_2}{\sqrt{k(s)}} \exp\left\{i\int_s^a k(s')ds'\right\},$$

and

$$\frac{c_3}{\sqrt{k(s)}} \exp\left\{-i\int_c^s k(s')ds'\right\} + \frac{c_4}{\sqrt{k(s)}} \exp\left\{i\int_c^s k(s')ds'\right\},$$

respectively, then the coefficients c_1 and c_2 are related to c_3 and c_4 by:

$$\begin{pmatrix} c_1 \\ c_2 \end{pmatrix} = C \begin{pmatrix} c_3 \\ c_4 \end{pmatrix},$$

where

$$C = \begin{pmatrix} i e^{-\pi\varepsilon} & [1+e^{-2\pi\varepsilon}]^{1/2} e^{i\phi(\varepsilon)} \\ [1+e^{-2\pi\varepsilon}]^{1/2} e^{-i\phi(\varepsilon)} & -i e^{-\pi\varepsilon} \end{pmatrix}.$$

Notice also that $C = C^{-1}$, that is C is a self-reciprocal matrix

2.3 CONNECTION FORMULAE FOR A PARABOLIC WELL

In this section exact solutions of the Schrödinger equation for a parabolic well will be used to derive the appropriate semiclassical connection formulae. In particular the wavefunction is taken to be exponentially decreasing in one classically inaccessible region and a semiclassical expression for its form in the other classically inaccessible region is found. The method follows similar lines to that already described in Section (2.2).

The potential energy for a parabolic well is:

$$V(s) = V(b) + \tfrac{1}{2}\mu\tilde{\omega}^2(s-b)^2, \qquad (2.24)$$

where $\tilde{\omega}$ is the classical angular vibration frequency for the well and b is the classical equilibrium value of s (the notation of Figure (3) will be used). With the change of variable

$$\tilde{\epsilon} = \frac{E - V(b)}{\hbar\tilde{\omega}},$$

$$\alpha = \left(\frac{2\mu\tilde{\omega}}{\hbar}\right)^{1/2}(s-b),$$

Figure 3

The potential energy curve V(s). V(s) is assumed to be quadratic in s near its minimum. a and c denote the classical turning points and b is the position of the well minimum. E is the total energy of the system.

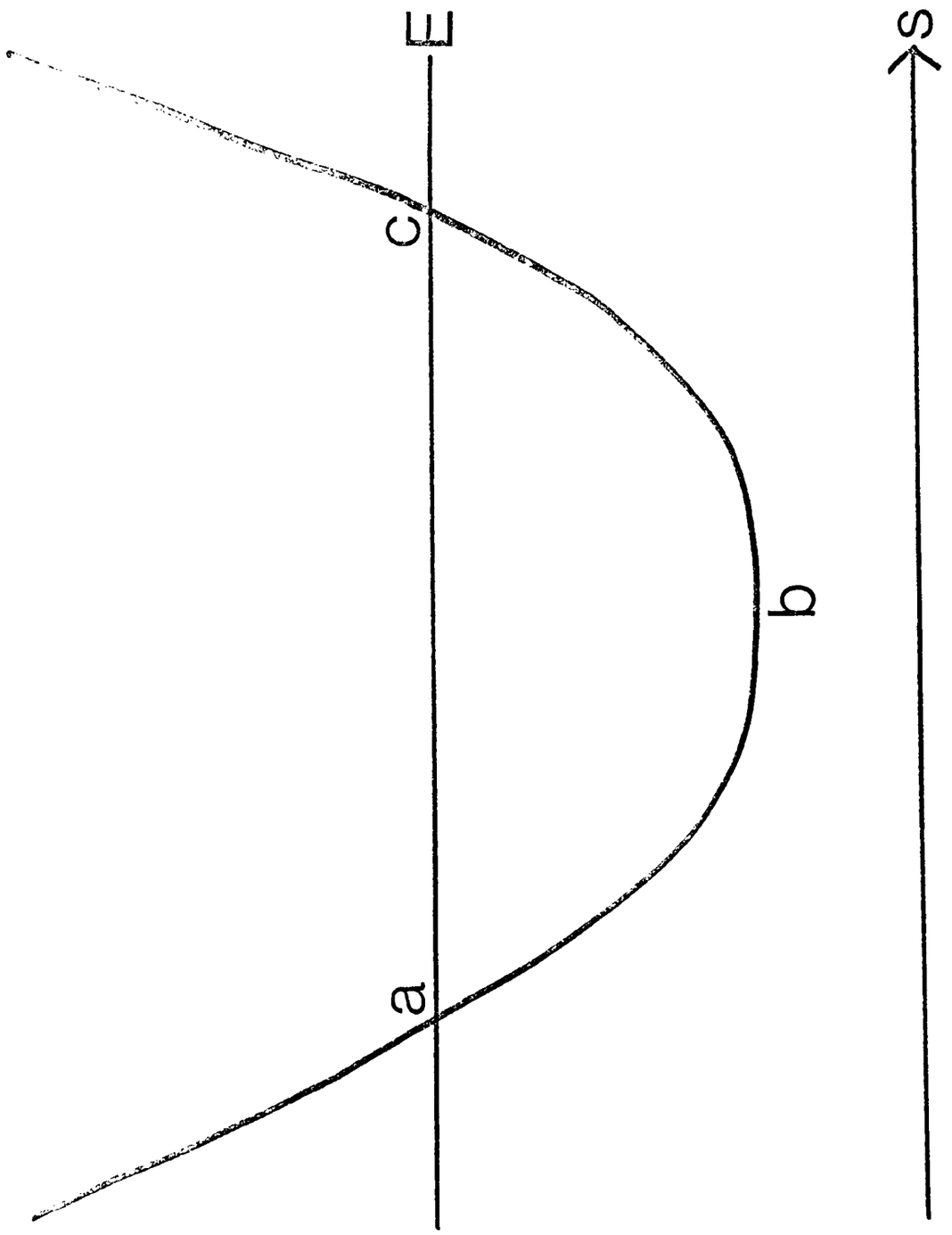
E
S
c
b
a

equation (2.1) together with equation (2.24) becomes:

$$\frac{d^2\psi(x)}{dx^2} + \left[\tilde{\varepsilon} - \frac{x^2}{4}\right]\psi(x) = 0, \tag{2.25}$$

A solution of equation (2.25) with the desired form (exponentially decreasing for $x \gg 0$) is in terms of Weber parabolic cylinder functions:

$$\psi(x) = U(-\tilde{\varepsilon}, x), \tag{2.26}$$

with an asymptotic representation valid for $|x| \gg |\tilde{\varepsilon}|$ of:

$$\psi(x) \sim \frac{1}{\sqrt{x}} \exp\left(-\frac{x^2}{4} + \tilde{\varepsilon}\ln x\right), \tag{2.27}$$

for $x \gg 0$ and since:[42,43]

$$\pi V(-\tilde{\varepsilon}, x) = \Gamma\left(\tfrac{1}{2} - \tilde{\varepsilon}\right)\left[U(-\tilde{\varepsilon}, -x) - \sin\pi\tilde{\varepsilon}\, U(-\tilde{\varepsilon}, x)\right],$$

and

$$V(-\tilde{\varepsilon}, x) \sim \left(\frac{2}{\pi}\right)^{1/2} \frac{1}{\sqrt{x}} \exp\left(+\frac{x^2}{4} - \tilde{\varepsilon}\ln x\right),$$

the asymptotic representation for $x \ll 0$ is

$$\psi(x) \sim \frac{\sin\pi\tilde{\varepsilon}}{\sqrt{|x|}} e^{-x^2/4 + \tilde{\varepsilon}\ln|x|} + \frac{(2\pi)^{1/2}}{\Gamma\left(\frac{1}{2} - \tilde{\varepsilon}\right)\sqrt{|x|}} e^{x^2/4 - \tilde{\varepsilon}\ln|x|}, \tag{2.28}$$

and terms of order x^{-2} have been neglected in equations (2.27) and (2.28). For $\tilde{\varepsilon} \geqslant 0$, the semi-classical solution of equation (2.25) corresponding to equation (2.27) is

$$\psi(x) = \left[\frac{x^2}{4} - \tilde{\varepsilon}\right]^{-1/4} \exp\left\{-\int_{2\sqrt{\tilde{\varepsilon}}}^{x} \left[\frac{x'^2}{4} - \tilde{\varepsilon}\right]^{1/2} dx'\right\}, \qquad (2.29)$$

$$\sim \left(\frac{2}{x}\right)^{1/2} \exp\left\{-\frac{x^2}{4} + \tilde{\varepsilon}\ln x + \frac{\tilde{\varepsilon}}{2} - \frac{\tilde{\varepsilon}}{2}\ln\tilde{\varepsilon}\right\}, \qquad (2.30)$$

where the lower integration limit has been chosen as the classical turning point ($x = 2\sqrt{\tilde{\varepsilon}}$) in equation (2.29) and in equation (2.30) terms of order x^{-2} have again been neglected. Similar semiclassical solutions may be written down that correspond to the asymptotic forms (2.28). By comparing these semiclassical solutions with equations (2.27) and (2.28) the following connection formula may be deduced. The function:

$$\frac{1}{\sqrt{|k(s)|}} \exp\left\{-\int_{c}^{s} |k(s')|\, ds'\right\}, \qquad (2.31)$$

valid for $s \gg c$ connects with

$$\frac{\sin \pi \tilde{\varepsilon}}{\sqrt{|k(s)|}} \exp\left\{ -\int_s^a |k(s')| ds' \right\} + \frac{A(\tilde{\varepsilon})}{\sqrt{|k(s)|}} \exp\left\{ \int_s^a |k(s')| ds' \right\}, \qquad (2.32)$$

valid for $s \ll a$, where

$$A(\tilde{\varepsilon}) = \frac{(2\pi)^{1/2}}{\Gamma(\frac{1}{2} - \tilde{\varepsilon})} \exp\left(\tilde{\varepsilon} - \tilde{\varepsilon} \ln |\tilde{\varepsilon}| \right). \qquad (2.33)$$

Equations (2.31)-(2.33) provide one of the desired connection formulae. A similar analysis based on the solution:

$$\psi(x) = U(-\tilde{\varepsilon}, -x),$$

of equation (2.25) leads to the second connection formula, namely for $\tilde{\varepsilon} \gg 0$ the function:

$$\frac{1}{\sqrt{|k(s)|}} \exp\left\{ -\int_s^a |k(s')| ds' \right\}, \qquad (2.34)$$

valid for $s \ll a$ connects with:

$$\frac{\sin \pi \tilde{\varepsilon}}{\sqrt{|k(s)|}} \exp\left\{ -\int_c^s |k(s')| ds' \right\} + \frac{A(\tilde{\varepsilon})}{\sqrt{|k(s)|}} \exp\left\{ \int_c^s |k(s')| ds' \right\}, \qquad (2.35)$$

valid for $s \gg c$ and $A(\tilde{\varepsilon})$ is again defined by equation (2.33). The functions (2.31)-(2.35) may

also be shown to be valid for $\tilde{\varepsilon}<0$ provided the classical turning points a and c are replaced by b, the classical equilibrium value of s. Thus the connection formulae are valid for energies which lie either above or below the bottom of the well and they provide a direct connection between one classically inaccessible region and another.

The behaviour of $A(\tilde{\varepsilon})$ as a function of $\tilde{\varepsilon}$ is shown in Figure (4). For $\tilde{\varepsilon}>0$ the function oscillates whilst for $\tilde{\varepsilon}<0$ the function asymptotically approaches unity. For $\tilde{\varepsilon}\gg 0$ equation (2.33) may be written:

$$A(\tilde{\varepsilon}) = 2\cos\pi\tilde{\varepsilon}\, e^{-\chi(\tilde{\varepsilon})}, \qquad (2.36)$$

where the quantum correction function $\chi(\tilde{\varepsilon})$ is defined by:

$$\chi(\tilde{\varepsilon}) = \tilde{\varepsilon}\ln\tilde{\varepsilon} - \tilde{\varepsilon} - \ln\Gamma(\tfrac{1}{2}+\tilde{\varepsilon}) + \tfrac{1}{2}\ln 2\pi, \qquad (2.37)$$

The reflection formula:

$$\Gamma(\tfrac{1}{2}-z)\Gamma(\tfrac{1}{2}+z) = \pi/\cos\pi z,$$

has been used in deriving equations (2.36) and (2.37). $\chi(\tilde{\varepsilon})$ in equation (2.37) takes the values 0.35 at $\tilde{\varepsilon} = 0$, and then decays to zero being 0.07 at $\tilde{\varepsilon} = 0.5$,

Figure 4

The function $A(\tilde{\varepsilon})$.

The full line is equation (2.33).

The dashed lines are equations

(2.38) and (2.39).

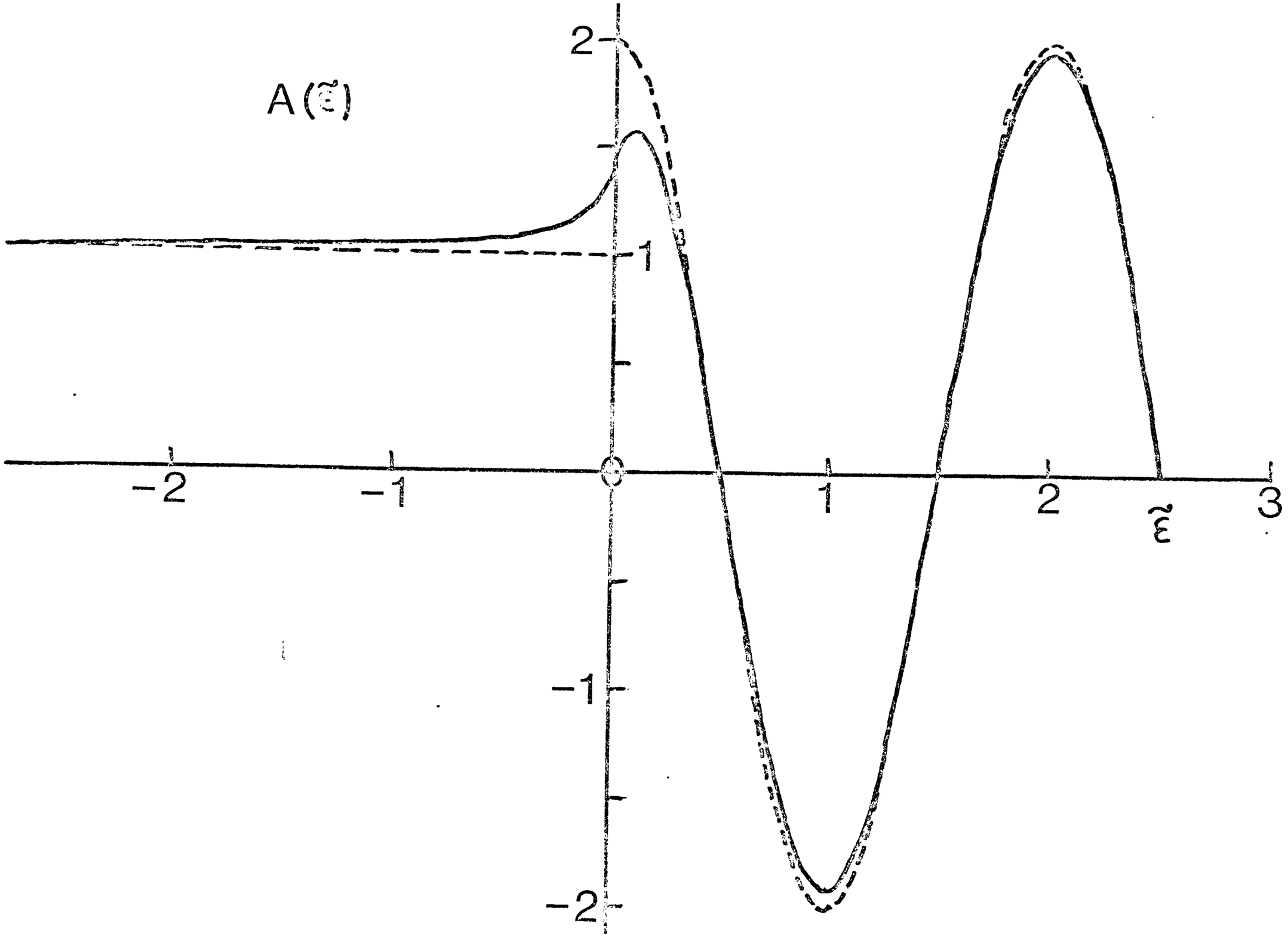
A(ξ)
2
1
−1
−2
−2
−1
0
1
2
3
ξ

0.04 at $\tilde{\varepsilon} = 1.0$ and 0.02 at $\tilde{\varepsilon} = 2.0$. Numerical values of $\chi(\tilde{\varepsilon})$ are given in Table (2). Notice also that $\chi(\tilde{\varepsilon})$ possesses a logarithmic singularity at $\tilde{\varepsilon} = 0$ and that the slope of $\chi(\tilde{\varepsilon})$ is infinite there (compare $\phi(\varepsilon)$). With the help of Burnside's formula:[46]

$$\ln \Gamma(z) \sim (z-\tfrac{1}{2})\ln(z-\tfrac{1}{2}) - z - \tfrac{1}{2} + \tfrac{1}{2}\ln 2\pi ,$$

the asymptotic form of $A(\tilde{\varepsilon})$ for $\tilde{\varepsilon} \gg 0$ becomes:

$$A(\tilde{\varepsilon}) \sim 2\cos\pi\tilde{\varepsilon} . \qquad (2.38)$$

In a similar way, for $\tilde{\varepsilon} \ll 0$:

$$A(\tilde{\varepsilon}) \sim 1 . \qquad (2.39)$$

Equations (2.38) and (2.39) give $A(\tilde{\varepsilon})$ to within 10% of its exact value for $|\tilde{\varepsilon}| > 0.4$. Their behaviour is also shown in Figure (4). Comparison of equation (2.15) with equation (2.37) shows that the quantum correction functions ϕ and χ are related via:

$$\phi(x) = -\mathrm{Im}\,\chi(ix) .$$

It is clear that for large s the exponentially increasing terms in the connection formulae (2.32) and (2.35) completely dominate the exponentially

Table 2

Numerical values of $\chi(\tilde{\varepsilon}) = \tilde{\varepsilon}\ln\tilde{\varepsilon} - \tilde{\varepsilon} - \ln\Gamma(\frac{1}{2}+\tilde{\varepsilon}) + \frac{1}{2}\ln 2\pi$.

$\tilde{\varepsilon}$	$\chi(\tilde{\varepsilon})$
0.0	0.347**
0.1	0.192
0.2	0.136
0.3	0.106
0.4	0.087
0.5	0.072
0.6	0.062
0.7	0.054
0.8	0.049
0.9	0.044
1.0	0.040
1.2	0.033
1.4	0.028
1.6	0.026
1.8	0.023
2.0	0.021
2.5	0.016

** Using $\lim_{\tilde{\varepsilon}\to 0} \tilde{\varepsilon}\ln\tilde{\varepsilon} = 0$

decreasing terms except when

$$\tilde{\varepsilon} = n + \tfrac{1}{2} \qquad n = 0, 1, 2, \cdots, \tag{2.40}$$

in which case according to equation (2.36) the coefficient of the increasing term vanishes. Equation (2.40) then gives the eigenvalues of the corresponding bound state problem. It is this abrupt disappearance and subsequent change in sign of the coefficient of the leading term that gives rise to resonance effects in orbiting collisions discussed in Chapter (3). On the other hand, for $\tilde{\varepsilon} < 0$ according to equations (2.33) and (2.39), $A(\tilde{\varepsilon})$ is always finite and no resonant behaviour is expected.

When the well is only approximately parabolic, analogous substitutions to those employed in Section (2.2) may be used, namely:

$$\left.\begin{aligned} \pi\tilde{\varepsilon} &\longrightarrow \int_a^c k(s)\,ds\,, \qquad \tilde{\varepsilon} > 0\,, \\ \pi\tilde{\varepsilon} &\longrightarrow \mathrm{Re}\, i\int_{ia}^{ic} |k(s)|\,ds\,, \qquad \tilde{\varepsilon} < 0\,. \end{aligned}\right\} \tag{2.41}$$

The arrows become equality signs when the well is exactly parabolic.

For use in later applications connection formulae based on a linear turning point are summarized below.[5] For the first turning point in Figure (1) the functions:

$$\frac{1}{\sqrt{k(s)}} \exp\left\{ \pm i \int_s^a k(s')ds' \pm i\frac{\pi}{4} \right\}, \tag{2.42}$$

valid for $s \ll a$ connect with:

$$\frac{1}{\sqrt{|k(s)|}} \exp\left\{ \int_a^s |k(s')|ds' \right\} \pm \frac{i}{2\sqrt{|k(s)|}} \exp\left\{ -\int_a^s |k(s')|ds' \right\}, \tag{2.43}$$

valid for $s \gg a$. For the second turning point in Figure (1) the functions:

$$\frac{1}{\sqrt{k(s)}} \exp\left\{ \pm i \int_c^s k(s')ds' \pm i\frac{\pi}{4} \right\}, \tag{2.44}$$

valid for $s \gg c$ connect with:

$$\frac{1}{\sqrt{|k(s)|}} \exp\left\{ \int_s^c |k(s')|ds' \right\} \mp \frac{i}{2\sqrt{|k(s)|}} \exp\left\{ -\int_s^c |k(s')|ds' \right\}, \tag{2.45}$$

valid for $s \ll c$.

CHAPTER THREE: ORBITING COLLISIONS

3.1 INTRODUCTION

The system under consideration consists of two particles interacting via a single spherically symmetrical potential energy curve. Systems of this type have been the object of considerable study by molecular beam techniques and a large amount of information has been acquired.[2-4] The Schrödinger equation that determines the scattering is:

$$-\frac{\hbar^2}{2\mu}\nabla^2\psi(\vec{r}) + [V(r) - E]\psi(\vec{r}) = 0, \qquad (3.1)$$

where μ is the reduced mass of the particles, V(r) is the interaction potential and E is the initial relative kinetic energy or collision energy. It is always possible to remove the centre of mass motion provided the particles move in a homogeneous space. Equation (3.1) is subject to the boundary condition that asymptotically $\psi(\vec{r})$ represents an incoming plane wave and an outgoing scattered wave:

$$\psi(\vec{r}) \sim e^{ikr\cos\theta} + f(\theta)\frac{e^{ikr}}{r}, \qquad (3.2)$$

where θ is the scattering angle and $f(\theta)$ the scattering amplitude. The asymptotic form (3.2) holds provided $V(r)$ drops off more rapidly than r^{-1}.[47] The method of partial waves gives for $f(\theta)$:[8]

$$f(\theta) = \frac{1}{2ik} \sum_{\ell=0}^{\infty} (2\ell+1)(e^{2i\delta_\ell} - 1) P_\ell(\cos\theta), \qquad (3.3)$$

where in equation (3.3) $k = (2\mu E/\hbar^2)^{\frac{1}{2}}$ is the incident wave number, $P_\ell(\cos\theta)$ is the Legendre polynomial in $\cos\theta$ and δ_ℓ is the ℓth order phase shift defined below. The scattering problem thus reduces to the determination of the phase shifts, which in turn are found from the asymptotic form of the regular solution of the radial wave equation:

$$-\frac{\hbar^2}{2\mu}\frac{d^2R_\ell(r)}{dr^2} + \left[V(r) + \frac{\ell(\ell+1)\hbar^2}{2\mu r^2} - E\right]R_\ell(r) = 0, \qquad (3.4)$$

with

$$R_\ell(r) \sim \sin(kr - \ell\pi/2 + \delta_\ell), \qquad (3.5)$$

and

$$R_\ell(0) = 0. \qquad (3.6)$$

The reference phase in equation (3.5) is that determined by the asymptotic form of the corresponding

ℓth order spherical Bessel function, that is the free particle solution. A semiclassical expression for δ_ℓ in the orbiting case is derived below. Important measurable quantities are the differential and total cross sections, $I(\theta)$ and σ which are given in terms of the phase shifts by:[8]

$$I(\theta) = |f(\theta)|^2, \tag{3.7}$$

$$\sigma = \frac{4\pi}{k^2} \sum_{\ell}^{(2\ell+1)} \lambda^2 \sin^2 \delta_\ell . \tag{3.8}$$

The orbiting phenomenon arises from the form of V(r), which typically has a short range repulsive part and a long range attractive part so that the effective potential defined by:

$$V_\ell(r) = V(r) + \frac{\ell(\ell+1)\hbar^2}{2\mu r^2},$$

has a maximum and a minimum for a certain range of ℓ values and for a certain range of energy, $E - V_\ell(r)$ possesses three zeros or classical turning points. (An additional possibility is that V(r) itself possesses a maximum and minimum). This situation, which is illustrated in Figure (5), gives rise to the phenomenon of orbiting or spiralling.[48] Classically

Figure 5

The effective potential energy curve $V_\ell(r)$. E denotes the collision energy. a_ℓ, c_ℓ, e_ℓ are the classical turning points. d_ℓ is the position of the barrier maximum and b_ℓ is the position of the well minimum.

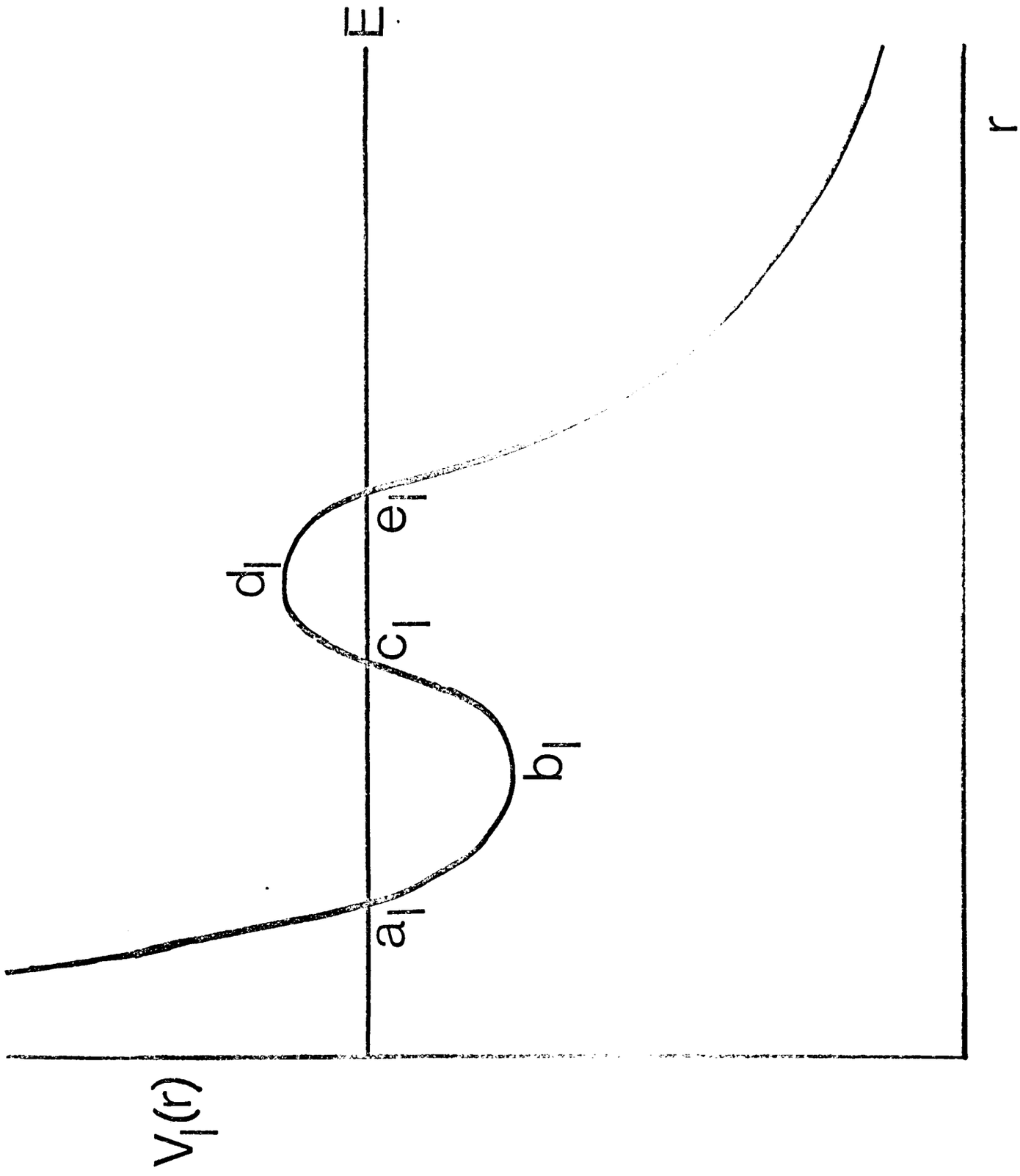
E
r
$V_l(r)$
a_l
b_l
c_l
d_l
e_l

orbiting occurs when the collision energy equals the value of the effective potential at its maximum, that is when $E = V_\ell(d_\ell)$ in the notation of Figure (5), and the particles then orbit around each other for an infinite length of time. It is shown below that in a semiclassical treatment this infinite lifetime is replaced by a finite one. For E somewhat greater (or somewhat less) than $V_\ell(d_\ell)$ the two particles execute several orbits before separating again. This type of behaviour will also be encountered in Chapters (4)-(6).

Figure (5) also shows that quasi-stationary states may exist in the dip of the effective potential. From a classical viewpoint these states are stable but quantum mechanically they have a finite lifetime because of the possibility of tunnelling through the barrier. Such quasi-stationary behaviour may be understood in terms of complex energies, whose real and imaginary parts determine the resonance energies and widths of the states respectively. In Sections (3.2) and (3.3) expressions for the resonance energies and their widths are determined from the semiclassical expressions for the wavefunction derived with the help of the connection formulae

given in Chapter (2).

Using the boundary condition that the wavefunction is regular at the origin, together with linear and parabolic connection formulae the form of the wavefunction in the region $r \gg e_\ell$ is found. For energies near the maximum in the effective potential, connection formulae for a parabolic barrier are valid for the semiclassical analysis, whilst for energies near the bottom of the well, connection formulae for a parabolic well must be used. Imposing the further boundary condition that there be no incoming wave in the region $r \gg e_\ell$ yields a complex Bohr-Sommerfeld quantization condition for the resonance energies and widths of the quasi-stationary states. This quantization condition may be solved to give explicit expressions for the resonance energies and their widths when the separation of the states is much greater than their widths. It is shown below that these expressions allow the phase shift and cross sections to be expressed in a Breit-Wigner resonance form.

Orbiting collisions are of interest in a variety of collision processes and related phenomena. These include atom-atom,[2-4] atom-molecule,[10,49]

ion-molecule,[50] and α particle collisions,[51,52] rotational predissociation[53](which may be regarded as the inverse process to orbiting), the effect of curve crossing on elastic scattering[54,55] (the existing semiclassical theory breaks down when $E \approx V_l(d_l)$ for a lower adiabatic curve of the shape shown in Figure (5)),and three body recombination reactions.[56,57] In the last example,a recent theory of three body recombination reactions assumes the mechanism:

$$X + X \rightleftharpoons X_2^*,$$

where X_2^* denotes an orbiting complex,which then suffers an inelastic collision with a third body M

$$X_2^* + M \rightarrow X_2 + M.$$

3.2 SEMICLASSICAL ANALYSIS

The choice of connection formulae is determined by the value of the collision energy relative to the minimum and maximum in the effective potential. In the first instance it is supposed the collision energy is near the barrier maximum so that the use of parabolic connection formulae for a barrier is valid for the semiclassical analysis. When the collision energy is near the minimum in the effective potential, parabolic connection formulae for a well must be used.

The boundary condition (3.6) that $R_\ell(r)$ be regular at the origin requires that the semiclassical solution of equation (3.4) be exponentially decreasing in the region $r \ll a_\ell$. This boundary condition cannot be satisfied by the ordinary semiclassical solution however because $V_\ell(r)$ varies rapidly for $r \approx 0$. By means of the Langer transformation[37] it is possible to use the semiclassical approximation near the origin provided that $\ell(\ell+1)$ is replaced by $(\ell+\frac{1}{2})^2$ in the effective potential. The semiclassical solution in the region $r \ll a_\ell$ is therefore:

$$R_\ell(r) = \frac{K}{\sqrt{|k_\ell(r)|}} \exp\left\{ -\int_r^{a_\ell} |k_\ell(r')| dr' \right\}, \qquad (3.9)$$

where

$$k_\ell(r) = \left\{ \frac{2\mu}{\hbar^2}\left[E - V(r) - \frac{(\ell+\frac{1}{2})^2\hbar^2}{2\mu r^2} \right] \right\}^{1/2},$$

and K is a constant whose value is chosen later. The use of linear connection formulae, equations (2.44) and (2.45) gives for the semiclassical solution in the region $a_\ell \ll r \ll c_\ell$ which connects with equation (3.9):

$$R_\ell(r) = \frac{2K}{\sqrt{k_\ell(r)}} \cos\left\{ \int_{a_\ell}^{r} k_\ell(r')dr' - \frac{\pi}{4} \right\}. \qquad (3.10)$$

Equation (3.10) may be written in terms of the phase reference point c_ℓ (or d_ℓ when $E > V_\ell(d_\ell)$):

$$R_\ell(r) = \frac{K}{\sqrt{k_\ell(r)}}\left[e^{i\alpha_\ell(E)} \exp\left\{ -i\int_r^{c_\ell} k_\ell(r')dr' - i\frac{\pi}{4} \right\} + e^{-i\alpha_\ell(E)} \exp\left\{ i\int_r^{c_\ell} k_\ell(r')dr' + i\frac{\pi}{4} \right\} \right], \qquad (3.11)$$

where $\alpha_\ell(E)$ denotes the phase integral:

$$\alpha_\ell(E) = \int_{a_\ell}^{c_\ell} k_\ell(r)dr. \qquad (3.12)$$

Equation (3.11) is now in a form suitable for the application of parabolic connection formulae for a barrier (equations (2.16) and (2.17)). The result for the wavefunction in the region $r \gg e_\ell$ is:

$$R_\ell(r) = \frac{K}{\sqrt{k_\ell(r)}}\left[A\exp\left\{i\int_{e_\ell}^{r} k_\ell(r')dr' - i\frac{\pi}{4}\right\} + A^*\exp\left\{-i\int_{e_\ell}^{r} k_\ell(r')dr' + i\frac{\pi}{4}\right\}\right], \tag{3.13}$$

where

$$A = e^{i[\alpha_\ell(E)-\phi(\varepsilon_\ell)]}\left[1+e^{-2\pi\varepsilon_\ell}\right]^{1/2} + e^{-i\alpha_\ell(E)}e^{-\pi\varepsilon_\ell}, \tag{3.14}$$

and

$$\varepsilon_\ell = \frac{E - V_\ell(d_\ell)}{\hbar\omega_\ell^*}, \tag{3.15}$$

with ω_ℓ^* the classical angular frequency of vibration in the upturned barrier. To avoid cumbersome equations in what follows the notation $\pi\varepsilon_\ell$ will be retained for the integral substitutions (2.23). Equation (3.13) (together with equations (3.14) and (3.15)) is the key equation in what follows. From it is derived the phase shift and the resonance energies and widths of the quasi-stationary states. Notice that the first term in equation (3.13) is the complex conjugate of the second term - in accord with the conservation of flux.

Equation (3.13) may be rewritten as:

$$R_\ell(r) = \frac{1}{\sqrt{k_\ell(r)}} \sin\left\{ \int_{e_\ell}^{r} k_\ell(r')dr' + \frac{\pi}{4} - \tfrac{1}{2}\phi(\varepsilon_\ell) + \delta_\ell^{(r)}(E)\right\}, \qquad (3.16)$$

where

$$\delta_\ell^{(r)}(E) = \tan^{-1}\left\{ \frac{T(\varepsilon_\ell)-1}{T(\varepsilon_\ell)+1} \tan\left[\alpha_\ell(E) - \tfrac{1}{2}\phi(\varepsilon_\ell)\right]\right\}, \qquad (3.17)$$

with

$$T(\varepsilon_\ell) = \left[1 + e^{2\pi\varepsilon_\ell}\right]^{1/2},$$

and the branch of the arctangent is determined by the continuity of $\delta_\ell^{(r)}(E)$ in equation (3.17). The constant K in equation (3.13) has been chosen so that the coefficient of the sine wave in equation (3.16) is unity. The reference phase is that determined by the asymptotic form of the ℓth order spherical Bessel function (see equation (3.5)) so that the phase shift $\delta_\ell(E)$ for this three turning point problem is:

$$\delta_\ell(E) = \delta_\ell^{(0)}(E) + \delta_\ell^{(r)}(E), \qquad (3.18)$$

where

$$\delta_\ell^{(0)}(E) = \lim_{r\to\infty}\left\{ \int_{e_\ell}^{r} k_\ell(r')dr' - kr\right\} + (\ell+\tfrac{1}{2})\tfrac{\pi}{2} - \tfrac{1}{2}\phi(\varepsilon_\ell). \qquad (3.19)$$

In the energy region $\varepsilon_\ell \gg 0$ the factor $(T(\varepsilon_\ell)-1)(T(\varepsilon_\ell)+1)^{-1}$ rapidly approaches unity so that $\delta_\ell^{(r)}(E)$ contributes a term $\alpha_\ell(E)$ to the phase shift ($\phi(\varepsilon_\ell) \longrightarrow 0$ as $\varepsilon_\ell \to \infty$), which becomes:

$$\delta_\ell(E) = \lim_{r\to\infty} \left\{ \int_{a_\ell}^{r} k_\ell(r')dr' - kr \right\} + (\ell+\tfrac{1}{2})\tfrac{\pi}{2}. \qquad (3.20)$$

Equation (3.20) is just the value for the phase shift in the absence of a barrier.[3]

When $\varepsilon_\ell \approx 0$ the phase integrals occurring in equations (3.17) and (3.19) may be expanded in a similar manner to that employed in Chapter (2):

$$\left.\begin{aligned} \alpha_\ell(E) &= \tfrac{\varepsilon_\ell}{2} - \tfrac{\varepsilon_\ell}{2}\ln|\varepsilon_\ell| + \text{other terms}, \\ \int_{a_\ell}^{r} k_\ell(r')dr' &= \tfrac{\varepsilon_\ell}{2} - \tfrac{\varepsilon_\ell}{2}\ln|\varepsilon_\ell| + \text{other terms}, \end{aligned}\right\} \qquad (3.21)$$

where 'other terms' denotes contributions not related to the top of the barrier. In the absence of the quantum correction function $\phi(\varepsilon_\ell)$, equation (3.21) would predict an infinite rate of change of the phase shift with ε_ℓ at $\varepsilon_\ell = 0$ and derivatives of the phase shift (such as the deflection function $\Theta = 2\,\partial\delta_\ell(E)/\partial\ell$) would be divergent at $\varepsilon_\ell = 0$. This is

the orbiting singularity. Recalling the definition of $\phi(\varepsilon_\ell)$ (equation (2.15)) it is seen that this singularity is exactly cancelled and the divergences do not occur.

In the energy region $\varepsilon_\ell \ll 0$ the factor $(T(\varepsilon_\ell)-1)(T(\varepsilon_\ell)+1)^{-1}$ is very small and consequently the contribution from $\delta_\ell^{(1)}(E)$ is constant except when:

$$\alpha_\ell(E) \approx (n+\tfrac{1}{2})\pi + \tfrac{1}{2}\phi(\varepsilon_\ell), \quad n = 0, 1, 2, \ldots, \qquad (3.22)$$

in which case according to equation (3.17) the phase shift rapidly increases by π. In this energy region $\delta_\ell^{(1)}(E)$ is the resonance contribution to the phase shift whilst $\delta_\ell^{(0)}(E)$ is the non-resonance or 'potential' contribution. In section (3.3) it is shown how, with the help of equation (3.14), equation (3.17) may be reduced to a Breit-Wigner resonance form.

It is instructive to compare the phase shift given by equations (3.17) and (3.19) with the simple semiclassical result for this problem. The latter may be written:[41]

$$\delta_\ell(E) = \lim_{r\to\infty}\left\{\int_{a_\ell}^{r} k_\ell(r')dr' - kr\right\} + (\ell+\tfrac{1}{2})\tfrac{\pi}{2} \qquad (3.23)$$

$$+ \tan^{-1}\left\{\theta(\varepsilon_\ell)\tan\alpha_\ell(E)\right\},$$

where $\theta(\varepsilon_\ell)$ is a step function:

$$\theta(\varepsilon_\ell) = 1 \qquad \varepsilon_\ell > 0 ,$$

$$= 0 \qquad \varepsilon_\ell < 0 .$$

Comparing equations (3.17) and (3.19) with equation (3.23) shows that the latter contains no provision for tunnelling through the barrier or resonance effects when $\varepsilon_\ell<0$ or for the partial reflection of the incoming wave by the centrifugal barrier when $\varepsilon_\ell>0$. The failure of the simple semiclassical phase shift (3.23) in comparison with the exact phase shift obtained by numerical integration of the radial wave equation in the orbiting region is well known.[58-60]

Ford, Hill, Wakano and Wheeler[6] have obtained an expression for the phase shift by fitting a parabola to the maximum in the effective potential. However their result is not expressed in terms of classical phase integrals and is consequently very complicated. Herm[61] and Dubrovsky[62] have obtained expressions in closed form for the phase shift and it may be shown that the simple result contained in equation (3.18) is equivalent to their much more complicated results.

Herm[61] has compared his semiclassical phase shift with the exact numerical results of Bernstein, Curtiss, Iman-Rahajoe and Wood for a Lennard-Jones (12,6) potential.[59] Excellent qualitative and good quantitative agreement was found. The semiclassical result began to fail for small values of the orbital angular momentum quantum number ($\ell \lesssim 10$).

Phase integral methods have also been used to derive phase shifts for this three turning point problem. Miller[41] has explicitly demonstrated that in this approach $\phi(\varepsilon_\ell)$ is of an unknown magnitude. Livingston[63] has also applied phase integral methods to this problem and has concluded that resonance effects are associated with pairs of virtual energy levels in the dip of the effective potential. Since the semiclassical phase shifts discussed above (and those mentioned in references (64) and (65) below) show no such pairing effect (nor have calculations involving numerical integration of the radial wave equation[58-60]), it is important that this discrepancy in the theory be resolved. It is shown below that whilst Livingston's expression for the phase shift is essentially correct, the pairing effect arises from an incorrect specification of the

resonance conditions in reference (63).

A resonance occurs when a small increase in energy results in a rapid but smooth increase in the phase shift. The centre of the resonance is the point of maximum rate of this increase - a point of inflection in the phase shift . Equation (3.17) shows that the points of inflection which determine the resonance conditions are given by:

$$\alpha_\ell(E_{n\ell}) = (n+\tfrac{1}{2})\pi - \tfrac{1}{2}\phi(|\varepsilon_{n\ell}|), \quad n = 0, 1, 2 \ldots . \tag{3.24}$$

Equation (3.24) is an extension of the standard semiclassical quantization condition ($\frac{1}{2}\phi(|\varepsilon_{n\ell}|)$ represents a level shift). Livingston's expression for the phase shift may be written:

$$\delta_\ell(E) = \delta_\ell^{(0)}(E) + \frac{1}{2}\tan^{-1}\left[\frac{(T^2+1)^{-1}(T^2-1)\sin\{2[\alpha_\ell(E)-\frac{1}{2}\phi(\varepsilon_\ell)]\}}{2T(T^2+1)^{-1} + \cos\{2[\alpha_\ell(E)-\frac{1}{2}\phi(\varepsilon_\ell)]\}}\right] - \frac{\pi}{2}, \tag{3.25}$$

which is obtained from equation (3.17) via the identity:

$$\tan^{-1}(-z^{-1}) = \frac{1}{2}\tan^{-1}[2z(1-z^2)^{-1}] - \frac{\pi}{2},$$

with

$$z = (1+T)\Big/\{(1-T)\tan[\alpha_\ell(E) - \tfrac{1}{2}\phi(\varepsilon_\ell)]\}.$$

As noted above, a phase integral derivation of equations (3.17) and (3.25) does not allow the magnitude of $\phi(\varepsilon_\ell)$ to be determined. Comparison of equation (3.15) with equation (30) of reference (63) shows that the latter corresponds to the choice $\phi(\varepsilon_\ell) = \pm\pi$. From the preceding discussion it is clear that this choice is incorrect. The form of equation (3.25) led Livingston to conclude that a resonance occurs whenever the denominator of equation (3.25) vanishes, or equivalently whenever

$$\cos\left[\alpha_\ell(E) - \tfrac{1}{2}\phi(\varepsilon_\ell)\right] = \pm (T+1)(T-1)^{-1},$$

that is, resonance pairs situated on either side of $\alpha_\ell(E) = (n+\tfrac{1}{2})\pi + \tfrac{1}{2}\phi(\varepsilon_\ell)$. It is easy to show however that this resonance condition is incorrect since it does not correspond to a point of inflection in the phase shift. The points of inflection are of course given by equation (3.24) because equations (3.17) and (3.25) are identical. The prediction of resonance pairs must therefore be abandoned.**

**Livingston (private communication) has agreed with the above analysis.

An important case not covered by equation (3.13) occurs when the collision energy takes on values near the minimum of the effective potential well. Connection formulae for a parabolic well must then be used in the semiclassical analysis. Imposing the boundary condition that $R_\ell(r)$ be regular at the origin gives equation (3.9) as the solution valid for $r \ll a_\ell$. In the region $c_\ell \ll r \ll e_\ell$, the connection formula (2.35) gives for the solution there:

$$\frac{\sin \pi \tilde{\varepsilon}_\ell}{\sqrt{|k_\ell(r)|}} \exp\left\{ -\int_{c_\ell}^{r} |k_\ell(r')| dr' \right\} + \frac{A(\tilde{\varepsilon}_\ell)}{\sqrt{|k_\ell(r)|}} \exp\left\{ \int_{c_\ell}^{r} |k_\ell(r')| dr' \right\}, \quad (3.26)$$

where

$$\tilde{\varepsilon}_\ell = \frac{E - V_\ell(b_\ell)}{\hbar \tilde{\omega}_\ell},$$

and $\tilde{\omega}_\ell$ is the classical angular frequency of oscillation in the potential well. In addition:

$$A(\tilde{\varepsilon}_\ell) = \frac{(2\pi)^{1/2}}{\Gamma(\frac{1}{2} - \tilde{\varepsilon}_\ell)} \exp\left[\tilde{\varepsilon}_\ell - \tilde{\varepsilon}_\ell \ln|\tilde{\varepsilon}_\ell| \right],$$

$$= 2 \cos(\pi \tilde{\varepsilon}_\ell) \exp(-\chi(\tilde{\varepsilon}_\ell)) \quad \text{for } \tilde{\varepsilon}_\ell \gg 0.$$

The phase integrals in (3.26) may be written in terms of the phase reference point e_ℓ and linear connection formulae, equations (2.44) and (2.45) used to find the solution valid for $r \gg e_\ell$. The result is:

$$R_\ell(r) = \frac{\widetilde{K}}{\sqrt{k_\ell(r)}}\left[B\exp\left\{ i\int_{e_\ell}^{r} k_\ell(r')dr' - i\frac{\pi}{4}\right\} + B^*\exp\left\{ -i\int_{e_\ell}^{r} k_\ell(r')dr' + i\frac{\pi}{4}\right\}\right], \tag{3.27}$$

where

$$B = i\sin(\pi\tilde{\varepsilon}_\ell)\exp\left[-\beta_\ell(E)\right] + \cos(\pi\tilde{\varepsilon}_\ell)\exp\left[\beta_\ell(E) - \chi(\tilde{\varepsilon}_\ell)\right],$$

and where $\beta_\ell(E)$ denotes the phase integral:

$$\beta_\ell(E) = \int_{c_\ell}^{e_\ell} |k_\ell(r)|dr .$$

$\widetilde{K}$ is a constant in equation (3.27). Equation (3.27) is restricted to $\tilde{\varepsilon}_\ell \gtrsim 0$, the energy range where resonance effects are observed. Equation (3.27) may be written in the form:

$$R_\ell(r) = \frac{1}{\sqrt{k_\ell(r)}}\sin\left\{ \int_{e_\ell}^{r} k_\ell(r')dr' + \frac{\pi}{4} + \delta_\ell^{(r)}(E)\right\}, \tag{3.28}$$

with $\widetilde{K}$ having been chosen so that the coefficient of the sine wave is unity. In equation (3.28):

$$\delta_\ell^{(1)}(E) = \tan^{-1}\left\{ \frac{1}{4} \exp\left[-2\left\{\beta_\ell(E) - \tfrac{1}{2}\chi(\tilde{\varepsilon}_\ell)\right\}\right] \tan \pi \tilde{\varepsilon}_\ell \right\}, \quad (3.29)$$

and the phase shift becomes:

$$\delta_\ell(E) = \delta_\ell^{(0)}(E) + \delta_\ell^{(1)}(E), \quad (3.30)$$

with

$$\delta_\ell^{(0)}(E) = \lim_{r \to \infty} \left\{ \int_{e_\ell}^{r} k_\ell(r')dr' - kr \right\} + \left(\ell + \tfrac{1}{2}\right)\frac{\pi}{2}. \quad (3.31)$$

For energies near the bottom of the well $\beta_\ell(E)$ may be expanded (compare equations (3.21)):

$$\beta_\ell(E) = -\frac{\tilde{\varepsilon}_\ell}{2} + \frac{\tilde{\varepsilon}_\ell}{2} \ln \tilde{\varepsilon}_\ell + \text{other terms},$$

and recalling the definition of $\chi(\tilde{\varepsilon}_\ell)$ (equation (2.37)) it is seen that the logarithmic singularity in $\beta_\ell(E)$ is exactly cancelled by that in $\chi(\tilde{\varepsilon}_\ell)$.

Buckingham and Dalgarno[64] and Berry[65] have derived formulae for the phase shift equivalent to equations (3.29) and (3.31) but from which the quantum correction function $\chi(\tilde{\varepsilon}_\ell)$ is absent. Miller[41] has demonstrated by phase integral methods the necessity for a factor of this type, but the correction function that he

suggests is analogous to that for a potential barrier and therefore incorrect.*

Equations (3.17) and (3.19) hold for energies near the maximum in the effective potential, whilst equations (3.29) and (3.31) are valid for energies near the minimum in the effective potential. The connection between these two cases follows from the observation that equation (3.17) reduces to:

$$\delta_\ell^{(r)}(E) = \tan^{-1}\left\{ \frac{1}{4} e^{-2\pi|\varepsilon_\ell|} \tan \alpha_\ell(E) \right\}, \qquad (3.32)$$

for $\varepsilon_\ell \ll 0$, which together with the integral representations for ε_ℓ and $\tilde{\varepsilon}_\ell$ (equations (2.23) and (2.41)) and the results:

$$\phi(|\varepsilon_\ell|) \to 0, \quad |\varepsilon_\ell| \to \infty,$$

$$\chi(\tilde{\varepsilon}_\ell) \to 0, \quad \tilde{\varepsilon}_\ell \to \infty,$$

shows that the phase shifts (3.18) and (3.30) become equivalent in the energy region in which

---

** Miller (private communication) has agreed that $\chi(\tilde{\varepsilon}_\ell)$ is the appropriate quantum correction function to use.

they overlap. In particular the argument and coefficient of the tangent term in equations (3.17) and (3.29) are within 10% of those in equation (3.32) for $\varepsilon_\ell \leqslant -0.25$ and $\tilde{\varepsilon}_\ell \geqslant 0.40$, where for convenience the identifications $\beta_\ell = \pi/|\varepsilon_\ell|$ and $\alpha_\ell = \pi\tilde{\varepsilon}_\ell \geqslant \pi/2$ (the value at the first resonance) are made. On the other hand if the dip in the potential is so slight that the true three-turning-point problem cannot be regarded as a composite of one- and two-turning-point regions, the above analysis breaks down and another approach is required.

The derivation of the phase shift presented above appears to break down in certain other cases also. For example for energies above the barrier maximum the range in which connection formulae for a parabolic barrier can be used between a_ℓ and d_ℓ decreases as the energy increases (see Chapter (2)), but as $\delta_\ell(E)$ rapidly approaches the value of the phase shift in the absence of a dip, equation (3.18) may be taken as valid in this region. A similar consideration applies to energies below the minimum in the effective potential.

3.3 COMPLEX ENERGY FORMALISM

The quasi-stationary states in the dip of the effective potential have a finite lifetime because of the possibility of tunnelling through the barrier. This situation is represented by imposing the boundary condition that solutions of equation (3.4) represent outgoing waves at infinity.[8] This boundary condition requires that the energy be complex.

In the first case it is assumed that the solution valid for $r \gg e_\ell$ is given by equation (3.13). The complex eigenvalues of the energy are found by equating the amplitude of the incoming wave in equation (3.13) to zero (that is A* = 0). This leads to:

$$\alpha_\ell(E) = (n+\tfrac{1}{2})\pi + \tfrac{1}{2}\phi(\varepsilon_\ell) - \frac{i}{4}\ln\left(1+e^{2\pi\varepsilon_\ell}\right), \qquad (3.33)$$

with n = 0,1,2,... which is a complex Bohr-Sommerfeld quantization condition. If the potential barriers surrounding the dip were infinitely high and wide so that $\varepsilon_\ell \to -\infty$, equation (3.33) would reduce to:

$$\alpha_\ell(E_{n\ell}) = \int_{a_\ell}^{c_\ell} k_\ell(r)\,dr = (n+\tfrac{1}{2})\pi, \qquad (3.34)$$

the usual Bohr-Sommerfeld quantization condition for a potential well. The extra terms on the right hand side of equation (3.33) thus arise from the quasi-stationary nature of the states. The introduction of a complex energy:

$$E = E_{n\ell} - \tfrac{i}{2}\Gamma_{n\ell}, \quad E_{n\ell} > 0, \ \Gamma_{n\ell} > 0, \qquad (3.35)$$

characterizes these properties in a simple way.[8] In equation (3.35) $E_{n\ell}$ is the resonance energy and $\Gamma_{n\ell}$ the level width with the physical interpretation that the system decays according to the exponential law $\exp(-\Gamma_{n\ell}t/\hbar)$ and the lifetime $\tau_{n\ell}$ of a state is given by $\tau_{n\ell} = \hbar/\Gamma_{n\ell}$.

There is an alternative physical interpretation for $\Gamma_{n\ell}$ however. If the amplitude of the outgoing wave in equation (3.13) is set equal to zero, there results the quantization condition:

$$\alpha_\ell(E) = (n+\tfrac{1}{2})\pi + \tfrac{1}{2}\phi(\varepsilon_\ell) + \tfrac{i}{4}\ln(1+e^{2\pi\varepsilon_\ell}), \qquad (3.36)$$

with n = 0,1,2,.... Associated with equation (3.36)

is the complex energy:

$$E = E_{n\ell} + \tfrac{i}{2}\gamma_{n\ell}\,, \quad E_{n\ell} > 0\,, \quad \gamma_{n\ell} > 0\,,$$

with the physical interpretation that the system builds up in time according to $\exp(\gamma_{n\ell}t/\hbar)$. It is also clear that $\gamma_{n\ell} = \Gamma_{n\ell}$. In Chapter (5) it will be shown that setting the amplitude of the incoming and outgoing waves to zero in the semiclassical description of resonance tunnelling reactions will result in $\gamma_{n\ell} \neq \Gamma_{n\ell}$.

Equation (3.33) (and equation (3.36)) is valid for energies above or below the barrier maximum but physically the most interesting case is when the energy levels within the dip possess small widths compared with their separation. For this case equation (3.33) may be written:

$$\int_{a_\ell}^{c_\ell} k_\ell(r)\,dr = (n+\tfrac{1}{2})\pi - \tfrac{1}{2}\phi(|\varepsilon_\ell|) - \tfrac{i}{4}\ln\left(1+e^{-2\pi|\varepsilon_\ell|}\right), \qquad (3.37)$$

Inserting the complex energy (3.35) into $k_\ell(r)$ and expanding to first order in $\Gamma_{n\ell}$ (a valid procedure since $\Gamma_{n\gamma} \ll E_{n\ell}$ for sharp resonances) gives:

$$\int_{a_\ell}^{c_\ell} k_\ell(r)\,dr \approx \frac{1}{\hbar}\int_{a_\ell}^{c_\ell}\left\{2\mu\left[E_{n\ell} - V_\ell(r)\right]\right\}^{1/2}dr - \frac{i\Gamma_{n\ell}\pi}{2\hbar\omega_{n\ell}}\,, \qquad (3.38)$$

where

$$\omega_{n\ell}(E_{n\ell}) = \pi \Big/ \mu \int_{a_\ell}^{c_\ell} \{2\mu[E_{n\ell} - V_\ell(r)]\}^{-1/2} dr,$$

is the classical angular frequency of vibration for the well. If the minimum of the well is quadratic in r then the integral (3.37) may be evaluated directly in which case the expansion (3.38) is exact. Comparing the real and imaginary parts of equation (3.37) and (3.38) yields:

$$\frac{1}{\hbar} \int_{a_\ell}^{c_\ell} \{2\mu[E_{n\ell} - V_\ell(r)]\}^{1/2} dr = (n+\tfrac{1}{2})\pi - \tfrac{1}{2}\phi(|\varepsilon_{n\ell}|), \qquad (3.39)$$

$$\Gamma_{n\ell} = \frac{\hbar\omega_{n\ell}}{2\pi} \ln\left(1 + e^{-2\pi|\varepsilon_{n\ell}|}\right). \qquad (3.40)$$

The subscript n on $\varepsilon_{n\ell}$ in equations (3.39) and (3.40) indicates that E has been replaced by $E_{n\ell}$ in the equation defining ε_ℓ (equation (3.15)) since terms arising from the imaginary part of E in the right hand side of equation (3.37) may be neglected in this order of approximation. Comparing equation (3.39) with equation (3.34) shows that the resonance energy has been lowered relative to the

energy levels of the bounded system since $\phi(|\varepsilon_{n\ell}|) \gg 0$, in accord with the greater freedom of the system.

A similar analysis may be carried out for the case of collision energies near the bottom of the well. Equating to zero the amplitude of the incoming wave of equation (3.27) yields the following complex quantization condition:

$$\pi \tilde{\varepsilon}_\ell = (n+\tfrac{1}{2})\pi - i \coth^{-1}\{4 \exp[2\beta_\ell(E) - \chi(\tilde{\varepsilon}_\ell)]\}, \qquad (3.41)$$

and introducing the complex energy (3.35) into equation (3.41) gives:

$$\tilde{\varepsilon}_{n\ell} = n + \tfrac{1}{2}, \qquad (3.42)$$

and

$$\Gamma_{n\ell} = \frac{2\hbar\tilde{\omega}_{n\ell}}{\pi} \coth^{-1}\{4 \exp[2\beta_\ell(E_{n\ell}) - \chi(\varepsilon_{n\ell})]\}, \qquad (3.43)$$

for the resonance energies and widths of the quasi-stationary states respectively. Equations (3.42) and (3.43) become equivalent to equations (3.39) and (3.40) in the energy region where the two cases overlap.

Equations (3.39),(3.40),(3.42) and (3.43) provide expressions for the resonance energies and widths of

the quasi-stationary levels when the widths of the levels are small compared with their separation. These states may be regarded as a continuation of the true bound states embedded in the continuum by the centrifugal barrier and thus may be characterized by a vibrational and rotational quantum number (n and ℓ). In particular the orbital angular momentum quantum number becomes the internal rotational quantum number of the collision complex. An approximate solution of equation (3.39) may be found by writing:

$$V_\ell(r) = V_{min} + \tfrac{1}{2}\mu\omega^2 r^2 + \frac{\ell(\ell+1)\hbar^2}{2I_0},$$

on the assumption that the potential well is sufficiently localized to allow the moment of inertia I_0 of the complex to be regarded as constant and that the interaction potential possesses a quadratic minimum. V_{min} is the minimum value of V(r). Equation (3.39) gives in this case:

$$E_{n\ell} = V_{min} + (n+\tfrac{1}{2})\hbar\omega + \frac{\ell(\ell+1)\hbar^2}{2I_0}, \qquad (3.44)$$

and the small term that represents a level shift in equation (3.39) has been neglected. Then equation (3.44) shows explicitly that a resonance occurs whenever the collision energy coincides with one of the vibration-rotation states of the complex. Equation (3.42) can be treated in a similar manner.

Returning now to the real energy case, when the collision energy is near a resonance:

$$E = E_{n\ell} + \delta E$$

where $E_{n\ell}$ and δE are both real and $|\delta E| \ll E_{n\ell}$ and following the derivation of equation (3.38):

$$\int_{a_\ell}^{c_\ell} k_\ell(r)\,dr \approx \frac{1}{\hbar}\int_{a_\ell}^{c_\ell} \{2\mu[E_{n\ell} - V_\ell(r)]\}^{1/2} dr + \frac{\delta E \cdot \pi}{\hbar \omega_{n\ell}}, \qquad (3.45)$$

Substituting equation (3.45) into the expression for the phase shift, equation (3.18), and making the approximation valid for all $\varepsilon_{n\ell}$:

$$\frac{1}{4}\ln\left(1 + e^{-2\pi|\varepsilon_{n\ell}|}\right) \approx \frac{T(\varepsilon_{n\ell}) - 1}{T(\varepsilon_{n\ell}) + 1},$$

together with equations (3.39) and (3.40) allows the phase shift to be written:

$$\delta_\ell(E) = \delta_\ell^{(0)}(E) + \tan^{-1}\frac{\Gamma_{n\ell}}{2(E_{n\ell}-E)} . \qquad (3.46)$$

Equation (3.46) is an expression of Breit-Wigner form,[8] and clearly demonstrates the increase of π in $\delta_\ell(E)$ on passing through a resonance. In a similar way for energies near the well minimum, equation (3.30) together with equations (3.42) and (3.43) may be reduced to the resonance form of equation (3.46).

From equation (3.46) the scattering amplitude, differential and total elastic cross sections may be written down.[8] If only a relatively small number of partial waves contribute to the scattering amplitude (3.3), it is possible to associate the special features observed in the differential cross section (3.7) with individual partial waves.[66] When a large number of partial waves contribute, the standard semiclassical techniques for the evaluation of the scattering amplitude cannot be used as these require $\delta_\ell(E)$ to be a slowly varying function of ℓ.[3]

The total elastic cross section (3.8) is given by:

$$\sigma(E) = \frac{4\pi}{k^2} \sum_{\ell}^{(2\ell+1)} \lambda \sin^2[\delta_\ell(E)], \qquad (3.47)$$

where

$$\sin^2\delta_\ell(E) = \frac{(E_{n\ell}-E)^2}{(E_{n\ell}-E)^2+(\Gamma_{n\ell}/2)^2} \sin^2\delta_\ell^{(0)} + \frac{(\Gamma_{n\ell}/2)^2}{(E_{n\ell}-E)^2+(\Gamma_{n\ell}/2)^2} \cos^2\delta_\ell^{(0)}$$

$$+ \frac{(\Gamma_{n\ell}/2)(E_{n\ell}-E)}{(E_{n\ell}-E)^2+(\Gamma_{n\ell}/2)^2} \sin 2\delta_\ell^{(0)}. \qquad (3.48)$$

Equation (3.48) shows that a resonance occurs for $E = E_{n\ell}$ and that the shape of the resonance is determined by the value of $\delta_\ell^{(0)}$. When $\delta_\ell^{(0)} = n\pi$ a large positive spike appears in the total cross section on passing through a resonance whilst for $\delta_\ell^{(0)} = (n+\frac{1}{2})\pi$ a large negative spike is present. For other values of $\delta_\ell^{(0)}$ both positive and negative contributions will be present.

The measured total cross section will not be that given by equations (3.47) and (3.48) because in an experimental determination there will be a certain energy spread ΔE with $\Delta E \gg \Gamma_{n\ell}$. The

measured total cross section $\Delta\sigma_\ell$ from a single resonance spanned by ΔE is:

$$\Delta\sigma_\ell = \frac{4\pi}{k^2}(2\ell+1)\frac{1}{\Delta E}\int_{E_{n\ell}-\Delta E/2}^{E_{n\ell}+\Delta E/2} \sin^2[\delta_\ell(E)]\,dE,$$

$$= \frac{4\pi}{k^2}(2\ell+1)\left[\sin^2\delta_\ell^{(0)} + \frac{\pi\Gamma_{n\ell}}{2\Delta E}\cos 2\delta_\ell^{(0)}\right], \qquad (3.49)$$

and the resonant behaviour of the cross section is now determined by the second term in equation (3.49).

Equation (3.49) has a bearing on a recent controversy concerning the correct classical limit for the three turning point problem.[65,67-69] Curtiss and Powers[67,68] derived an expression for the semi-classical phase shift (using a formalism based on the density of states) which indicated that in the classical limit there is a contribution from the classically inaccessible potential well region $a_\ell \ll r \ll c_\ell$ but that this contribution (as was pointed out by Barker and Johnson[69]) is independent of the height or shape of the barrier in the region $c_\ell \leqslant r \leqslant e_\ell$. This difficulty has been resolved by the work of Berry[65]. Berry points out that the phase

shift is not an observable quantity and that the correct procedure in passing to the classical limit is to take averages of observable quantities such as cross sections. When this done, the contributions of classically inaccessible regions to averages of observable quantities vanishes in the classical limit.[65] It is clear that the second term in equation (3.49) vanishes for $\hbar \to 0$ since, from equations (3.40) and (3.43) the width varies as $a\hbar \exp(-b/\hbar)$. This is also the case if equation (3.48) is averaged over many resonances (the level separation varies as $c\hbar$) so that the contribution from the potential well disappears in the classical limit.

As a general guide to the detection of the resonances, the strongest well-resolved resonances may be taken to have a width equal to the rotational constant $\hbar^2/2I_o$ of the collison complex because from equation (3.44), although resonances with low ℓ values would overlap, those with high ℓ values would be well resolved.[24]

The orbiting resonances will appear as additional structure superimposed on the glory oscillations of the total elastic cross section.[3] The glory oscillations arise because the partial wave summation for the

total cross section, equation (3.8) contains two ranges of l values for which δ_l is a slowly varying function[3]. Calculations of the total cross section using equation (3.8) together with phase shifts obtained by numerical integration of the radial wave equation have clearly shown the expected resonance effects.[66,70,71] The first experimental detection of these resonances (for the system H + Hg) has been reported by Stwalley, Niehaus and Herschbach.[71] However the resolution was poor and no detailed information could be deduced.

CHAPTER FOUR: REACTIVE MOLECULAR COLLISIONS - THREE DIMENSIONAL MODEL

4.1 INTRODUCTION

In this Chapter a tractable formalism is developed for the calculation of the differential and total elastic and reactive cross sections for the electronically adiabatic bimolecular exchange reaction:

$$A + BC \rightarrow AB + C. \qquad (4.1)$$

The model chosen to describe the reaction (4.1) is one in which the three atoms are at all times in their preferred configuration (which is taken to be linear) and with the whole system free to rotate in three dimensions. The restriction of B having an infinite mass that is present in an earlier model is removed.[24] This model does not take into account the effect of the BC rotations on the reaction. An approach to this problem for a two dimensional system is described in Chapter (6).

The plan of this Chapter is as follows. The hamiltonian for the system is derived in Section (4.2). An important feature in the development of the theory is the introduction of a mathematically meaningful reaction coordinate which varies in value

from $-\infty$ at the beginning of the reaction to $+\infty$ at the end. In Sections (4.3) and (4.4) it is shown how an adiabatic separation of variables reduces the scattering problem to the solution of a one dimensional Schrödinger equation for motion along the reaction coordinate. A semiclassical determination of the phase shifts and reflection and transmission coefficients that occur in the partial wave expansions for the elastic and reactive scattering amplitudes is the subject of Section (4.5). Semiclassical approximations for the partial wave summations are also considered.

The remainder of the Chapter is concerned with the calculation of the phase shifts,deflection functions and elastic and reactive cross sections for three types of potential surface. The three potential profiles along the reaction coordinate that are chosen are (1) a profile of lorentzian shape; this also includes the special case of a flat potential surface along the reaction coordinate. This form of barrier is chosen because the phase shifts,deflection functions and cross sections may be explicitly evaluated in terms of elliptic and related integrals. (2) a profile of downhill type.

(3) a modification of the Lennard-Jones potential so that the resulting profile contains both a well and a barrier. It is shown that at relatively low collision energies,this potential surface gives rise to two quadratic rainbows in the elastic scattering pattern and that as the collision energy increases these coalesce to form a cubic rainbow. Cubic rainbows have not apparently been considered before and they are considered both classically and semiclassically in this Chapter.

4.2 HAMILTONIAN AND BOUNDARY CONDITIONS

The masses of A,B,C in reaction (4.1) are taken to be m_A, m_B, m_C respectively with the distance A to B and B to C being r_A and r_C respectively. It will also be useful to define $\rho_A(\rho_C)$ as the distance of A(C) to the centre of mass of BC(AB):

$$\rho_A = r_A + \frac{m_C}{m_B + m_C} r_C ,$$

$$\rho_C = r_C + \frac{m_A}{m_A + m_B} r_A .$$

The classical kinetic energy T for this system (after removal of the centre of mass motion) is[72]:

$$T = T_t + T_r ,$$

where

$$2T_t = \frac{1}{M}\left[m_A(m_B+m_C)\dot{r}_A^2 + 2m_A m_C \dot{r}_A \dot{r}_C + m_C(m_A+m_B)\dot{r}_C^2\right], \qquad (4.2)$$

$$2T_r = I\left(\dot{\theta}^2 + \sin^2\theta\,\dot{\phi}^2\right), \qquad (4.3)$$

and the dots denote differentiation with respect to time. In equations (4.2) and (4.3), M is the total mass

of the system:

$$M = m_A + m_B + m_C,$$

and I is the moment of inertia of the complex about its centre of mass:

$$I = \frac{1}{M}\left[m_A(m_B+m_C)r_A^2 + 2m_A m_C r_A r_C + m_C(m_A+m_B)r_C^2\right].$$

Finally θ and ϕ are the polar angles that characterize the position of A. It is well known that scaling r_A and r_C together with a skewing of the coordinate axes removes the cross terms in equation (4.2) and that this is equivalent to writing the kinetic energy in terms of r_C and ρ_A (or r_A and ρ_C).[72] This is illustrated in Figure (6). The following relations are apparent from that Figure:

$$y = k_C r_C \sin\gamma,$$

$$x = k_A r_A + k_C r_C \cos\gamma,$$

where k_A and k_C are mass scaling factors. The values chosen for k_C and k_A are:

$$k_C = \left[\frac{m_C(m_A+m_B)}{M}\right]^{1/2},$$

Figure 6

The coordinate system.

The quantities r_A, r_C, k_A, k_C, x, y, α, and γ are defined in the text.

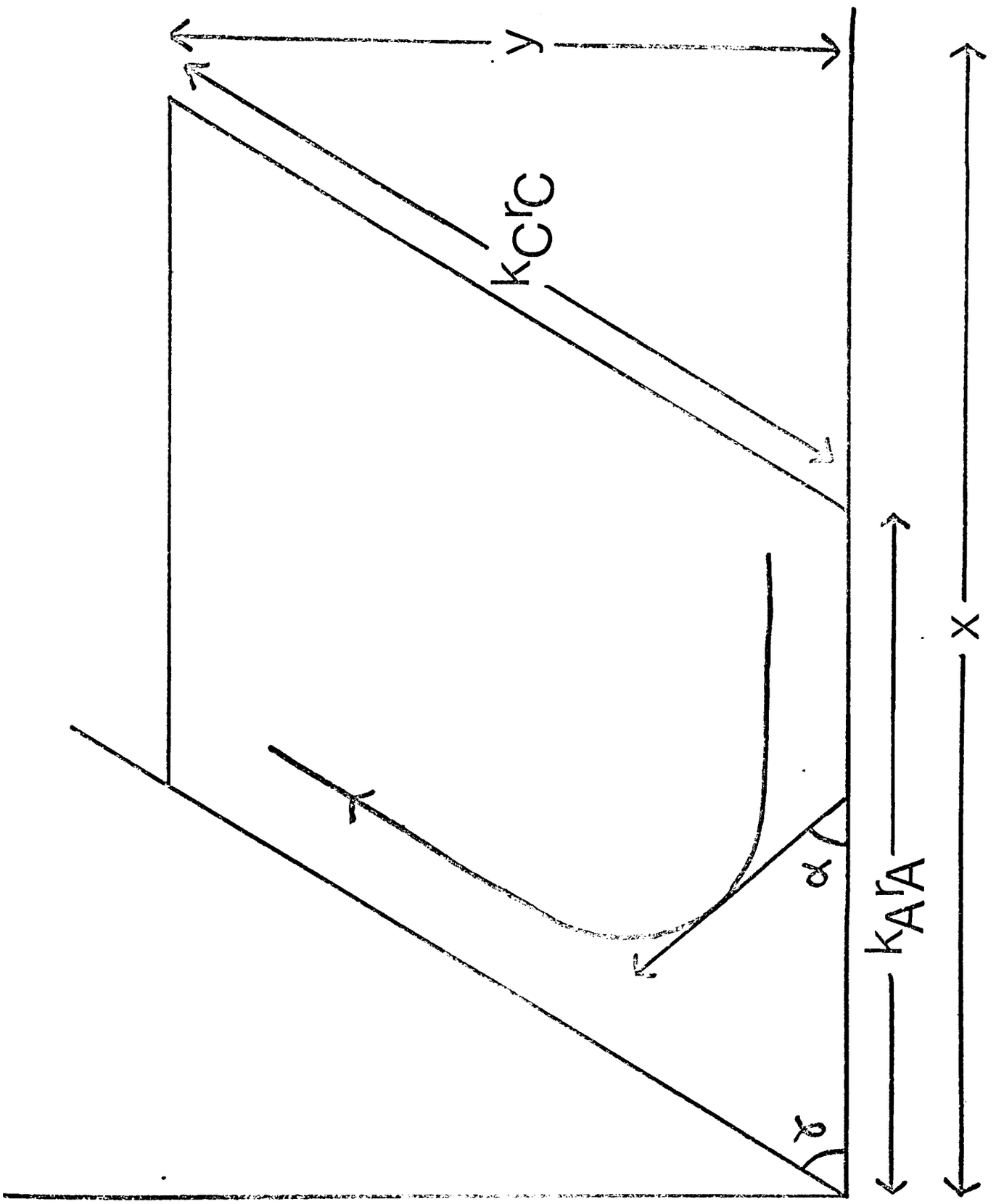
y
$k_C r_C$
$k_A r_A$
x
α
γ

$$k_A = \left[\frac{m_A(m_B+m_C)}{M}\right]^{1/2},$$

and γ is calculated from:

$$\tan\gamma = \left[\frac{m_B M}{m_A m_C}\right]^{1/2}.$$

For example $\gamma = 90^\circ$ if B is of infinite mass and $\gamma = 60^\circ$ if the three particles are of equal mass. In terms of r_C and ρ_A:

$$y = \left[\frac{m_B m_C}{m_B+m_C}\right]^{1/2} r_C,$$

$$x = \left[\frac{m_A(m_B+m_C)}{M}\right]^{1/2} \rho_A,$$

and the kinetic energy takes the simple form:

$$2T = \dot{x}^2 + \dot{y}^2 + (x^2+y^2)(\dot{\theta}^2 + \sin^2\theta\dot{\phi}^2).$$

Plots of the potential energy in the (x,y) space normally possess two valleys, one of which corresponds with the initially separated reactants and the other with the finally separated products. These valleys may be separated by one or more saddle points. If no saddle point is present the surface is of the

downhill (or uphill) type. Surfaces of the downhill type and those possessing one saddle point are considered in this Chapter; surfaces with two saddle points are treated in Chapter (5). The reaction path for the surface is defined as the path of minimal potential energy in passing from the reactants region to the products region. If it is assumed that the only energetically accessible regions of the surface are those close to the reaction path then it is useful to introduce two new coordinates: a reaction coordinate s and a vibrational coordinate v. If the tangent to the reaction path makes an acute angle α with the x coordinate (see Figure (6)) then s and v are defined by:[27]

$$\left.\begin{aligned} s &= -x\cos\alpha + y\sin\alpha , \\ v &= x\sin\alpha + y\cos\alpha . \end{aligned}\right\} \qquad (4.4)$$

At the beginning of the reaction $\alpha = 0$ and

$$s = -\left[\frac{m_A(m_B+m_C)}{M}\right]^{1/2}\rho_A ,$$

$$v = \left[\frac{m_B m_C}{m_B + m_C}\right]^{1/2} r_C ,$$

Thus initially s and v are proportional to the distance of A to the centre of mass of BC and the BC bond distance respectively, with mass weighting factors equal to the square roots of the reduced mass of the reactants and the BC molecule respectively. Near s = 0, that is in the central region of the potential where the three atoms are interacting strongly, s and v represent the asymmetric and symmetric stretching vibrations of the ABC complex respectively. Finally, at the end of the reaction where $\alpha = \pi - \gamma$:

$$s = \left[\frac{m_C(m_A + m_B)}{M}\right]^{1/2} \rho_C ,$$

$$v = \left[\frac{m_A m_B}{m_A + m_B}\right]^{1/2} r_A ,$$

so that s is proportional to the distance of C to the centre of mass of AB with mass weighting factor equaling the square root of the reduced mass of the products and v equals the AB bond distance multiplied by the square root of

the reduced mass of AB. The mass weighting factors therefore change as the reaction proceeds.

In terms of these natural collision coordinates the classical kinetic energy becomes:

$$2T_t = \dot{v}^2 + \dot{s}^2\left(1 + \kappa^2 s^2 - 2\frac{dv}{ds}\kappa s + 2\kappa v + \kappa^2 v^2\right), \qquad (4.5)$$

$$2T_r = (s^2+v^2)(\dot{\theta}^2 + \sin^2\theta\,\dot{\phi}^2),$$

where $\kappa(s) = -d\alpha/ds$ is the curvature of the reaction path at each s. Marcus[28] has derived for the kinetic energy of a linear collision:

$$2T_t = \dot{v}_M^2 + \dot{s}_M^2\left(1 - 2\kappa_M v_M + \kappa_M^2 v_M^2\right), \qquad (4.6)$$

where the subscript M indicates that the definition of s and v differ from those employed in equation (4.4). Comparing equation (4.5) with (4.6), it is seen that the two expressions are similar except for the curvature terms. These terms are neglected in what follows; their most important effect is to induce vibrational transitions as the system passes round the curved portion of the reaction path. The kinetic energy expression becomes:

$$2T = \dot{s}^2 + \dot{v}^2 + (s^2+v^2)(\dot{\theta}^2 + \sin^2\theta\,\dot{\phi}^2). \qquad (4.7)$$

In terms of the conjugate momenta $p_\alpha = \partial T/\partial \dot{q}_\alpha$ equation (4.7) becomes:

$$2T = p_s^2 + p_v^2 + \frac{1}{s^2+v^2} p_\theta^2 + \frac{1}{(s^2+v^2)\sin^2\theta} p_\phi^2, \qquad (4.8)$$

and the kinetic energy operator is now in a suitable form for quantization.

When the classical kinetic energy is given by:

$$2T = \sum_{ij} g^{ij} p_i p_j,$$

where g^{ij} is an element of the conjugate metric tensor, the corresponding quantum mechanical hamiltonian is given by:[73]

$$\mathcal{H} = -\frac{\hbar^2}{2} r^{-1/2} g^{1/4} \sum_i \frac{\partial}{\partial q_i} g^{-1/2} \sum_j g^{ij} \frac{\partial}{\partial q_j} g^{1/4} r^{1/2} + V, \qquad (4.9)$$

where V is the potential energy of the system, $g = \det(g^{ij})$, and the normalization volume element is $r\prod_i dq_i$.

In the first instance the choice made for r is $r = g^{-\frac{1}{2}}$, that is the volume element $(s^2+v^2)\sin\theta\,ds\,dv\,d\theta\,d\phi$

of mass weighted three dimensional space. From equations (4.8) and (4.9) the hamiltonian in this space is:

$$\mathcal{H} = -\frac{\hbar^2}{2}\left\{\frac{\partial^2}{\partial s^2} + \frac{2s}{s^2+v^2}\frac{\partial}{\partial s} + \frac{\partial^2}{\partial v^2} + \frac{2v}{s^2+v^2}\frac{\partial}{\partial v}\right\} + \frac{\hbar^2\hat{L}^2}{2(s^2+v^2)} + V(s,v),$$

where $\hbar^2\hat{L}^2$ is the total angular momentum operator:

$$\hat{L}^2 = -\frac{1}{\sin\theta}\frac{\partial}{\partial\theta}\sin\theta\frac{\partial}{\partial\theta} - \frac{1}{\sin^2\theta}\frac{\partial^2}{\partial\phi^2}.$$

The Schrödinger equation is:

$$\mathcal{H}\Psi = E\Psi,$$

with boundary conditions:

$$\left.\begin{aligned}\Psi(s,v,\theta) &\underset{s\to-\infty}{\sim} e^{-ik^{(-)}s\cos\theta}\xi_n(v) + \sum_{k^{(-)},n}\frac{e^{-ik^{(-)}s}}{(-s)}f^{(-)}(\theta)\xi_n(v),\\ &\underset{s\to+\infty}{\sim} \sum_{k^{(+)},n}\frac{e^{ik^{(+)}s}}{s}f^{(+)}(\theta)\xi_n(v).\end{aligned}\right\} \quad (4.10)$$

The first term in (4.10) represents the motion of A as an incoming plane wave moving in the z direction and with BC in the vibrational state n (with

eigenfunction $\xi_n(v)$). The second term corresponds with non-reactive elastic and inelastic scattering whilst the third term corresponds to reactive scattering (outgoing waves only). The notation used in (4.10) anticipates the further development of the theory where it will be shown that the scattering problem may be reduced to consideration of only two channels: an initial elastic channel and a final reactive channel (these will be denoted by a superscript (-) and (+) sign respectively). $f^{(-)}(\theta)$ and $f^{(+)}(\theta)$ are the respective scattering amplitudes and $k^{(-)}$ and $k^{(+)}$ are the initial and final mass reduced wave numbers. The summations in (4.10) must be consistent with the conservation of energy.

For the immediate development of the theory it is convenient to define a (non-physical) space with volume element $\sin\theta ds dv d\theta d\phi$. The hamiltonian in this space is (from equation (4.9)):

$$H = -\frac{\hbar^2}{2}\left\{\frac{\partial^2}{\partial s^2} + \frac{\partial^2}{\partial v^2}\right\} + \frac{\hbar^2(\hat{L}^2+1)}{2(s^2+v^2)} + V(s,v),$$

and the Schrödinger equation is:

$$H\psi = E\psi. \qquad (4.11)$$

Comparing the volume elements of these two spaces shows that:

$$\Phi = \psi (s^2 + v^2)^{-1/2}, \tag{4.12}$$

and this may be verified by direct substitution. From equations (4.10) and (4.12) the boundary condition on ψ becomes:

$$\left.\begin{aligned} \psi(s,v,\theta) &\underset{s\to-\infty}{\sim} (-s) e^{-ik^{(-)}s\cos\theta} \xi_n(v) + \sum_{k^{(-)},n} e^{-ik^{(-)}s} f^{(-)}(\theta) \xi_n(v), \\ &\underset{s\to+\infty}{\sim} \sum_{k^{(+)},n} e^{ik^{(+)}s} f^{(+)}(\theta) \xi_n(v). \end{aligned}\right\} \tag{4.13}$$

4.3 ADIABATIC SEPARATION OF VARIABLES

For many systems the purely vibrational motion of the atoms is much faster than the motion along the reaction coordinate, a circumstance which allows an adiabatic separation of variables to be carried out.[24]

The internal vibrational wavefunctions $\chi_n(s;v)$ at each s are defined by:

$$\left[-\frac{\hbar^2}{2}\frac{\partial^2}{\partial v^2} + V(s,v)\right]\chi_n(s;v) = V_n(s)\,\chi_n(s;v), \qquad (4.14)$$

where $V_n(s)$ is the internal vibrational energy and both $\chi_n(s;v)$ and $V_n(s)$ depend parametrically on s. For $s \to -\infty$ $(+\infty)$ $\chi_n(s;v)$ and $V_n(s)$ become the vibrational eigenfunctions and eigenvalues of the reactant (product) molecules respectively. An approximate solution of equation (4.14) is obtained by assuming that the displacement along v is small at each s so that V(s,v) may be taken to be quadratic in v: $\chi_n(s;v)$ and $V_n(s)$ are then harmonic oscillator eigenfunctions and eigenvalues respectively.

Since the $\chi_n(s;v)$ form a complete set of functions at each s, the total wavefunction may be expanded in

terms of them:

$$\psi(s,v,\theta) = \sum_n \psi_n(s,\theta)\xi_n(s;v) . \qquad (4.15)$$

Substituting the expansion (4.15) into the Schrödinger equation (4.11), multiplying by $\xi_n^*(s;v)$ and integrating over dv yields an equation obeyed by $\psi_n(s,\theta)$:

$$\left[-\frac{\hbar^2}{2}\frac{\partial^2}{\partial s^2} + V_n(s) + \frac{\hbar^2(\hat{L}^2+1)}{2(s^2+v_e^2)} - E\right]\psi_n(s,\theta) = \sum_{n'} C_{nn'}(s)\psi_{n'}(s,\theta), \qquad (4.16)$$

where

$$C_{nn'}(s) = \frac{\hbar^2}{2}\int \xi_n^*(s;v)\frac{\partial^2}{\partial s^2}\xi_{n'}(s;v)dv + \hbar^2\int \xi_n^*(s;v)\frac{\partial}{\partial s}\xi_{n'}(s;v)dv\frac{\partial}{\partial s},$$

and v_e is the equilibrium value of v. The terms $C_{nn'}(s)$ on the right hand side of equation (4.16) couple together different vibrational states of the system. Neglect of these terms means that the system always stays in the same vibrational state: the reaction is vibrationally adiabatic, and the expansion (4.15) then consists of a single term. The purpose of introducing natural collision coordinates is to minimize this coupling as far as possible. In many reactive systems it should be possible to treat the $C_{nn'}(s)$ terms as perturbations. However if different

vibrational states become strongly coupled as the reaction proceeds the above approach breaks down. With neglect of the coupling terms the equation for $\psi_n(s,\theta)$ simplifies to:

$$\left[-\frac{\hbar^2}{2}\frac{\partial^2}{\partial s^2} + V_n(s) + \frac{\hbar^2(\hat{L}^2+1)}{2(s^2+v_2^2)} - E\right]\psi_n(s,\theta) = 0, \qquad (4.17)$$

and from equations(4.13) and (4.15),the boundary condition for $\psi_n(s,\theta)$ becomes:

$$\left.\begin{aligned}\psi_n(s,\theta) \underset{s\to-\infty}{\sim} (-s)e^{-ik^{(-)}s\cos\theta} &+ e^{-ik^{(-)}s}f^{(-)}(\theta),\\ \underset{s\to+\infty}{\sim} & \; e^{ik^{(+)}s}f^{(+)}(\theta).\end{aligned}\right\} \qquad (4.18)$$

Only two channels therefore remain in the theory: an initial (elastic) channel and a final (reactive) channel.

4.4 PARTIAL WAVE ANALYSIS

The wavefunction $\psi_n(s,\theta)$ may be expanded as a sum over an infinite number of partial waves:

$$\psi_n(s,\theta) = \sum_{L=0}^{\infty} A_L S_{nL}(s) P_L(\cos\theta), \qquad (4.19)$$

where L is the total angular momentum quantum number and A_L is a constant to be chosen in accord with the boundary conditions (4.18). Substituting the expansion (4.19) into equation (4.17) gives an equation obeyed by $S_{nL}(s)$:

$$\left[\frac{d^2}{ds^2} + k_L^2(s)\right] S_{nL}(s) = 0, \qquad (4.20)$$

where

$$k_L^2(s) = \frac{2}{\hbar^2}\left[E - V_{nL}(s)\right],$$

and

$$V_{nL}(s) = V_n(s) + \frac{\hbar^2\left[L(L+1)+1\right]}{2(s^2+v_e^2)}. \qquad (4.21)$$

The effect of the potential barrier $V_{nL}(s)$ is to cause partial reflection and partial transmission

of the incident wave. Equation (4.21) shows explicitly that the barrier to reaction along the reaction coordinate has three contributions: (1) the potential energy barrier (if any) belonging to the original potential surface along the reaction coordinate, (2) the change in internal vibrational energy as a function of s. These two contributions are contained in the term $V_n(s)$, (3) the centrifugal potential associated with the conservation of angular momentum. It may also be noted that $k^{(\pm)} = k_L(\pm\infty)$. The boundary condition for $S_{nL}(s)$ is written in the form:

$$S_{nL}(s) \underset{s\to-\infty}{\sim} e^{ik^{(-)}s + i(L+1)\pi} + R_L e^{2i\delta_L^{(-)}} e^{-ik^{(-)}s}, \qquad \underset{s\to+\infty}{\sim} \left(\frac{k^{(-)}}{k^{(+)}}\right)^{1/2} T_L e^{2i\delta_L^{(+)}} e^{ik^{(+)}s}, \tag{4.22}$$

where the reflection coefficient R_L, transmission coefficient T_L and phase shifts $\delta_L^{(-)}$ and $\delta_L^{(+)}$ are all real quantities. The first term in (4.22) represents the phase of the incoming part of a plane wave:

$$(-s)e^{-ik^{(-)}s\cos\theta} \sim \frac{1}{2ik^{(-)}} \sum_L (2L+1)\left[e^{-ik^{(-)}s} + e^{i(L+1)\pi} e^{ik^{(-)}s}\right] P_L(\cos\theta). \tag{4.23}$$

The phases of the elastically and reactively scattered waves in (4.22) have been written in such a way as to bring out the similarity with pure elastic scattering from a central potential. The semiclassical determination of $R_L, T_L, \delta_L^{(-)}, \delta_L^{(+)}$ is the subject of the next section and also Chapter (5).

Substituting the partial wave expansion (4.19) into the boundary condition (4.22) and comparing with (4.18) (into which (4.23) has been substituted) it follows that:

$$A_L = \frac{(2L+1)}{2ik^{(-)}},$$

and that the elastic and reactive scattering amplitudes are given by:

$$f^{(-)}(\theta) = \frac{1}{2ik^{(-)}} \sum_L (2L+1)\left[R_L e^{2i\delta_L^{(-)}} - 1\right] P_L(\cos\theta), \qquad (4.24)$$

$$f^{(+)}(\theta) = \frac{1}{2i\left[k^{(-)}k^{(+)}\right]^{1/2}} \sum_L (2L+1)\, T_L e^{2i\delta_L^{(+)}} P_L(\cos\theta), \qquad (4.25)$$

From equation (4.24) the elastic differential cross section is given by:

$$I^{(-)}(\theta) = |f^{(-)}(\theta)|^2, \tag{4.26}$$

and the total elastic cross section is:

$$\sigma^{(-)} = 2\pi \int_0^{\pi} \sin\theta \, I^{(-)}(\theta) \, d\theta, \tag{4.27}$$

$$= \frac{\pi}{k^{(-)2}} \sum_L (2L+1)\left[4 R_L \sin^2\delta_L^{(-)} + (R_L - 1)^2\right]. \tag{4.28}$$

In a similar way, the reactive differential cross section is:

$$I^{(+)}(\theta) = \frac{k^{(+)}}{k^{(-)}} |f^{(+)}(\theta)|^2, \tag{4.29}$$

and the total reactive cross section is:

$$\sigma^{(+)} = 2\pi \int_0^{\pi} \sin\theta \, I^{(+)}(\theta) \, d\theta, \tag{4.30}$$

$$= \frac{\pi}{k^{(-)2}} \sum_L (2L+1) \, T_L^2. \tag{4.31}$$

When $R_L = 1$, $T_L = 0$ there is no contribution from the reactive scattering and equations (4.24) and (4.28) reduce to the pure elastic scattering case,

compare equations (3.3) and (3.8). When $R_L = 0$, $T_L = 1$ on the other hand, equations (4.28) and (4.31) show that the partial elastic and reactive cross sections $\sigma_L^{(\pm)}$ ($\sigma^{(\pm)} = \sum_L \sigma_L^{(\pm)}$) become equal and are of magnitude $\pi(2L+1)/k^{(-)2}$. This is in agreement with more formal results available in the literature.[74]

4.5 SEMICLASSICAL ANALYSIS

In this Section, semiclassical expressions are derived for the reflection coefficient R_L, transmission coefficient T_L, and the phase shifts $\delta_L^{(-)}$ and $\delta_L^{(+)}$ that occur in the partial wave expansions for the elastic and reactive scattering amplitudes (4.24) and (4.25). Since these partial wave expansions will typically involve many partial waves, semiclassical procedures analogous to those used in atom-atom scattering may be applied to the evaluation of $f^{(-)}(\theta)$ and $f^{(+)}(\theta)$. This is described in the latter part of this section.

The problem is first to find the semiclassical form of the elastically and reactively scattered waves in the boundary condition (4.22) given the form of the initial incoming wave.

In the first case it is assumed that $E \gg V_{nL}(s)$ in equation (4.20). The incoming wave in equation (4.22) may be written semiclassically as:

$$\left(\frac{k^{(-)}}{k_L(s)}\right)^{1/2} \exp\left\{ i\int_{-\infty}^{s} [k_L(s') - k^{(-)}]\, ds' \right\} e^{ik^{(-)}s + i(L+1)\pi}, \qquad (4.32)$$

an expression valid for all s. If $k^{(-)} = k^{(+)}$ the boundary condition (4.22) together with the expression (4.32) immediately give for the reactive phase shift and transmission coefficient:

$$2\delta_L^{(+)} = \int_{-\infty}^{\infty} [k_L(s) - k^{(-)}]\, ds + (L+1)\pi, \tag{4.33}$$

and

$$T_L = 1.$$

In this approximation there is no reflected wave; all the incoming wave is transmitted. When $k^{(-)} \neq k^{(+)}$ integrals of the type (4.33) no longer converge and one must proceed as follows. If b_L is an arbitrary phase reference point (a convenient choice is $b_L = 0$) then the wavefunction (4.32) may be written as:

$$\left(\frac{k^{(-)}}{k_L(s)}\right)^{1/2} \exp\left\{ i\int_{-\infty}^{b_L} [k_L(s) - k^{(-)}]\, ds + i\int_{b_L}^{s} [k_L(s') - k^{(+)}]\, ds' + i[k^{(-)} - k^{(+)}]b_L + i(L+1)\pi + ik^{(-)}s \right\}. \tag{4.34}$$

Taking the limit $s \to \infty$ in (4.34) and comparing with the boundary condition (4.22) leads to:

$$2\delta_L^{(+)} = \int_{-\infty}^{b_L} [k_L(s) - k^{(-)}]\, ds + \int_{b_L}^{\infty} [k_L(s) - k^{(+)}]\, ds + [k^{(-)} - k^{(+)}]b_L + (L+1)\pi, \tag{4.35}$$

and

$$T_L = 1.$$

Notice that the derivation given above does not make it necessary to assume any particular shape for $V_{nL}(s)$ (except that required for the validity of the semiclassical method).

In the second case considered in this Chapter, E is allowed to have any value relative to $V_{nL}(s)$ but $V_{nL}(s)$ is restricted to having a single maximum which is assumed to be approximately quadratic in s. This allows the use of connection formulae for a parabolic barrier to bridge the regions where the semiclassical solution (4.32) fails. The notation of Figure (1) will be used.

The incoming wave in the boundary condition (4.22) may be written semiclassically in terms of the turning point a_L (or b_L when $E > V_{nL}(b_L)$) as:

$$\left(\frac{k^{(-)}}{k_L(s)}\right)^{1/2} \exp\left\{ i\int_{-\infty}^{a_L} [k_L(s) - k^{(-)}]\,ds - i\int_{s}^{a_L} k_L(s')\,ds' + ik^{(-)}a_L + i(L+1)\pi \right\}, \qquad (4.36)$$

which is valid for $s \ll a_L$. The parabolic connection formulae (2.13) and (2.14) may be reexpressed in a form convenient for application to the expression (4.36) namely:

The incident wave:

$$\frac{1}{\sqrt{k_L(s)}} \exp\left\{ -i\int_s^{a_L} k_L(s')ds' \right\}, \tag{4.37}$$

valid for $s \ll a_L$ connects with the reflected wave:

$$\frac{1}{\sqrt{k_L(s)}} \exp\left\{ i\int_s^{a_L} k_L(s')ds' - i\phi(\varepsilon_L) - i\frac{\pi}{2} \right\} \left[1 + e^{2\pi\varepsilon_L}\right]^{-1/2}, \tag{4.38}$$

valid for $s \ll a_L$ and connects with the transmitted wave:

$$\frac{1}{\sqrt{k_L(s)}} \exp\left\{ i\int_{c_L}^{s} k_L(s')ds' - i\phi(\varepsilon_L) \right\} \left[1 + e^{-2\pi\varepsilon_L}\right]^{-1/2}, \tag{4.39}$$

valid for $s \gg c_L$. In the formulae (4.38) and (4.39):

$$\varepsilon_L = \frac{E - V_{nL}(b_L)}{\hbar\omega_L^*},$$

where ω_L^* is the classical angular frequency of oscillation in the upturned barrier. Applying the connection formula (4.37)-(4.39) to the incoming wave (4.36), taking the limit $s \to -\infty$ (or $+\infty$ as appropriate) and comparing with the boundary condition (4.22) gives:

$$2\delta_L^{(+)} = \int_{-\infty}^{a_L} [k_L(s) - k^{(-)}]\,ds + \int_{c_L}^{\infty} [k_L(s) - k^{(+)}]\,ds + k^{(-)}a_L - k^{(+)}c_L - \phi(\varepsilon_L) + (L+1)\pi, \qquad (4.40)$$

$$2\delta_L^{(-)} = 2\int_{-\infty}^{a_L} [k_L(s) - k^{(-)}]\,ds + 2k^{(-)}a_L - \phi(\varepsilon_L) + (L+\tfrac{1}{2})\pi, \qquad (4.41)$$

$$T_L = [1 + e^{-2\pi\varepsilon_L}]^{-1/2}, \qquad (4.42)$$

$$R_L = [1 + e^{2\pi\varepsilon_L}]^{-1/2}. \qquad (4.43)$$

In the limit $T_L \to 1$ the expression (4.40) goes over to the phase shift (4.35) already derived whilst in the limit $R_L \to 1$, the expression (4.41) becomes equivalent to the phase shift based on a linear turning point, equation (3.20). Equations (4.40)-(4.43) may therefore be considered valid for all energies. From the discussion of Section (3.2) it is clear that the singular contribution to the phase integrals in equations (4.40) and (4.41) is exactly cancelled by the quantum correction function $\phi(\varepsilon_L)$. The numerical evaluation

of $\delta_L^{(+)}$ and $\delta_L^{(-)}$ is considered in the next section. Plots of $\delta_L^{(\pm)}$ for the potential profiles shown in Figure (7) are illustrated in Figures (8)-(10).

Since, in a typical case, many partial waves will contribute to the scattering, semiclassical techniques similar to those used in elastic scattering from a central potential may be used to evaluate the elastic and reactive scattering amplitudes (4.24) and (4.25).[3,75] The deflection function $\Theta^{(\pm)} = 2\partial\delta_L^{(\pm)}/\partial L$ plays an important role in the analysis as is shown below.

The first case considered is the elastic scattering amplitude $f^{(-)}(\theta)$. For angles $\theta \neq 0$:

$$\sum_L (2L+1) P_L(\cos\theta) = 0,$$

so that equation (4.24) becomes:

$$f^{(-)}(\theta) = \frac{1}{2ik^{(-)}} \sum_L (2L+1) R_L e^{2i\delta_L^{(-)}} P_L(\cos\theta). \qquad (4.44)$$

The following four approximations are now introduced into equation (4.44):[3,75] (1) $\delta_L^{(-)}$ is replaced by its semiclassical value, equation (4.41) (2) $P_L(\cos\theta)$ is replaced by its asymptotic value valid for $\sin\theta > 1/L$:

$$P_L(\cos\theta) \sim \left[\frac{2}{\pi(L+\tfrac{1}{2})\sin\theta}\right]^{1/2} \sin\left[(L+\tfrac{1}{2})\theta + \frac{\pi}{4}\right]. \qquad (4.45)$$

(3) the summation is replaced by an integration.

Equation (4.44) then becomes:

$$f^{(-)}(\theta) = \frac{-1}{K^{(-)}(2\pi\sin\theta)^{1/2}} \int_0^\infty dL\, R_L (L+\tfrac{1}{2})^{1/2} \left[e^{i\Phi_+(L)} - e^{i\Phi_-(L)}\right], \qquad (4.46)$$

where

$$\Phi_\pm(L) = 2\delta_L^{(-)} \pm (L+\tfrac{1}{2})\theta \pm \pi/4 .$$

The final approximation is (4) that the integral (4.46) may be evaluated by the method of stationary phase. The stationary points of the integrand are when $\partial\Phi_\pm(L)/\partial L = 0$ which leads to $\Theta^{(-)} = 2\partial\delta_L^{(-)}/\partial L$ where $\Theta^{(-)}$ is the elastic deflection function. $\Theta^{(-)}$ takes values from π to $-\infty$ and is to be distinguished from the scattering angle which (by convention) lies in the range $0 \leqslant \theta \leqslant \pi$. A similar analysis using the reactive scattering amplitude (4.25) results in $\Theta^{(+)} = 2\partial\delta_L^{(+)}/\partial L$. The overall result applicable to both elastic and reactive scattering may therefore be expressed as the semiclassical equivalence relationship:

$$\Theta^{(\pm)} = 2\frac{\partial \delta_L^{(\pm)}}{\partial L}, \qquad (4.47)$$

Section (4.7) is devoted to the numerical evaluation of $\Theta^{(\pm)}$ and typical plots for $\Theta^{(\pm)}$ are shown in Figures (11)-(15).

The scattering amplitude $f^{(-)}(\theta)$ may be further simplified by expanding $\Theta^{(-)}$ as a Taylor series:

$$\Theta^{(-)} = -\theta_1 + a(L-L_1) + q(L-L_1)^2 + c(L-L_1)^3 + \dots, \qquad (4.48)$$

where

$$a = \left.\frac{d\Theta^{(-)}}{dL}\right|_{L=L_1}, \quad q = \frac{1}{2}\left.\frac{d^2\Theta^{(-)}}{dL^2}\right|_{L=L_1}, \quad c = \frac{1}{6}\left.\frac{d^3\Theta^{(-)}}{dL^3}\right|_{L=L_1}.$$

For example if a = c = 0, then $\Theta^{(-)}$ possesses a maximum or a minimum (see Figures (12),(13) and (15)) whilst if a = q = 0, $\Theta^{(-)}$ possesses a point of inflection (see Figure (13)). From the semiclassical equivalence relationship (4.47),the phase shift is given by:

$$2\delta_L^{(-)} = 2\delta_1^{(-)} - \theta_1(L-L_1) + \frac{q}{2}(L-L_1)^2 + \frac{c}{3}(L-L_1)^3 + \frac{c}{4}(L-L_1)^4.$$

For the elastic deflection function,the region of of stationary phase is contained in the $\Phi_+(L)$ term

of equation (4.46) so that the elastic scattering amplitude becomes:

$$f^{(-)}(\theta) = \frac{-(L_1+\frac{1}{2})^{1/2} R_{L_1}}{k^{(-)}(2\pi \sin\theta)^{1/2}} \exp\left\{i\left[2\delta_1^{(-)} + (L_1+\tfrac{1}{2})\theta + \frac{\pi}{4}\right]\right\}$$

$$\times \int_{-\infty}^{\infty} du \exp\left\{i\left[(\theta-\theta_1)u + \frac{a}{2}u^2 + \frac{c}{3}u^3 + \frac{e}{4}u^4\right]\right\}, \qquad (4.49)$$

where $u = L-L_1$ and the lower limit of the integral has been extended to $-\infty$.

The simplest approximation that may be introduced into equations (4.48) and (4.49) is to set $q = c = 0$. The integral in equation (4.49) reduces to a Fresnel integral and the elastic differential cross section, equation (4.26) takes the simple form:

$$I^{(-)}(\theta)\sin\theta = \frac{(L_1+\frac{1}{2})R_{L_1}^2}{k^{(-)2}\left|\frac{d\Theta^{(-)}}{dL}\right|_{\Theta^{(-)}=\theta}} . \qquad (4.50)$$

Although derived for $\Theta^{(-)} < 0$, equation (4.50) is also valid for $\Theta^{(-)} > 0$. In a similar way the reactive differential cross section is given by (via equation (4.29)):

$$I^{(+)}(\theta)\sin\theta = \frac{(L_1+\frac{1}{2})\,T_{L_1}^{2}}{k^{(-)2}\left|\frac{d\Theta^{(+)}}{dL}\right|_{\Theta^{(+)}=\theta}} . \qquad (4.51)$$

Equations (4.50) and (4.51) are essentially the classical expressions for the differential cross sections. A rainbow occurs when $d\Theta^{(\pm)}/dL = 0$ and the classical cross sections (4.50) and (4.51) then become infinite. In a semiclassical analysis the classical singularities are replaced by finite peaks (see below).

When the elastic or reactive deflection functions possess more than one branch (that is when the scattering at a given Θ has a contribution from more than one impact parameter $b = (L+\frac{1}{2})/k^{(-)}$, it is necessary to sum equations (4.50) and (4.51) over the various branches:[3,75]

$$I^{(\pm)}(\theta) = \sum_{j=1}^{N} I_j^{(\pm)}(\theta) ,$$

where j labels the particular branch and N is the number of branches. Semiclassically there is interference between the branches as may be seen by writing the scattering amplitude in the form:

$$f^{(\pm)}(\theta) = \sum_{j=1}^{N} [I_j^{(\pm)}(\theta)]^{1/2} \exp[i\gamma_j^{(\pm)}], \qquad (4.52)$$

which is valid when the branches are well separated. $\gamma_j^{(\pm)}$ is a phase factor in equation (4.52).

The semiclassical analysis also allows for interference between branches of the deflection function which are not well separated.

Suppose in the first example $\Theta^{(-)}$ possesses a minimum (see Figures (12),(13) and (15)) so that:

$$\Theta^{(-)} = -\theta_n + q_n(L-L_n)^2, \quad q_n > 0, \qquad (4.53)$$

From equation (4.49) and (4.26),the differential cross section is:[75]

$$I^{(-)}(\theta)\sin\theta = \frac{R_{L_n}^2 (L_n+\frac{1}{2})}{k^{(-)2}} \cdot \frac{2\pi}{q_n^{2/3}} Ai^2\left(\frac{\theta-\theta_n}{q_n^{1/3}}\right), \qquad (4.54)$$

where Ai(x) is the Airy integral:

$$Ai(x) = \frac{1}{2\pi}\int_{-\infty}^{\infty} \exp\left(ixu + i\frac{u^3}{3}\right) du .$$

The corresponding classical result is from equation (4.50):

$$I^{(-)}(\theta)\sin\theta = \frac{R_{L_n}^2 (L_n+\frac{1}{2})}{k^{(-)2}} \frac{1}{2[q_n(\theta_n-\theta)]^{1/2}}, \quad \theta<\theta_n,$$
$$= 0, \quad \theta>\theta_n, \qquad (4.55)$$

assuming that no other branches contribute. The minimum corresponds to a 'negative' rainbow in the sense that in the angular distribution, intensity is focused into angles smaller than the extremum angle.[76,77] The dark side of this rainbow faces large angles and the bright side faces small angles (see Figures (21)-(23) and (25)).

$\Theta^{(-)}$ may also possess a maximum (see Figures (12) and (13)) so that in this case:

$$\Theta^{(-)} = -\theta_p - q_p(L-L_p)^2, \quad q_p>0, \qquad (4.56)$$

and following the derivation of equation (4.54), the semiclassical expression for the cross section is:

$$I^{(-)}(\theta)\sin\theta = \frac{R_{L_p}^2 (L_p+\frac{1}{2})}{k^{(-)2}} \cdot \frac{2\pi}{q_p^{4/3}} \cdot Ai^2\left(\frac{\theta_p-\theta}{q_p^{1/3}}\right), \qquad (4.57)$$

whilst from equations (4.50) and (4.56) the classical result is:

$$I^{(-)}(\theta)\sin\theta = \frac{R_{Lp}^2(L_p+\frac{1}{2})}{k^{(-)2}} \cdot \frac{1}{2[q_p(\theta-\theta_p)]^{1/2}}, \qquad \theta > \theta_p,$$

$$= 0 \qquad \theta < \theta_p. \qquad (4.58)$$

The rainbow corresponding to equations (4.57) and (4.58) is of 'positive' type since in the angular distribution, intensity is focused into angles larger than the extremum angle and the dark side faces small angles and the bright side large angles[76,77] (see Figures (21)-(23)).

Figure (13) shows that it is also necessary to consider a cubic variation of $\Theta^{(-)}$ with L:

$$\Theta^{(-)} = -\theta_c + c(L-L_c)^3, \qquad c > 0, \qquad (4.59)$$

This gives rise to a 'cubic' rainbow as opposed to the 'quadratic' rainbows of equations (4.53) and (4.56). Cubic rainbows have not been considered before either classically or semiclassically. From equation (4.49) the scattering amplitude is given by:

$$f^{(-)}(\theta) = \left[-(L_c+\tfrac{1}{2})^{1/2} R_{L_c} \exp\left\{i\left[2\delta_c^{(-)} + (L_c+\tfrac{1}{2})\theta + \tfrac{\pi}{4}\right]\right\}\right] \Big/ k^{(-)}(2\pi \sin\theta)^{1/2}$$

$$\times \left(\frac{2}{c^{1/2}}\right)^{1/2} C\left(\frac{\sqrt{2}\,(\theta-\theta_c)}{c^{1/4}}\right), \qquad (4.60)$$

where C(a) denotes the integral:

$$C(a) = \int_{-\infty}^{\infty} e^{i[ax+x^4]}\,dx\,. \qquad (4.61)$$

The integral in (4.61) therefore plays an analogous role to the Airy integral in the quadratic case, equations (4.54) and (4.57). The properties of C(a) together with its numerical evaluation are described in Appendix (A). From equation (4.60) the differential cross section is given by:

$$I^{(-)}(\theta)\sin\theta = \frac{R_{L_c}^2 (L_c+\tfrac{1}{2})}{k^{(-)2}} \cdot \frac{1}{\pi c^{1/2}} \left| C\left(\frac{\sqrt{2}\,(\theta-\theta_c)}{c^{1/4}}\right)\right|^2. \qquad (4.62)$$

The classical differential cross section for the deflection function (4.59) is from equation (4.50):

$$I^{(-)}(\theta)\sin\theta = \frac{R_{L_c}^2 (L_c+\frac{1}{2})}{K^{(-)2}} \cdot \frac{1}{3[c(\theta-\theta_c)^2]^{1/3}}, \qquad (4.63)$$

for both $\theta < \theta_c$ and $\theta > \theta_c$. If the integral C(a) in equation (4.62) is replaced by its asymptotic representation, equation (A5), the classical expression (4.63) is obtained. As in the case of the quadratic rainbow the classical infinity is replaced by a finite peak (see Figure (24)).

4.6 PHASE SHIFTS

This Section is devoted to the numerical evaluation of the phase shifts $\delta_L^{(+)}$ and $\delta_L^{(-)}$ that are defined by equations (4.40) and (4.41) respectively. Three potential energy profiles are chosen for the potential function $V_n(s)$.

The first potential barrier that is considered is one of lorentzian shape:

$$V_n(s) = \frac{H\hbar^2}{2(s^2+\sigma_2^2)}. \qquad (4.64)$$

This also includes the special case of a flat potential profile along the reaction coordinate by setting H = 0. The form of equation (4.64) is chosen because the phase integrals in equations (4.40) and (4.41) may be evaluated explicitly in terms of elliptic and related integrals. The remaining two choices require numerical methods for the evaluation of $\delta_L^{(+)}$ and $\delta_L^{(-)}$.

The second potential profile that is chosen is one of downhill type:

$$V_n(s) = -\varepsilon\left[1 + \tanh(s/A)\right], \qquad (4.65)$$

and the third choice is a modification of the

the Lennard-Jones (12,6) potential.

$$V_n(s) = \varepsilon\left[\frac{1}{1+(s/A)^{12}} - \frac{3(s/A)^2}{1+(s/A)^8}\right], \qquad (4.66)$$

The potential (4.66) possesses both a well and a barrier, varies as s^2 for small s and falls off as s^{-6} for large s. The potentials (4.64)-(4.66) are shown in Figure (7) plotted in terms of reduced variables. Also shown is the potential

$$V_n(s) = \varepsilon\left[e^{20(0.8+(s/A))} + \frac{1}{1+(s/A)^{12}} - \frac{3(s/A)^2}{1+(s/A)^8}\right], \quad s<0, \qquad (4.67)$$

which is the modified Lennard-Jones potential (4.66) to which a steeply repulsive contribution has been added. This potential is used later on to assess the extent to which deviations from the elastic differential cross section calculated from equation (4.67) can be attributed to reaction.

The potentials (4.64) and (4.66) are even in s so that $\delta_L^{(+)}$ and $\delta_L^{(-)}$ as given by equations (4.40) and (4.41) may be simplified:

$$\delta_L^{(-)} = \lim_{s\to\infty}\left\{\int_{c_L}^{s} k_L(s')ds' - k^{(-)}s\right\} - \tfrac{1}{2}\phi(\varepsilon_L) + (L+\tfrac{1}{2})\tfrac{\pi}{2}, \qquad (4.68)$$

$$\delta_L^{(+)} = \delta_L^{(-)} + \frac{\pi}{4}. \qquad (4.69)$$

Figure 7

The potential energy profiles (4.64) - (4.67) plotted in reduced units.

The solid line is the function:

$$V^*(x) = \frac{1}{1+x^{12}} - \frac{3x^2}{1+x^8} .$$

The dotted line is the function:

$$V^*(x) = e^{20[0.8+x]} + \frac{1}{1+x^{12}} - \frac{3x^2}{1+x^8} , \qquad x < 0 .$$

The dashed line is the function:

$$V^*(x) = \frac{1}{1+x^2} .$$

The dot-dash line is the function:

$$V^*(x) = -1 - \tanh x .$$

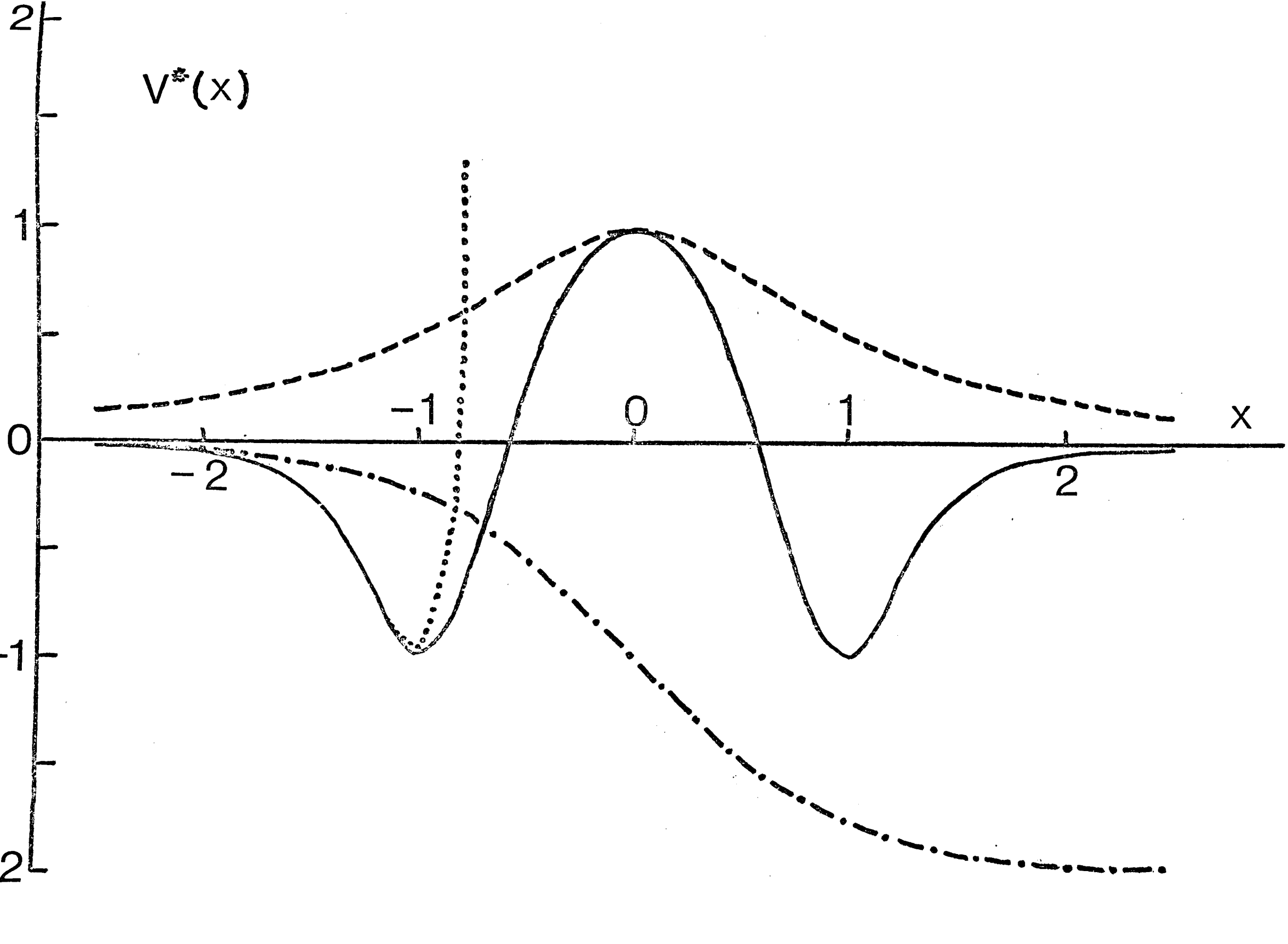
V*(x)
2
1
0
-1
-2
-2
-1
0
1
2
x

For these potentials it is therefore only necessary to calculate $\delta_L^{(-)}$ (say) as $\delta_L^{(+)}$ may be obtained from equation (4.69). If a classical cutoff is assumed in the angular momentum quantum number (L_0), only values of $L > L_0$ will determine the elastic scattering and likewise for the reactive scattering, only values for $L < L_0$ need be considered (see below).

For the lorentzian potential (4.64), the effective wave number is given by:

$$k_L^2(s) = k^{(-)2} - B_L/(s^2 + v_e^2), \tag{4.70}$$

where

$$B_L = H + L(L+1) + 1,$$

so that manipulation of the phase integral in equation (4.68) and the expression (4.70) allows $\delta_L^{(-)}$ to be expressed in terms of elliptic and related integrals. The result is:

$$\delta_L^{(-)} = -B_L^{1/2} \underset{\sim}{E}\left(k^{(-)}v_e/B_L^{1/2}\right) - \tfrac{1}{2}\phi(\varepsilon_L) + (L+\tfrac{1}{2})\tfrac{\pi}{2}, \tag{4.71}$$

when $k^{(+)}v_e < B_L^{1/2}$ and

$$\delta_L^{(-)} = -\frac{B_L}{k^{(-)}v_e} \underset{\sim}{B}\left(B_L^{1/2}/k^{(-)}v_e\right) - \tfrac{1}{2}\phi(\varepsilon_L) + (L+\tfrac{1}{2})\tfrac{\pi}{2}, \tag{4.72}$$

when $k^{(-)}v_e > B_L^{1/2}$ and $\underset{\sim}{E}$ and $\underset{\sim}{B}$ are the functions defined (and tabulated) by Jahnke and Emde.[78] From equation (2.23), ξ_L may also be evaluated in terms of elliptic integrals.

For the potentials (4.65) and (4.66), the phase integrals in equations (4.40) and (4.41) cannot be evaluated in terms of known functions and numerical methods must be used. However existing methods for the numerical evaluation of the phase integrals in (4.40) and (4.41) become inefficient as the turning points approach zero and break down altogether if $a_L = 0$, for example. To overcome this difficulty a scaled version of the Clenshaw-Curtis method recommended by Kennedy and Smith[79] was developed. The details of this procedure are given in Appendix (A).

Figures (8)-(10) show the results of the phase shift calculations for the potential (4.64)-(4.66) at several collision energies. The values chosen for the parameters occuring in the potentials are given in the Figure captions as are the classical cutoff values of the orbital angular momentum quantum number (the cutoffs are represented by arrows on the graphs). The choice of parameters is governed by

Figure 8

The elastic phase shift $\delta_L^{(c)}$ for the lorentzian potential (4.64).
The values of the parameters in equation (4.64) are H = 199.25, v_e = 10 Å amu$^{\frac{1}{2}}$.
The classical cutoff values are L_o = 47.5, 68.1, 98.5 for $k^{(c)}$(Å^{-1} amu$^{-\frac{1}{2}}$) = 5, 7, 10 respectively.

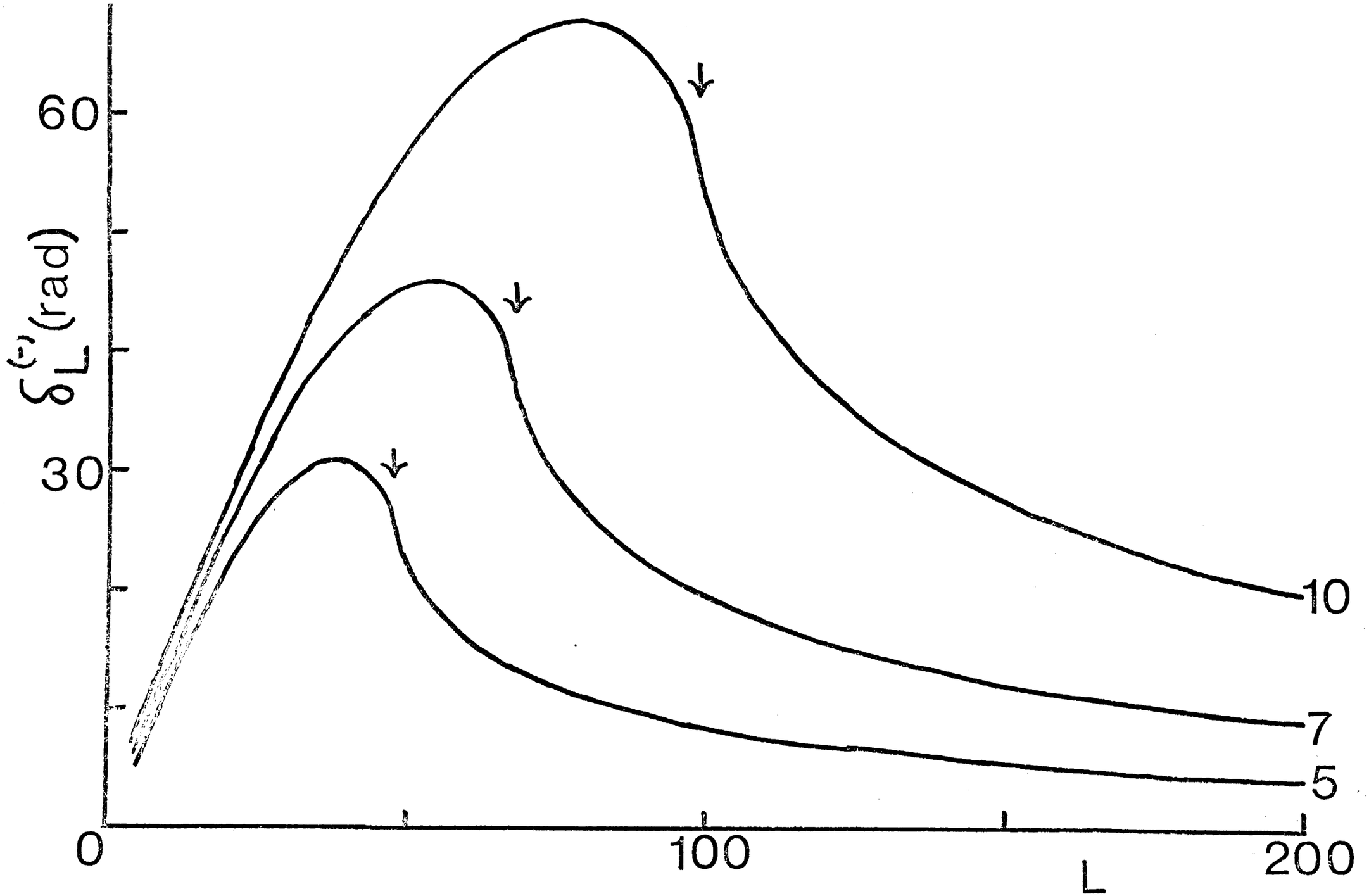
60
30
0
$\delta_L^{(\nu)}$(rad)
100
200
L
10
7
5

Figure 9

The elastic phase shift $\delta_L^{(-)}$ for the modified Lennard-Jones potential (4.66).

The values of the parameters in equation (4.66) are A = 9.487 Å $amu^{\frac{1}{2}}$, ε = 0.25 kcal $mole^{-1}$, v_e = 10 Å $amu^{\frac{1}{2}}$. The classical cutcffs are for L_o = 32.3, 44.0, 55.0, 65.7, 76.2, 86.5 for $k^{(-)}(Å^{-1}\ amu^{-\frac{1}{2}})$ = 4, 5, 6, 7, 8, 9 respectively.

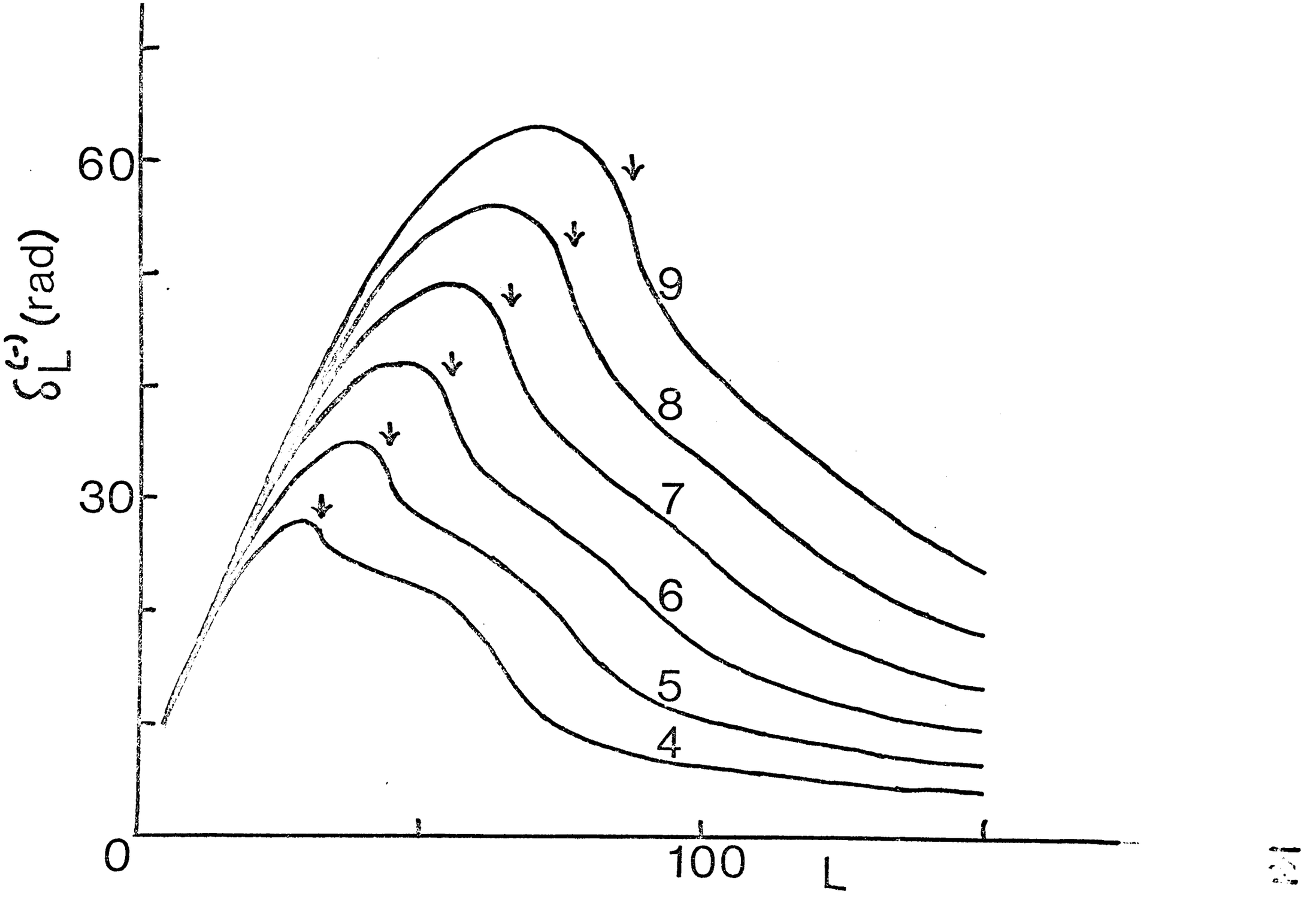
60
30
0
$\delta_L^{(-)}$ (rad)
100
L
9
8
7
6
5
4

Figure 10

The phase shift for the downhill potential (4.65). The values of the parameters in equation (4.65) are $A = 1.581$ Å amu$^{\frac{1}{2}}$, $\varepsilon = 5.0$ kcal mole^{-1}, $v_e = 10$ Å amu$^{\frac{1}{2}}$. The classical cutoffs occur at $L_o = 54.7, 75.5, 96.1$ for $k^{(4)}$(Å^{-1} amu$^{-\frac{1}{2}}$) = 5, 7, 9 respectively. $\delta_L^{(4)} - \pi/4$ is plotted for $L < L_o$ and $\delta_L^{(4)}$ for $L > L_o$.

phase shift (rad)
60
30
5
100
200
L
9
7
5

necessity for inclusion of sufficient partial waves to allow semiclassical analysis, without introducing an excessive computational burden. The term in $\phi(\varepsilon_L)$ has been neglected in calculating the phase shifts since it is only of significance for two or three partial waves and is very small in magnitude; the slopes of the phase shifts are therefore infinite at the classical cutoffs. Likewise, the reflection (transmission) coefficient changes in value from 0 to 1 (1 to 0) over two or three partial waves and has been replaced by its classical value. For the lorentzian and modified Lennard-Jones potentials, $\delta_L^{(-)}$ is plotted against L whilst for the downhill potential (4.65), $\delta_L^{(+)} - \pi/4$ is plotted for $L < L_o$ and $\delta_L^{(-)}$ for $L > L_o$.

The phase shifts for all three potentials are seen to be positive; the potentials (4.64)-(4.66) may therefore be described as attractive.[8] Considering first the phase shifts that contribute to the reactive scattering (that is the region to the left of the arrows in the Figures), it is seen that each one possesses a maximum. In the differential cross section this gives rise to a glory since the deflection function, equation (4.47) is then zero. Comparing

Figure (8) with Figure (9) shows that the well of the modified Lennard-Jones potential (4.66) has had little effect on the reactive scattering. The downhill potential gives rise to phase shifts whose maxima are closer to the classical cutoffs than is the case for the other two potentials.

The presence of a well for the potential (4.66) has a more dramatic effect on the elastic scattering (that is the region to the right of the arrows in the Figures). At small values of $k^{(-)}$ the elastic phase shift clearly possesses two points of inflection whereas this behaviour is absent for the potentials (4.64) and (4.65). In this region, Figure (9) shows that there is a range of L values for which $\delta_L^{(-)}$ is relatively slowly varying (in addition to the region of large L). It is therefore conceivable that the total elastic cross section will possess an oscillatory structure similar to the glory oscillations observed in the elastic scattering of two atoms.[3] In the atom-atom case however the oscillations arise because the phase shift possesses a maximum rather than a point of inflection.

4.7 DEFLECTION FUNCTION

This Section is devoted to the numerical evaluation of the delection function $\Theta^{(\pm)}$ defined by the semiclassical equivalence relationship (4.47) for the three potentials introduced in Section (4.6). Since $\delta_L^{(+)}$ and $\delta_L^{(-)}$ are not considered for L values which overlap in what follows, there will be no ambiguity in dropping the $(\mp)$ superscripts from $\Theta^{(\pm)}$ when it is convenient to do so. Recalling the semiclassical definition of $\delta_L^{(\pm)}$, equations (4.40) and (4.41), it follows that equation (4.47) is equivalent to:

$$\Theta^{(+)} = \pi - (L+\tfrac{1}{2})\int_{-\infty}^{a_L} \frac{ds}{(s^2+v_\infty^2)k_L(s)} - (L+\tfrac{1}{2})\int_{c_L}^{\infty} \frac{ds}{(s^2+v_\infty^2)k_L(s)} - \frac{\partial\phi(\epsilon_L)}{\partial L}, \quad (4.73)$$

$$\Theta^{(-)} = \pi - 2(L+\tfrac{1}{2})\int_{-\infty}^{a_L} \frac{ds}{(s^2+v_\infty^2)k_L(s)} - \frac{\partial\phi(\epsilon_L)}{\partial L}. \quad (4.74)$$

Figures (11)-(14) show graphs of Θ against L for the potentials defined in Section (4.6). The terms $\partial\phi(\epsilon_L)/\partial L$ have been neglected in the calculation; they are only important for two or three partial waves and in this region $\Theta^{(+)} + \partial\phi(\epsilon_L)/\partial L$ is large.

Figure 11

The deflection function for the lorentzian potential (4.64). The values of the parameters chosen for this potential are given in the caption to Figure (8).

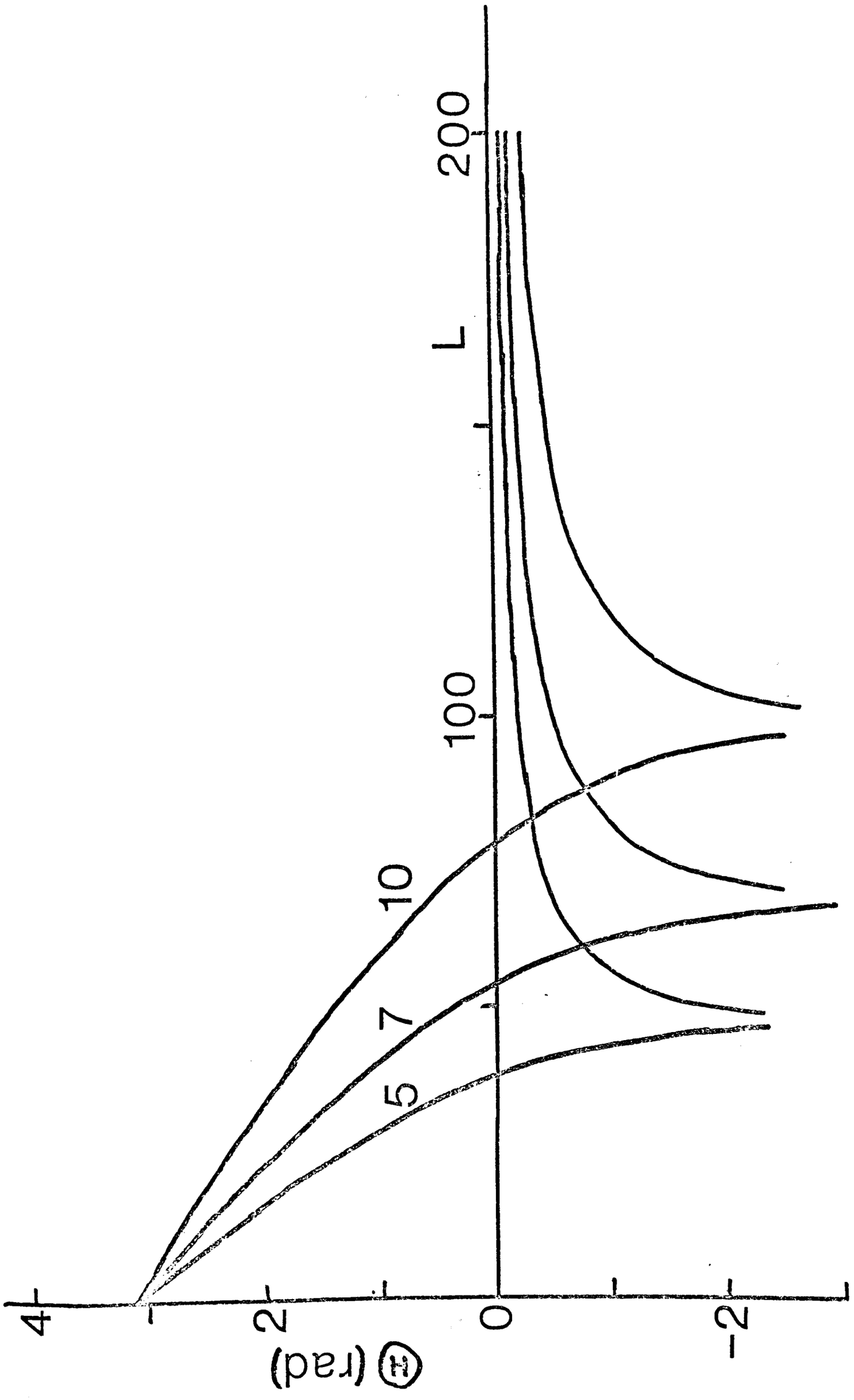
200
L
100
10
7
5
1
4
2
0
-2
Θ (rad)

Figure 12

The deflection function for the modified Lennard-Jones potential (4.66). The values of the parameters chosen for this potential are given in the caption to Figure (9).

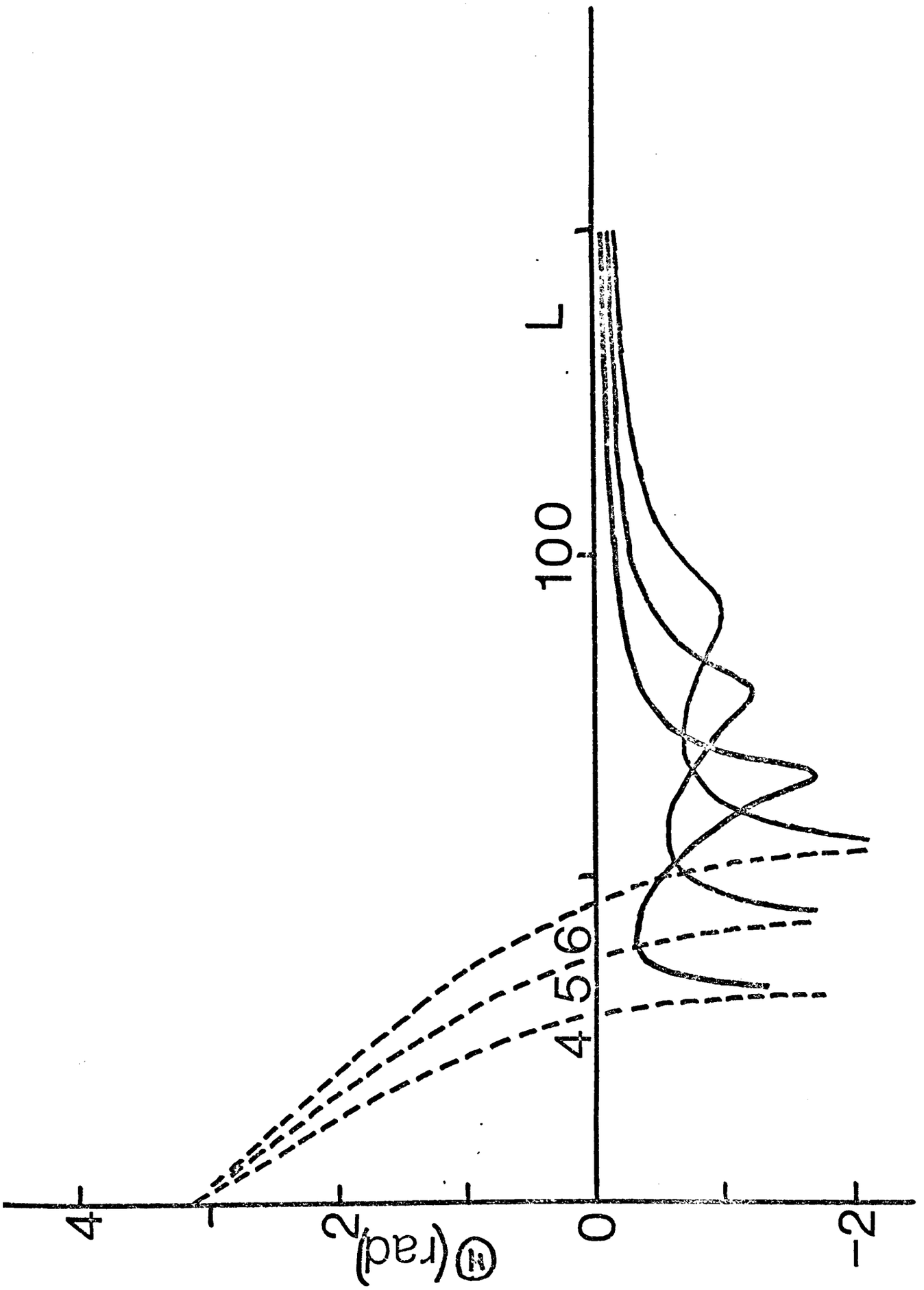
L
100
1
4
5
6
4
2
0
2
Θ(rad)

Figure 13

The deflection function for the modified Lennard-Jones potential (4.66). The values of the parameters chosen for this potential are given in the caption to Figure (9).

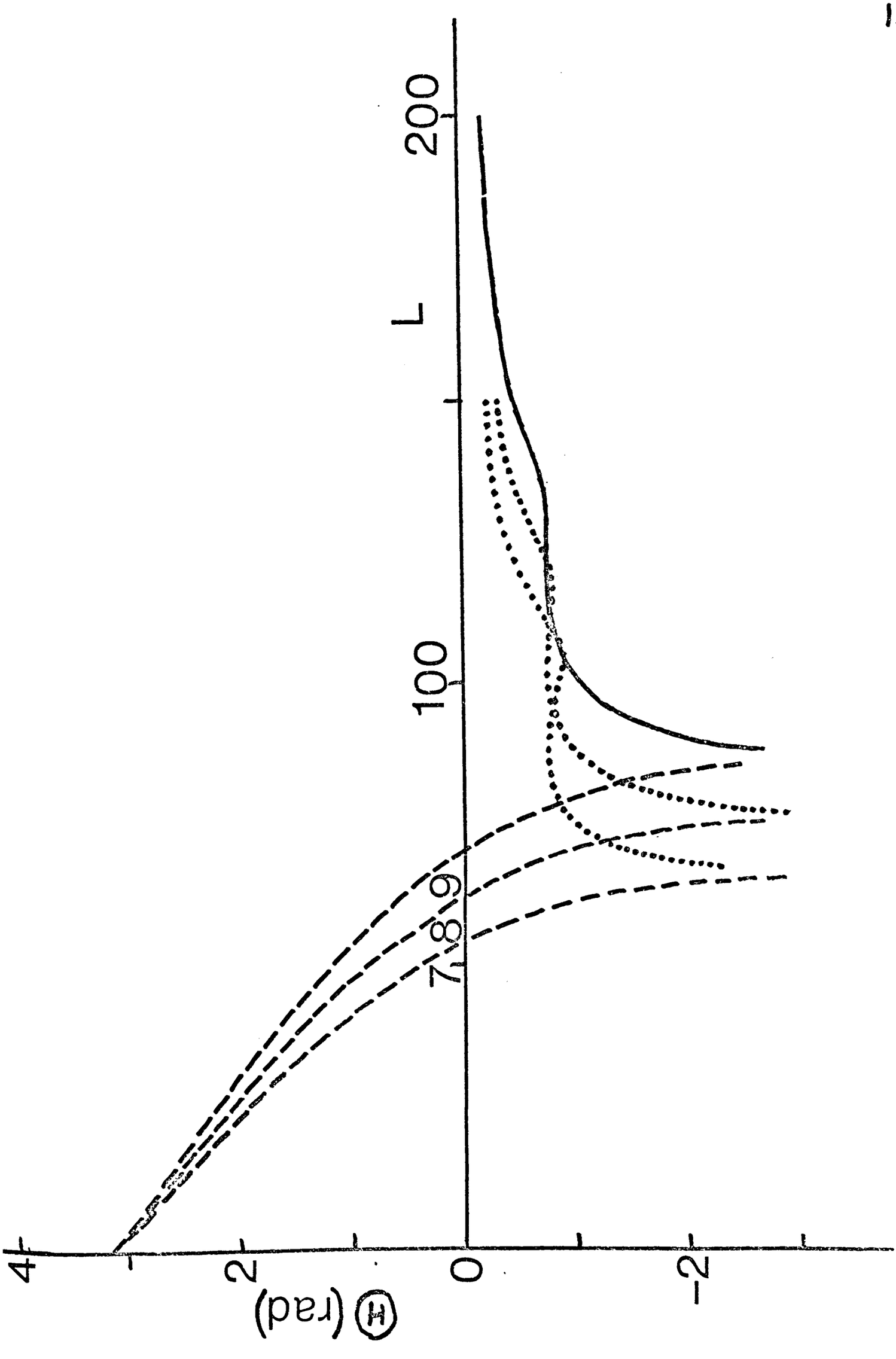
200
L
100
7
8
9
4
2
0
−2
Θ (rad)

Figure 14

The deflection function for the downhill potential (4.65). The values of the parameters chosen for this potential are given in the caption to Figure (10).

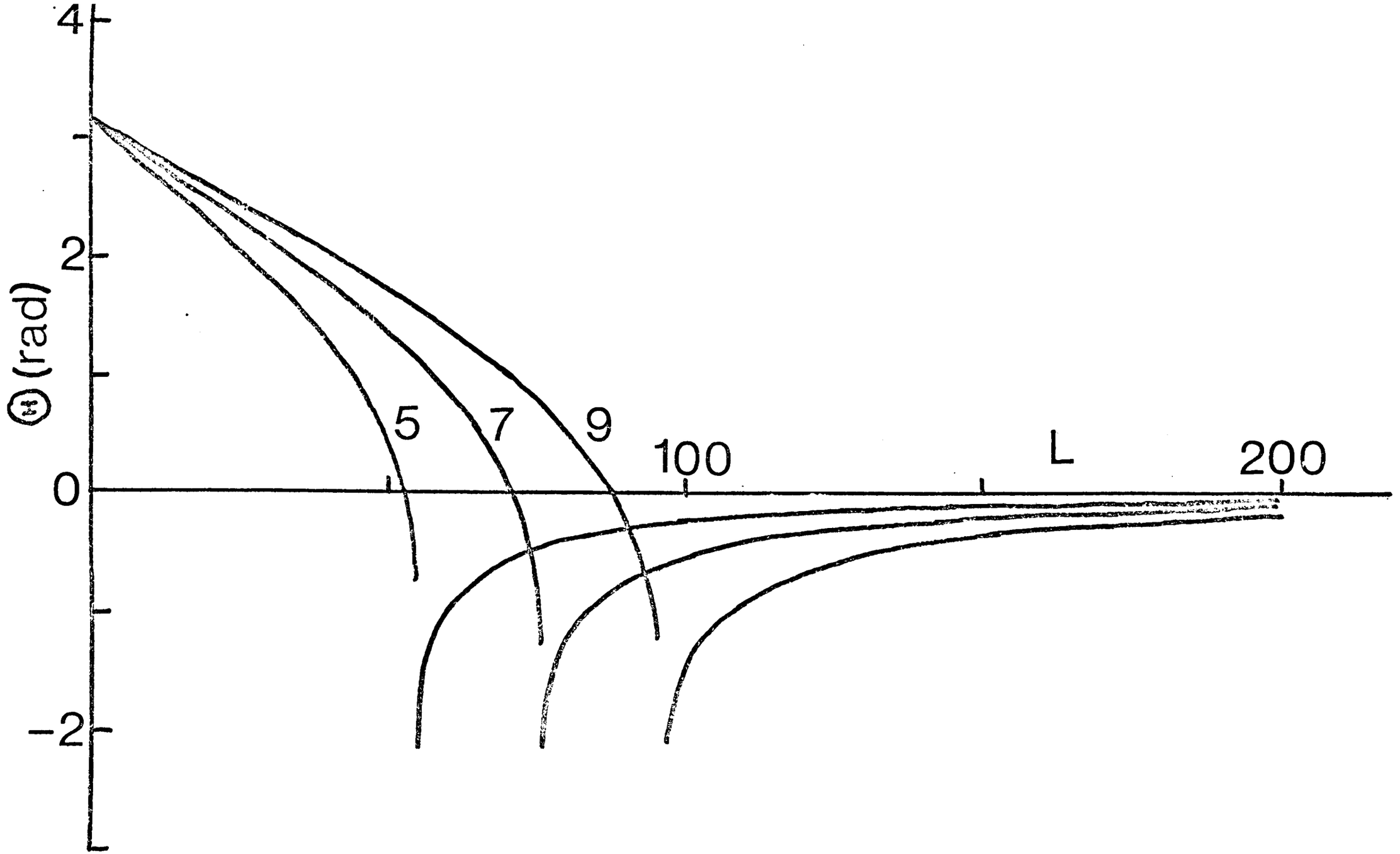
4
2
0
-2
Θ(rad)
5
7
9
100
L
200

Explicit expressions for $\textcircled{H}$ are available for the lorentzian potential (4.64). Differentiation of equations(4.71) and (4.72) gives:[78]

$$\textcircled{H}^{(-)} = \pi - \frac{2(L+\frac{1}{2})}{B_L^{1/2}} \underset{\sim}{K}\left(\frac{k^{(-)}\sigma_e}{B_L^{1/2}}\right) - \frac{\partial \phi(\varepsilon_L)}{\partial L}, \qquad (4.75)$$

$$\textcircled{H}^{(+)} = \pi - \frac{2(L+\frac{1}{2})}{k^{(-)}\sigma_e} \underset{\sim}{K}\left(\frac{B_L^{1/2}}{k^{(-)}\sigma_e}\right) - \frac{\partial \phi(\varepsilon_L)}{\partial L}. \qquad (4.76)$$

As in the case of the phase shifts,existing methods for the numerical evaluation of the integrals in equations (4.73) and (4.74) break down when $a_L = c_L = 0$. A scaled Gauss-Mehler quadrature designed to overcome this difficulty is described in Appendix (A).

Consider first of all the reactive deflection function $\textcircled{H}^{(+)}$. The shape of $\textcircled{H}^{(+)}$ is similar for all three potentials. The low impact parameter scattering corresponds to A approaching BC,picking up B and rebounding in the backward direction with C departing in the forward direction. As b increases $\textcircled{H}^{(+)}$ decreases until at the glory impact parameter $\textcircled{H}^{(+)} = 0$. This corresponds to the maximum in

the phase shift as previously mentioned. The value of the glory impact parameter also provides a test of consistency between the phase shift calculations and the deflection function calculations. For larger values of the impact parameter $\Theta^{(+)}$ goes over to an orbiting situation as the collision energy approaches the maximum in the effective potential.

The elastic deflection function $\Theta^{(-)}$ for the lorentzian potential (4.64) and the downhill potential (4.65) are seen to be similar in shape. $\Theta^{(-)}$ monotonically increases as the impact parameter increases and approaches zero as b tends to infinity. Of more interest is the behaviour of $\Theta^{(-)}$ for the modified Lennard-Jones potential (4.66). At low values of $k^{(-)}$, $\Theta^{(-)}$ possesses a maximum and minimum. These extrema correspond to the points of inflection in the phase shift $\delta_L^{(-)}$ of Figure (9) and give rise to rainbows in the differential cross sections (see Section (4.5)). As $k^{(-)}$ decreases below 4 Å^{-1} $\text{amu}^{-\frac{1}{2}}$ it is clear from Figure (12) that the negative rainbow would give away to orbiting. As $k^{(-)}$ increases the extremum behaviour in $\Theta^{(-)}$ becomes less pronounced until for

$k^{(-)} = 9\ \text{Å}^{-1}\ \text{amu}^{-\frac{1}{2}}$ the two quadratic rainbows have coalesced to form a cubic rainbow and $\Theta^{(-)}$ possesses a point of inflection (Figure(13)). For larger values of $k^{(-)}$ the behaviour of $\Theta^{(-)}$ approaches that of Figures (11) and (14). The influence of the well on the scattering has then become negligible.

It will also prove useful in the next Section to obtain an analytical approximation for Θ in the orbiting region. Consider first the case of the elastic deflection function $\Theta^{(-)}$. Expanding the phase integral in $\delta_L^{(-)}$ (equation (4.41)) about the orbiting maximum gives:

$$\int_{-\infty}^{a_{L_0}} k_{L_0}(s)\,ds = \frac{\varepsilon_{L_0}}{2} - \frac{\varepsilon_{L_0}}{2}\ln|\varepsilon_{L_0}| + \text{other terms.} \qquad (4.77)$$

In order to apply the semiclassical equivalence relationship (4.47) to obtain $\Theta^{(-)}$ it is first necessary to relate ε_{L_0} (which refers to variable E and fixed L_0) to the angular momentum displacement variable $L-L_0$ (which refers to variable L and fixed E). Recalling the definition of ε_{L_0} from Section (4.5) this relation to first order in $L-L_0$ is:

$$\varepsilon_{L_0} = -\frac{(L_0+\frac{1}{2})\hbar}{(b_{L_0}^2+\sigma_2^2)\,\omega_{L_0}^*}\cdot(L-L_0),$$

so that $\Theta^{(-)}$ may be written as:

$$\Theta^{(-)} = \theta_{>} + d \ln \frac{L-L_0}{L_0} \quad , \quad L > L_0 \, , \tag{4.78}$$

where

$$d = \frac{(L_0 + \frac{1}{2})\hbar}{(b_{L_0}^2 + v_e^2)\, \omega_{L_0}^{\ddagger}} \, . \tag{4.79}$$

In a similar manner $\Theta^{(+)}$ may be written as:

$$\Theta^{(+)} = \theta_{<} + d \ln \frac{L_0 - L}{L_0} \qquad L < L_0 \, , \tag{4.80}$$

where d is again defined by equation (4.79) and $\theta_{>}$ and $\theta_{<}$ are constants in equations (4.78) and (4.80) .

Figure (15) shows the deflection function calculated for the potential (4.67). It shows the usual negative rainbow that is characteristic of an attractive well in atom-atom scattering.

Figure 15

The deflection function for the potential (4.67).
The values of the parameters chosen for the potential (4.67) are $A = 9.487$ Å $amu^{\frac{1}{2}}$, $\epsilon = 0.25$ kcal $mole^{-1}$, $v_e = 10$ Å $amu^{\frac{1}{2}}$. The values of $k^{(-)}$ ($Å^{-1}$ $amu^{-\frac{1}{2}}$) are 4,5,7,9.

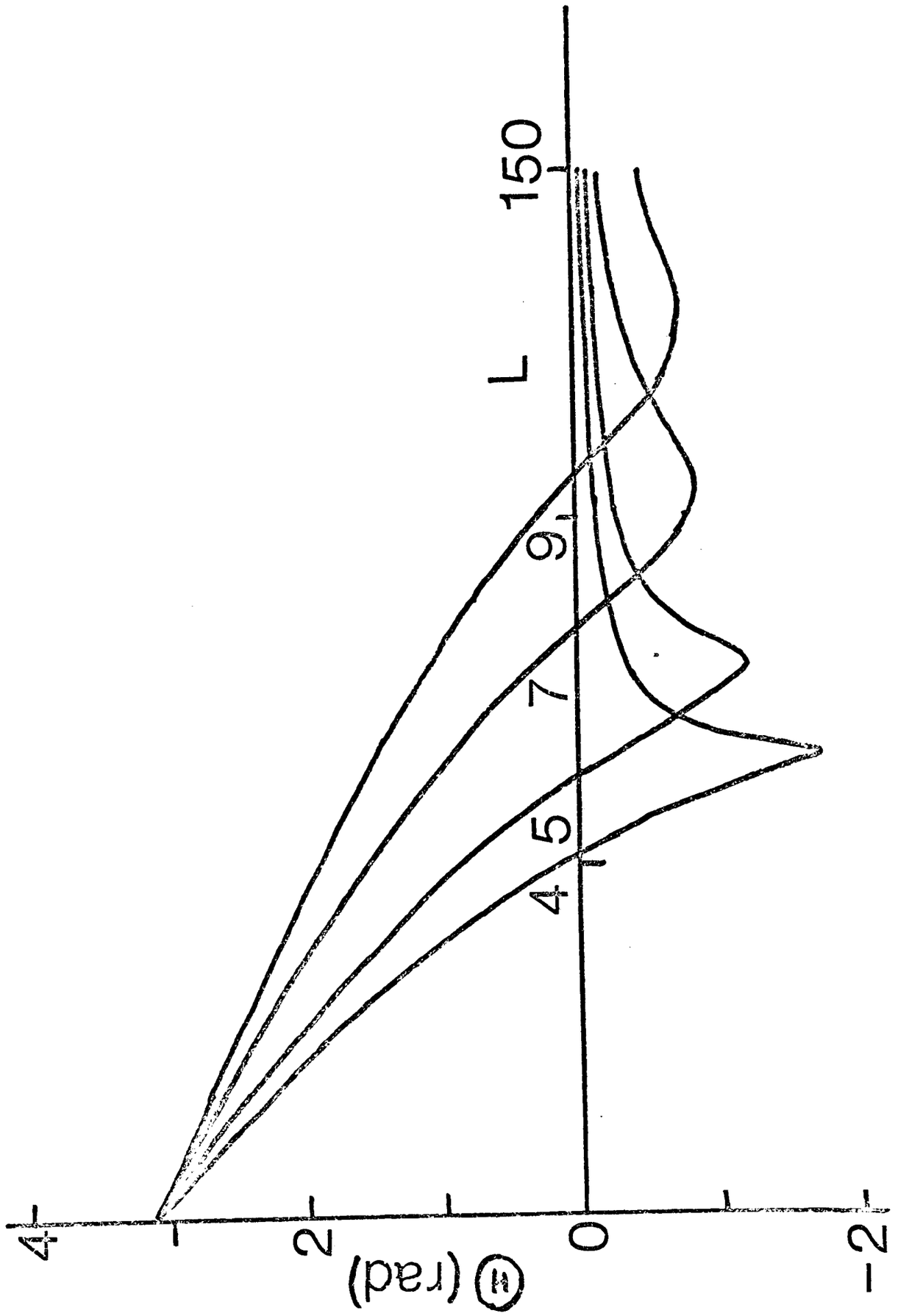
L
150
9
7
5
4
-4
-2
0
2
ω (rad)

4.8 DIFFERENTIAL CROSS SECTIONS

In this Section the angular distributions of the elastically and reactively scattered products are calculated using the deflection functions previously described.

The first point to be made is that Figures (11)-(14) show that interference effects (discussed in Section (4.5)) will be present in the reactive differential cross sections for all three potentials (4.64)-(4.66) and also in the elastic differential cross sections for the modified Lennard-Jones potential (4.66) at low values of $k^{(-)}$. Otherwise interference effects will be absent in the elastic scattering from the potentials (4.64) and (4.65) and also from the potential (4.66) at large values of $k^{(-)}$. (Interferences between the $\Theta^{(+)}$ and $\Theta^{(+)}$ branches and for values of $\Theta^{(\pm)} < -\pi$ have been neglected in making the above remarks). However the high frequency oscillations in the differential cross sections that arise from the interference effects will not be considered any further in what follows because experimentally they have not been observed in the scattering of reactive systems.[10-12]

(the oscillations have been detected in high resolution atom-atom scattering however[4])

Figures (16)-(18) show the reactive differential cross sections $I^{(+)}(\Theta)$ (weighted with $\sin\Theta$) calculated according to the classical expression (4.51) for the potentials (4.64)-(4.66). For the lorentzian potential (4.64), an explicit expression for $d\Theta^{(+)}/dL$ is obtained by differentiating equation (4.76) for $\Theta^{(+)}$:

$$\frac{d\Theta^{(+)}}{dL} = -\frac{2}{k^{(+)}v_e}\left[\underset{\sim}{K}\left(\frac{\beta_L^{1/2}}{k^{(+)}v_e}\right) + \frac{(L+\frac{1}{2})^2}{k^{(+)2}v_e^2-\beta_L}\underset{\sim}{\beta}\left(\frac{\beta_L^{1/2}}{k^{(+)}v_e}\right)\right] - \frac{\partial^2\phi(\varepsilon_L)}{\partial L^2}. \tag{4.81}$$

As in the calculation of the phase shift and deflection function, the term involving $\phi(\varepsilon_L)$ has been set equal to zero and the reflection and transmission coefficients given their classical values. This approximation breaks down only for two or three partial waves; their contribution to the cross section is however very small. For the downhill potential (4.65) and the modified Lennard-Jones potential (4.66), $d\Theta^{(+)}/dL$ was obtained by five point lagrangian numerical differentiation[80] of the deflection function. Comparison with the exact result (4.81) for the lorentzian potential

Figure 16

The reactive differential cross section $I^{(+)}(\Theta)$ ($Å^2$ amu) (weighted with $\sin(\Theta)$) for the lorentzian potential (4.64). The values of the parameters chosen for this potential are given in the caption to Figure (8).

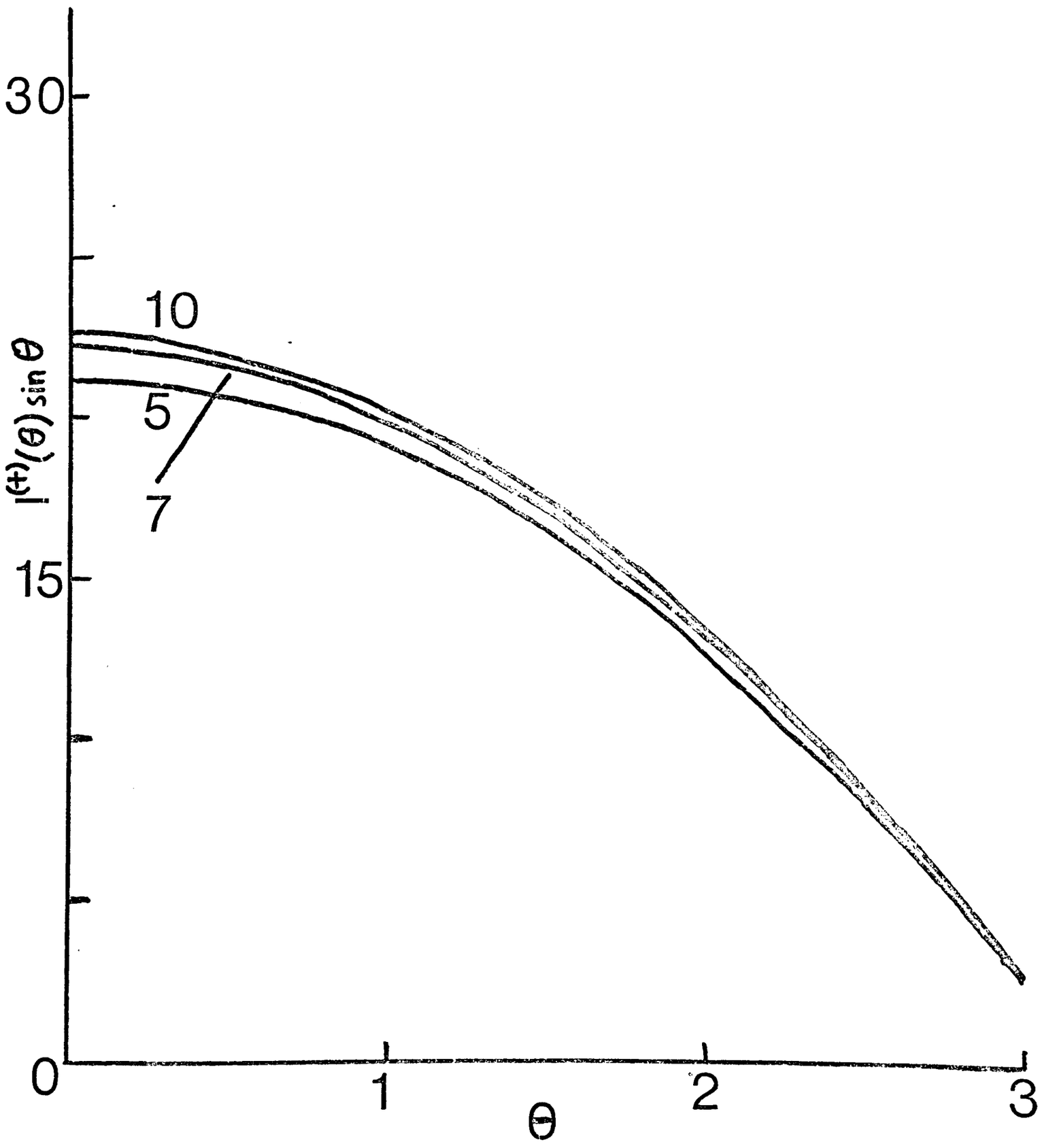
30
15
0
10
5
7
$I^{(+)}(\theta)\sin\theta$
1
2
3
θ

Figure 17

The reactive differential cross section $I^{(\theta)}(\Theta)$ ($Å^2$amu) (weighted with $\sin(\Theta)$) for the modified Lennard-Jones potential (4.66). The values of the parameters chosen for this potential are given in the caption to Figure (9)

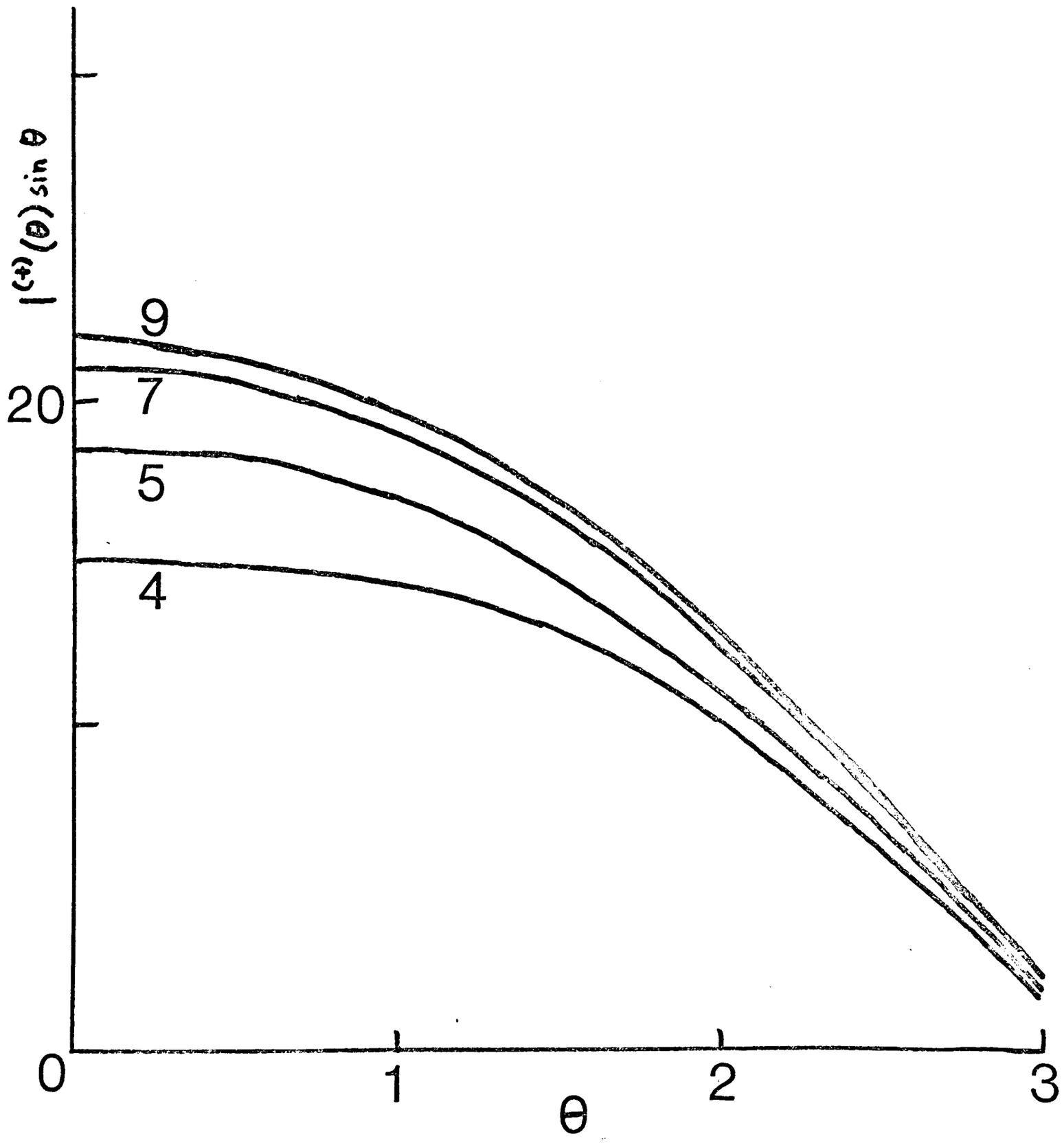
$I^{(+)}(\theta)\sin\theta$
9
7
5
4
20
0
1
2
3
θ

Figure 18

The reactive differential cross section $I^{(4)}(\theta)$ ($\mathring{A}^2$ amu) (weighted with $\sin(\theta)$) for the downhill potential (4.65). The values of the parameters chosen for this potential are given in the caption to Figure (10).

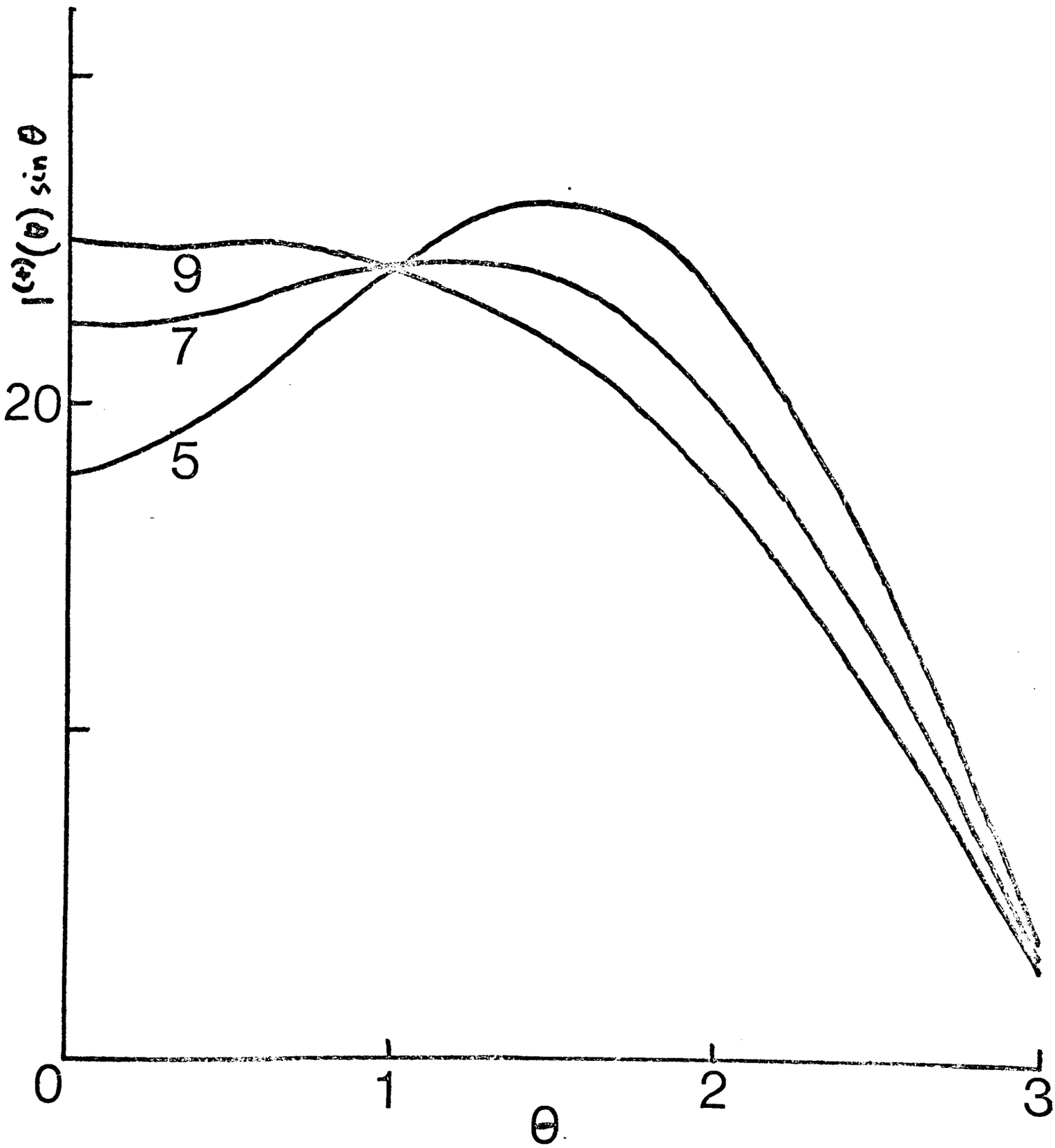
I(+)(θ) sin θ
9
7
5
20
0
1
2
3
θ

showed that the numerical differentiation procedure becomes unreliable in the orbiting region (that is when $d\Theta^{(+)}/dL$ is large). In this region therefore the deflection function was fitted to the analytical form (4.80), from which $d\Theta^{(+)}/dL = -d(L_o - L)$. Contributions to the differential cross section from angles $\Theta^{(+)} < -\pi$ were neglected. The angular distributions in Figures (16)-(18) are therefore a sum over the remaining two branches of $\Theta^{(+)}$. The shape of the angular distributions for the lorentzian potential (4.64) and modified Lennard-Jones potential (4.66) are seen to be similar. Both sets of distributions are broad and peaked in the forward ($\Theta = 0$) direction for all values of $k^{(-)}$ considered. In contrast the downhill potential (4.65) peaks at $\Theta \approx 1.5$ rad for $k^{(-)} = 5$ Å^{-1} $\text{amu}^{-\frac{1}{2}}$, the maximum moving in the forward direction as $k^{(-)}$ increases. The angular distribution is broad for this case also.

Figures (19)-(24) show the elastic differential cross sections $I^{(-)}(\Theta)$ (also weighted with $\sin\Theta$) calculated from the classical equation (4.50) (drawn as a solid line). For the lorenztian potential, differentiation of equation (4.75) gives:

Figure 19

The elastic differential cross section $I^{\Theta}(\theta)$ ($\mathring{A}^2$ amu) (weighted with $\sin(\theta)$) for the lorentzian potential (4.64). The values of the parameters chosen for this potential are given in the caption to Figure (8).

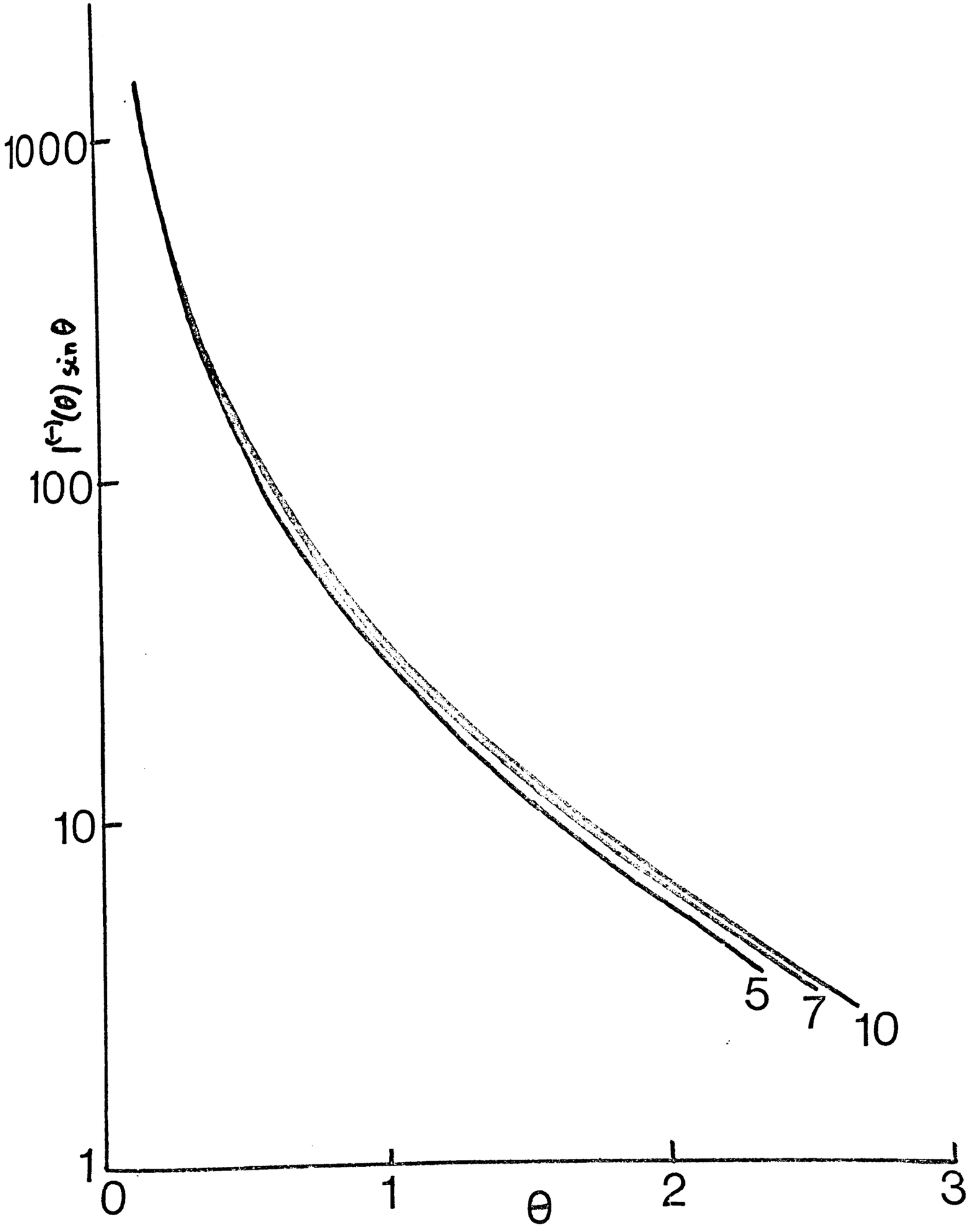
1000
100
10
1
$I^{(-)}(\theta)\sin\theta$
0
1
2
3
θ
5
7
10

Figure 20

The elastic differential cross section $I^{(-)}(\Theta)$ ($\mathring{A}^2$ amu) (weighted with $\sin(\Theta)$) for the downhill potential (4.65). The values of the parameters chosen for this potential are given in the caption to Figure (10).

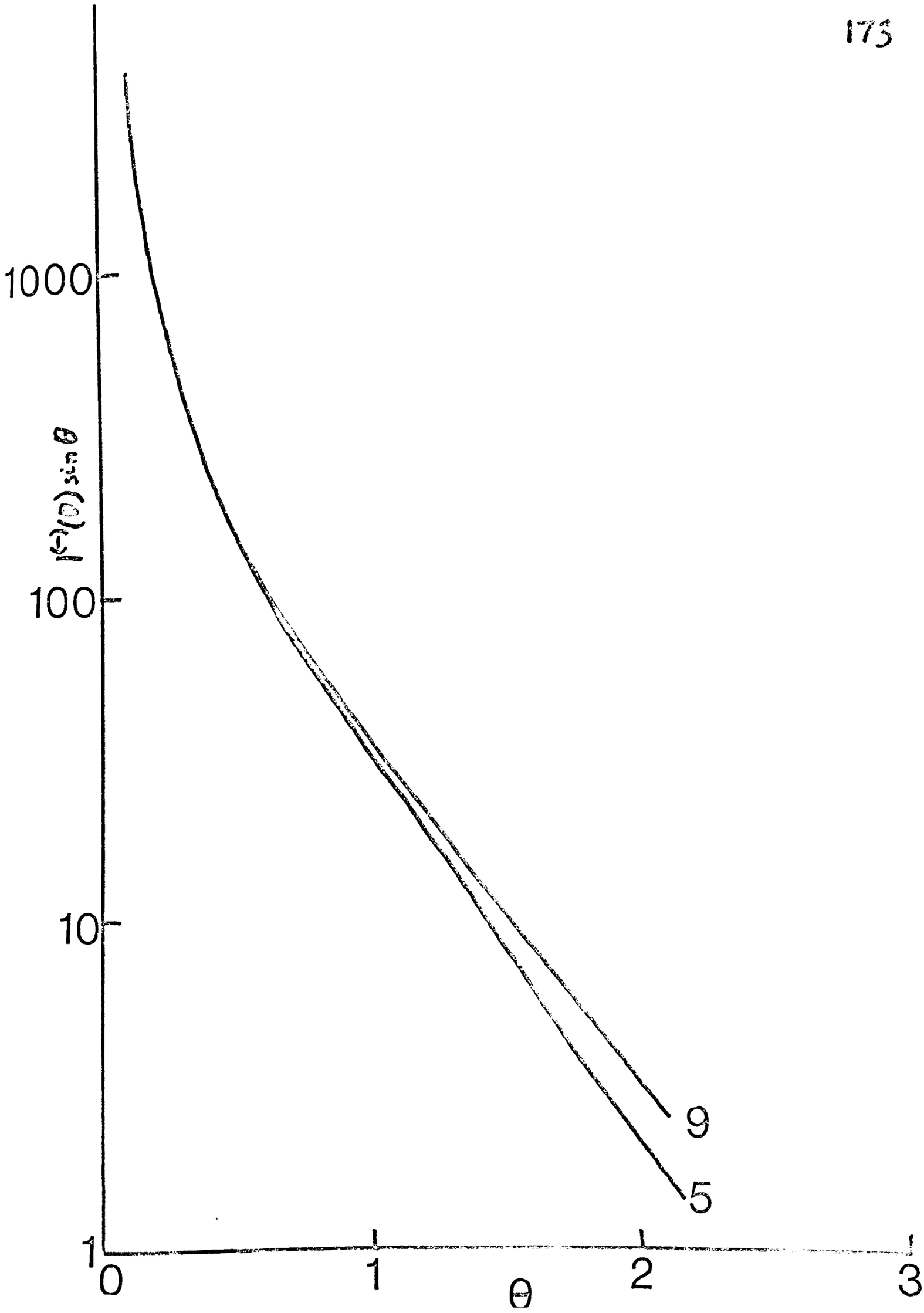
1000
100
10
1
$I^{(2)}(\theta)\sin\theta$
0
1
2
3
θ
9
5

Figure 21

The elastic differential cross section $I^{(-)}(\theta)$ ($\mathring{A}^2$ amu) (weighted with $\sin(\theta)$) for the modified Lennard-Jones potential (4.66) for $k^{(-)} = 4\ \mathring{A}^{-1}$ amu$^{-\frac{1}{2}}$. The values of the parameters chosen for this potential are given in the caption to Figure (9).

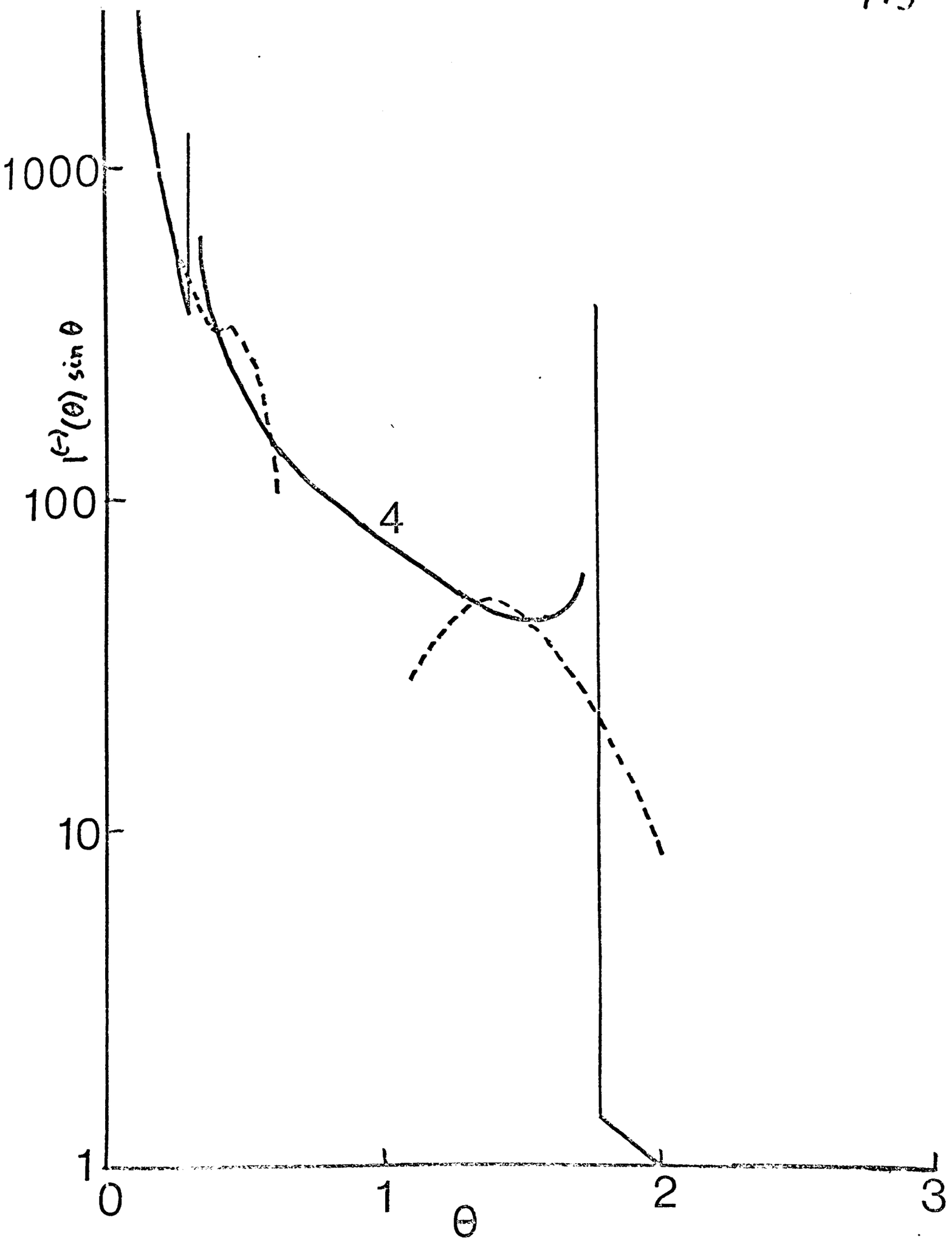
1000
100
10
1
$I^{(-)}(\theta)\sin\theta$
4
0
1
2
3
θ

Figure 22

The elastic differential cross section $I^{(-)}(\theta)$ ($\mathring{A}^2$ amu) (weighted with $\sin(\theta)$) for the modified Lennard-Jones potential (4.66) for $k^{(-)} = 5\ \mathring{A}^{-1}$ amu$^{-\frac{1}{2}}$. The values of the parameters chosen for this potential are given in the caption to Figure (9).

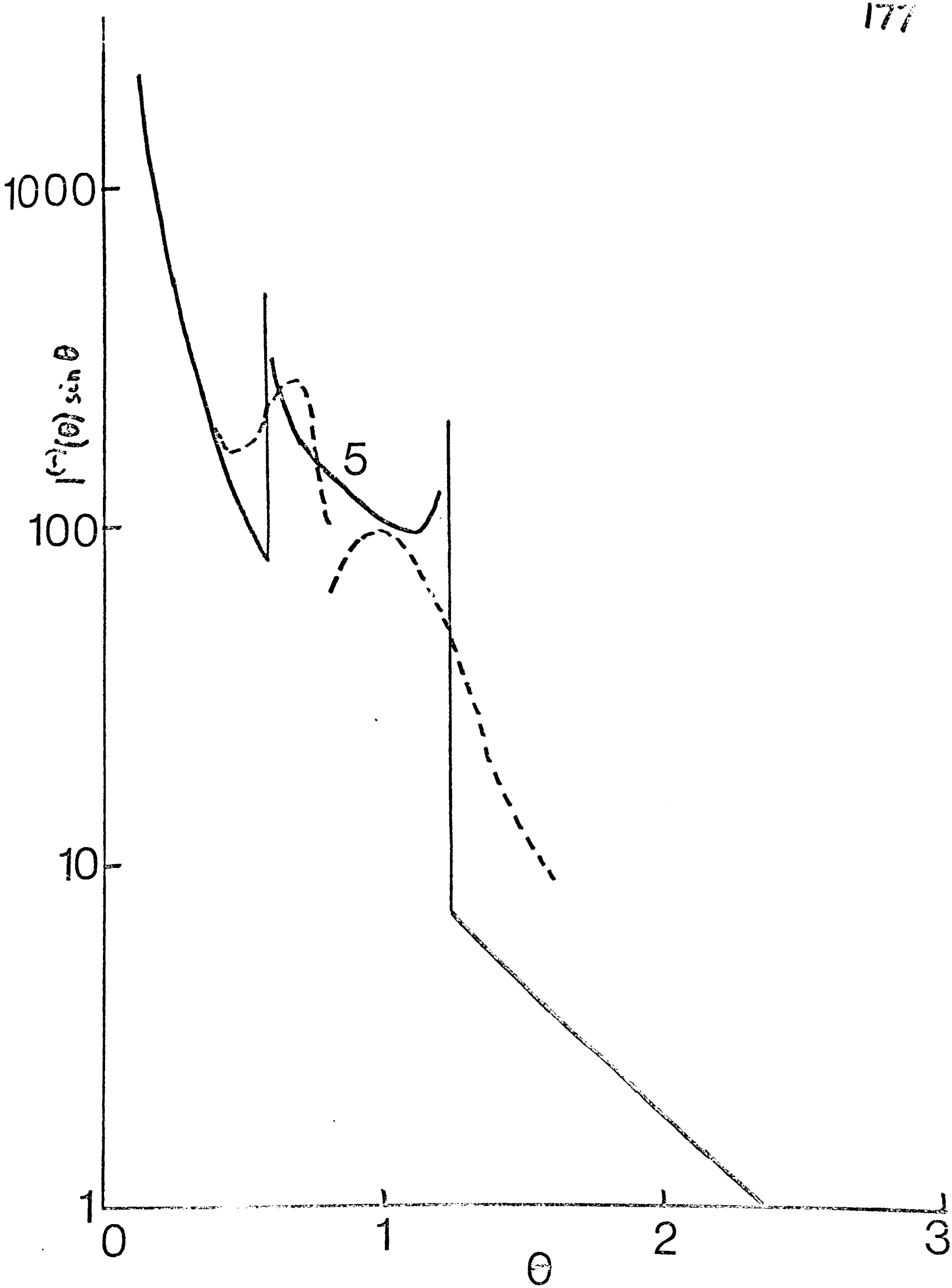
1000
100
10
1
$I^{(-)}(\theta) \sin\theta$
5
0
1
2
3
θ

Figure 23

The elastic differential cross section $I^{(-)}(\theta)$ ($\mathring{A}^2$ amu) (weighted with $\sin(\theta)$) for the modified Lennard-Jones potential (4.66) for $k^{(-)} = 7\ \mathring{A}^{-1}$ amu$^{-\frac{1}{2}}$. The values of the parameters chosen for this potential are given in the caption to Figure (9).

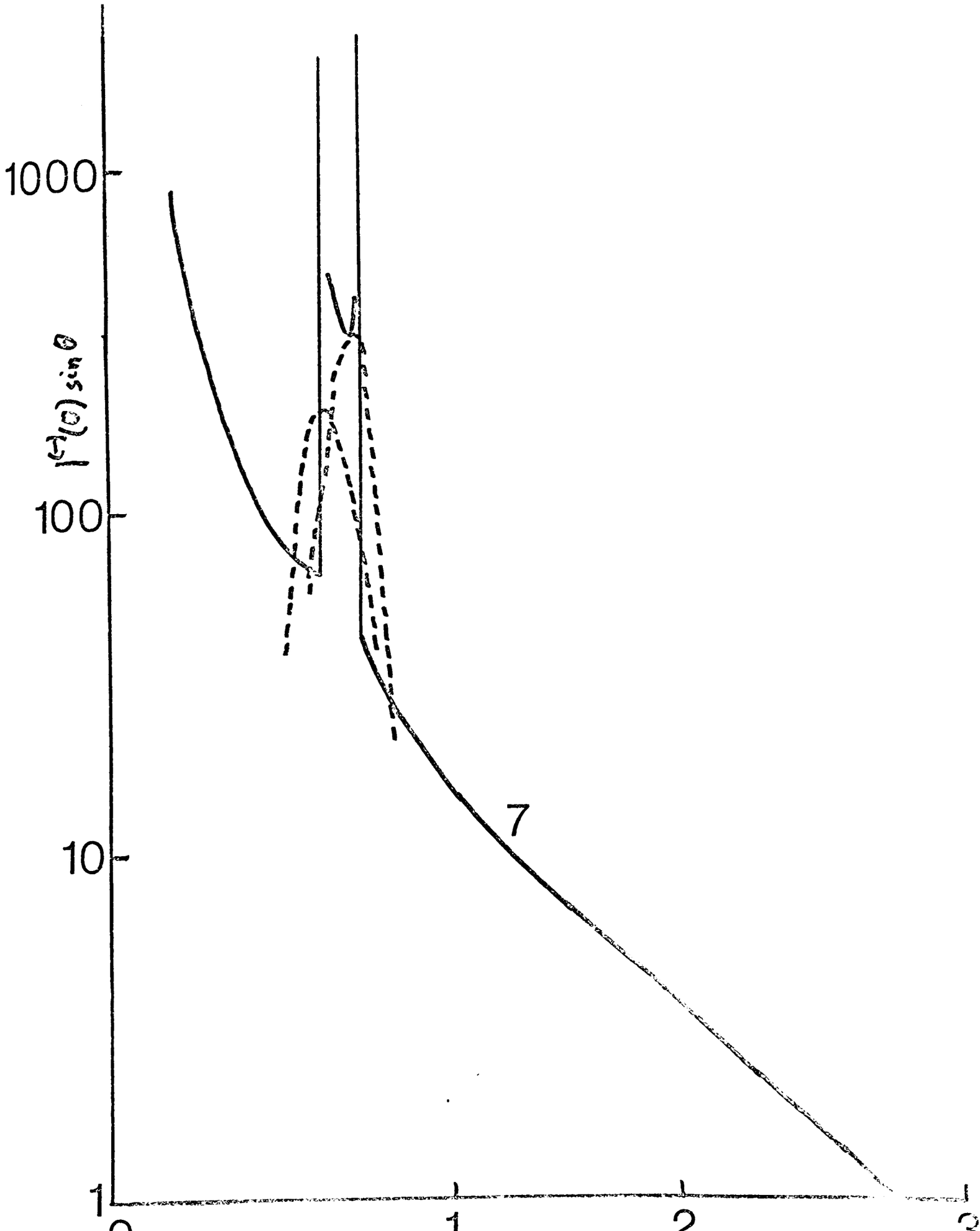
1000
100
10
1
$I^{(7)}(\theta)\sin\theta$
7
0
1
2
3
θ

Figure 24

The elastic differential cross section $I^{(-)}(\theta)$ ($\mathring{A}^2$ amu) (weighted with $\sin(\theta)$) for the modified Lennard-Jones potential (4.66) for $k^{(-)} = 9\ \mathring{A}^{-1}\ \text{amu}^{-\frac{1}{2}}$. The values of the parameters chosen for this potential are given in the caption to Figure (9).

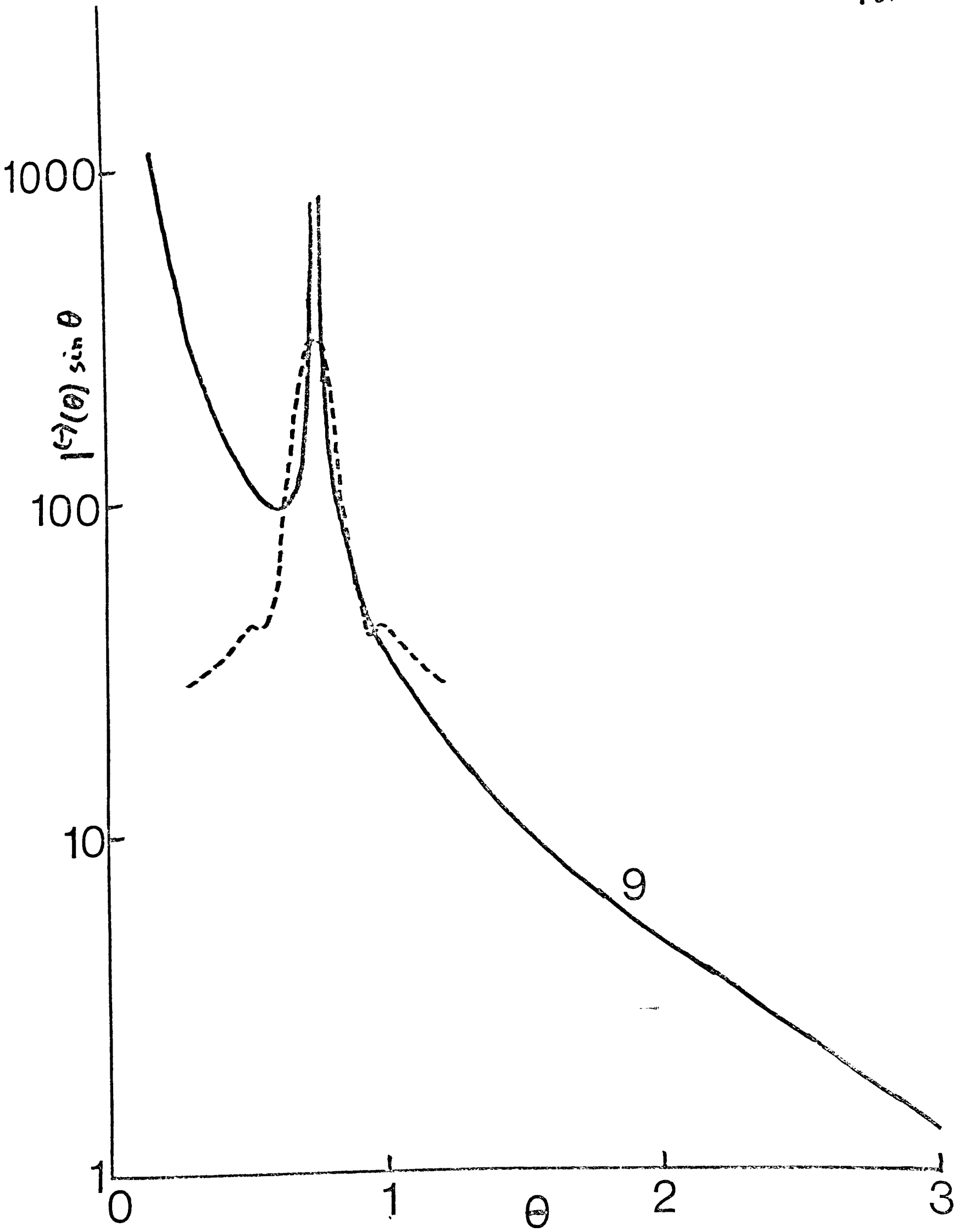
1000
100
10
1
$I^{(7)}(\theta) \sin\theta$
9
0
1
θ
2
3

$$\frac{d\Theta^{(-)}}{dL} = -\frac{2}{B_L^{1/2}}\left[\underset{\sim}{K}\left(\frac{k^{(-)}v_2}{B_L^{1/2}}\right) + \frac{(L+\frac{1}{2})^{\nu}}{k^{(-)2}v_2^2 - B_L}\,\underset{\sim}{E}\left(\frac{k^{(-)}v_2}{B_L^{1/2}}\right)\right] - \frac{\partial^2\phi(L)}{\partial L^2}.$$

For the remaining two potentials $d\Theta^{(-)}/dL$ was found by five point lagrangian numerical differentiation of the elastic deflection function, as in the reactive case. In the large angle orbiting region, the deflection function was fitted to the analytic form (4.78); this gives a cross section of the form:

$$I^{(-)}(\theta)\sin\theta = \frac{R_{L_0}^{\nu}(L_0+\frac{1}{2})}{k^{(-)2}}\,\frac{L_0}{d}\exp\left[-\frac{(\theta+\theta_r)}{d}\right], \qquad (4.82)$$

where $\Theta^{(-)} = -\theta$ for $-\pi \leqslant \Theta^{(-)} \leqslant 0$, that is exponentially decreasing for large angles. This limiting large angle behaviour is clearly visible from the graphs. The classical quadratic rainbow singularities in $I^{(-)}(\theta)$ expressed by equations (4.55) and (4.58) are also clearly illustrated in Figures (21)-(23). As $k^{(-)}$ increases the positive and negative rainbows move closer together until at $k^{(-)} = 9$ Å^{-1} amu$^{-\frac{1}{2}}$ they have coalesced to form a cubic rainbow (equation (4.63)). For higher values of $k^{(-)}$ the peak in the

cross section diminishes until the limiting behaviour of Figures (19) and (20) is reached. The region between the quadratic rainbows represents a sum over the three branches of the deflection function of Figures (12) and (13).

Figures (21)-(23) show as dotted lines the differential cross sections for the quadratic rainbows calculated according to equations (4.54) and (4.57). For $k^{(-)} = 4{,}5\ \text{Å}^{-1}\ \text{amu}^{-\frac{1}{2}}$ the contribution from the third branch of the deflection function has been added to that obtained from equations (4.54) and (4.57). Figure (24) shows the semiclassical differential cross section for the cubic rainbow calculated according to equation (4.62). The classical infinity is replaced by a finite peak. The semi-classical cross section also possesses a small oscillation; this may be described as a super-numerary cubic rainbow.[4]

Experimentally, the exponential fall off at large angles given by equation (4.82) has been observed for reactions with large cross sections and differential cross sections similar to those shown in Figures (19) and (20) have been found.[10]

No measurements of elastic differential cross sections possessing two maxima akin to those calculated here for the modified Lennard-Jones potential have been reported. It is clear from Figures (21)-(24) that the variation with angle of the rainbows as a function of $k^{(-)}$ would provide a decisive test of the present model as well as yielding detailed information on the intermolecular potential.

4.9 TOTAL REACTIVE CROSS SECTIONS

The total reactive cross sections are readily calculated from equation (4.31):

$$\sigma^{(r)} = \frac{\pi}{k^{(r)2}} \sum_{L} (2L+1) T_L^2,$$

$$\approx \frac{\pi}{k^{(r)2}} (L_0+1)^2. \qquad (4.83)$$

or from the area under the curves of Figures (16)-(18) by means of equation (4.30). The results are presented in Table (3). The total reactive cross section increases as $k^{(r)}$ increases for the lorentzian and modified Lennard-Jones potential but decreases as $k^{(r)}$ increases for the downhill potential. This is in accord with a simple classical model for the reactive cross section.[81]

Ross, Greene and Coworkers[49] have suggested that the difference between the observed elastic differential cross section in a reactive system and the elastic differential cross section calculated from a hypothetical potential for no reaction may be used to estimate the reactive total cross section. This hypothesis has been tested as follows. To the

Table 3 Total Reactive Cross Sections.

$k^{(-)}$ is the mass reduced incident wave number (in units of $\mathring{A}^{-1}$ $amu^{-\frac{1}{2}}$), L_o is the classical cutoff value in the orbital angular momentum quantum number, $\sigma^{(+)}$ is the total reactive cross section calculated from equation (4.83) (in units of $\mathring{A}^2$ amu), ESA (elastic scattering analysis) estimates the total reactive cross section (in units of $\mathring{A}^2$ amu) by an indirect method explained in the text.

Potential	$k^{(-)}$	L_o	$\sigma^{(+)}$	ESA
	5	47.5	295	
lorentzian	7	68.1	306	
(4.64)	10	98.5	311	
	5	54.7	390	
downhill	7	75.5	375	
(4.65)	9	96.1	365	
	4	32.3	218	130
modified	5	44.0	254	229
Lennard-Jones	7	65.7	285	193
(4.66)	9	86.5	297	161

modified Lennard-Jones potential (4.66) has been added a steeply repulsive wall (this is the potential (4.67) previously introduced and for which the deflection function was calculated in the previous section, Figure (15)) and elastic differential cross sections have been calculated for it by techniques similar to those described above. The results are shown in Figure (25). The negative rainbows are clearly visible as is the bow shaped high angle curve that is characteristic of scattering from a repulsive wall. It is known from detailed numerical studies[82] that the quadratic rainbow effect depends mainly on the nature of the potential beyond the well minimum. For the potentials (4.66) and (4.67) therefore the rainbows are very similar to each other (after the contribution from the third branch has been subtracted out). From Figure (25) an integral cross section was calculated for $\theta > \theta_n$ for the repulsive branch of the deflection function by the formula:

$$\sigma = 2\pi \int_{\theta_n}^{\pi} I(\theta) \sin\theta \, d\theta$$

A similar integral cross section was calculated from Figures (21)-(24) for the orbiting branch (also for

Figure 25

The elastic differential cross section $I(\theta)$ (Å^2 amu) (weighted with $\sin(\theta)$) for the potential (4.67) for $k^{(-)} = 4,5,7,9$ Å^{-1} $\text{amu}^{-\frac{1}{2}}$. The values of the parameters chosen for this potential are given in the caption to Figure (15).

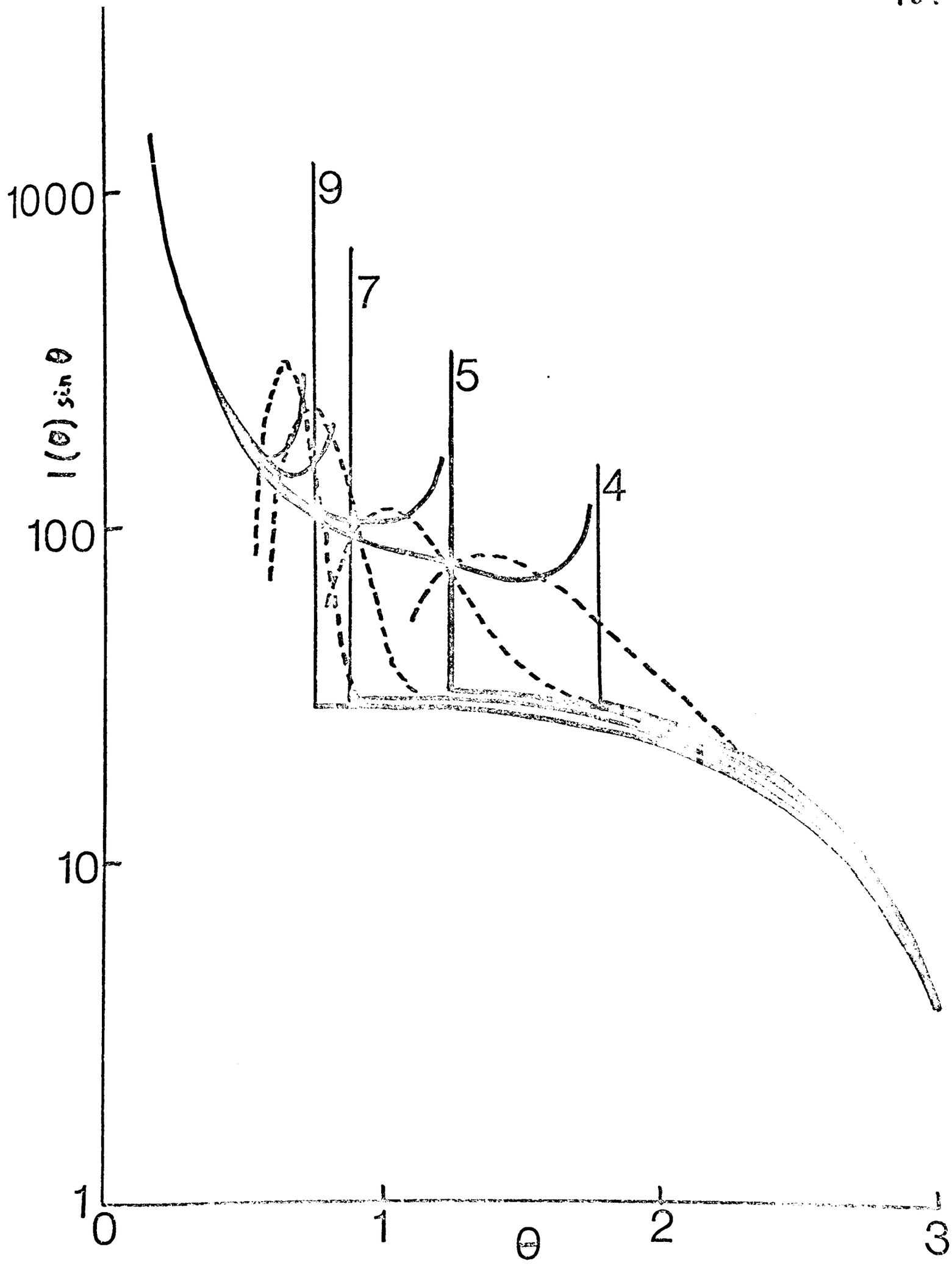
1000
100
10
1
I(θ) sin θ
9
7
5
4
0
1
2
3
θ

$\theta > \theta_n$). The difference between these two integral cross sections is also given in Table (3). The reactive cross section calculated via the elastic scattering is seen to be 40%,10%,32%,45% (for $k^{(-)} = 4,5,7,9$ Å^{-1} $\text{amu}^{-\frac{1}{2}}$ respectively) smaller than the true values. It thus appears that reaction cross sections for the modified Lennard-Jones potential (4.66) may be estimated to within a factor of approximately two from the deviations in the elastic scattering from the expected pattern in a simple central force field.

CHAPTER FIVE: RESONANCE TUNNELLING REACTIONS

5.1 INTRODUCTION

This Chapter investigates the effect of a dip in the activation barrier for a chemical reaction using the model developed in Chapter (4). In the previous Chapter it was shown that the theoretical treatment of the electronically adiabatic bimolecular exchange reaction:

$$A + BC = AB + C,$$

could be simplified by the introduction of a mathematically meaningful mass weighted reaction coordinate which varied in value from $-\infty$ at the beginning of the reaction to $+\infty$ at the end. Motion along the reaction coordinate could be separated from the angular motion of the system as well as the purely vibrational motion of the atoms and is determined by the one dimensional Schrödinger equation:

$$\left[-\frac{\hbar^2}{2}\frac{d^2}{ds^2} + V_{nL}(s) - E\right] S_{nL}(s) = 0 , \qquad (5.1)$$

with boundary conditions representing incident, reflected and transmitted waves:

$$S_{nL}(s) \underset{s\to-\infty}{\sim} e^{ik^{(-)}s + i(L+1)\pi} + R_L e^{2i\delta_L^{(-)}} e^{-ik^{(-)}s} \Bigg\} \quad (5.2)$$

$$\underset{s\to\infty}{\sim} \left(\frac{k^{(-)}}{k^{(+)}}\right)^{1/2} T_L e^{2i\delta_L^{(+)}} e^{ik^{(+)}s}.$$

The elastic and reactive differential and total cross sections are related to $\delta_L^{(-)}$, $\delta_L^{(+)}$, R_L, T_L by equations (4.24)-(4.31).

In the present case $V_n(s)$ is assumed to possess a dip in the activation barrier for the reaction at $s \approx 0$. For a certain range of values of the orbital angular momentum quantum number, the effective potential $V_{nL}(s)$ will also possess a dip. The volcano shape of $V_{nL}(s)$ in this case is shown in Figure (26). This effective potential profile therefore gives rise to a four turning point problem as opposed to the two turning point problems considered in Chapter (4) or the three turning point problem of Chapter (3).

The presence of a dip in the barrier implies the possibility of setting up quasi-stationary

Figure 26

The effective potential energy curve $V_{nL}(s)$. E denotes the total energy of the system. a_{1L}, c_{1L}, a_{2L}, c_{2L} are the classical turning points. b_{1L} and b_{2L} are the positions of the barrier maxima.

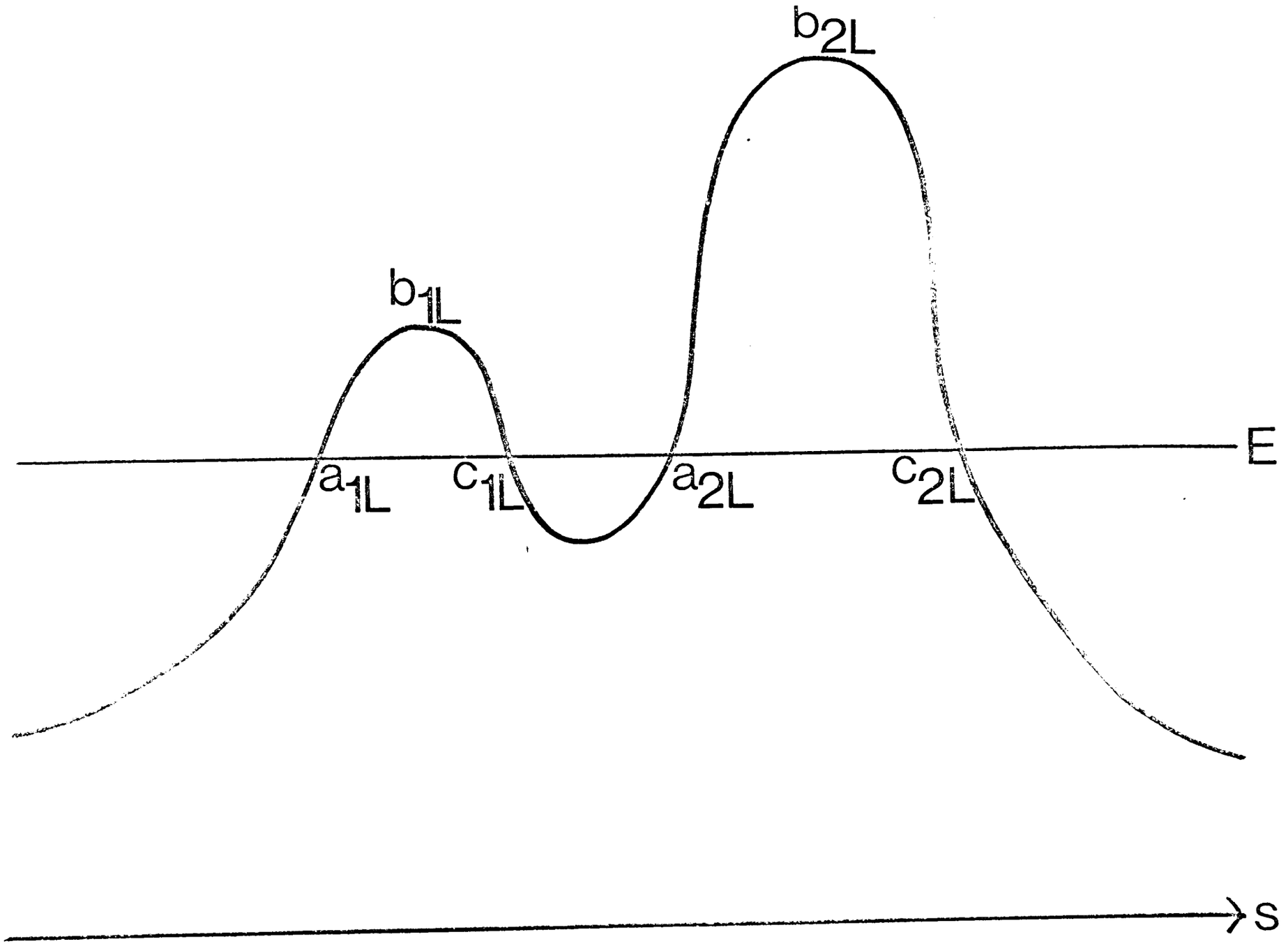

Fig

states (compare the orbiting resonance states of Chapter (3)). The existence of these states has been shown by Child[24] to have an important effect on the reaction cross section and rate constant. When the collision energy is in resonance with one of the asymmetric vibration-rotation states of the activated complex, tunnelling through the barrier can occur even when the collision energy is far below the barrier maxima. The reaction cross section then possesses a well resolved resonance structure and the rate constant shows a different behaviour from that expected for simple tunnelling through a single humped barrier. This phenomenon has been named resonance tunnelling[24].

This system is investigated using the parabolic connection formulae to derive the semiclassical form of $\delta_L^{(-)}$, $\delta_L^{(+)}$, R_L, T_L and the complex energy techniques developed in Chapter (3) are used to reduce these quantities to a Breit-Wigner resonance form.

A novel feature of this approach is the introduction of a complex energy:

$$E = E_{QL} + \frac{i\Gamma_{QL}}{2} ,$$

where γ_{qL} may be positive, negative or zero. Such a complex energy is the natural consequence of demanding that solutions of equation (5.1) represent incoming and transmitted waves only. When the second barrier is larger than the first in Figure (26) γ_{qL} is positive, whilst when the first barrier is larger than the second one γ_{qL} is negative. When the two barriers are of equal size γ_{qL} is zero. Clearly γ_{qL} may be interpreted in terms of the relative fluxes through the two barriers. The calculations described in this Chapter complement those in reference (24) where a complex energy approach was not used and where only the transmission coefficient T_L was calculated. The equations given here also correctly take the 'orbiting singularity' into account.

5.2 SEMICLASSICAL ANALYSIS

Semiclassical expressions for the transmission coefficient T_L, reflection coefficient R_L and phase shifts $\delta_L^{(-)}$ and $\delta_L^{(+)}$ that occur in the boundary condition (5.2) are determined in this Section and their properties described. The next Section shows how these quantities may be reduced to Breit-Wigner form by the application of complex boundary conditions.

The physical boundary condition to be imposed is that in the region $s \gg c_{2L}$ there is only a transmitted wave:

$$\left(\frac{k^{(-)}}{k^{(+)}}\right)^{1/2} T_L \exp\left[ik^{(+)}s + i2\delta_L^{(+)}\right], \tag{5.3}$$

where T_L and $\delta_L^{(+)}$ are as yet unknown quantities. In semiclassical form the expression (5.3) may be written:

$$\left(\frac{k^{(-)}}{k_L(s)}\right)^{1/2} T_L \exp\left\{-i\int_s^\infty \left[k_L(s') - k^{(+)}\right] ds'\right\} \exp\left[ik^{(+)}s + i2\delta_L^{(+)}\right], \tag{5.4}$$

(5.4) may now be reexpressed in terms of the phase reference point c_{2L} (or b_{2L} when $E > V_{nL}(b_{2L})$):

$$\left(\frac{k^{(-)}}{k_L(s)}\right)^{1/2} T_L \exp\left\{ i\int_{c_{2L}}^{s} k_L(s')ds' - i\int_{c_{2L}}^{\infty}[k_L(s)-k^{(+)}]ds + ik^{(+)}c_{2L} + 2i\delta_L^{(+)}\right\}. \qquad (5.5)$$

The expression (5.5) is now in a convenient form for application of parabolic connection formulae for a barrier, equations (2.13) and (2.14). Successive application of the connection formulae across the turning points gives (5.6) as the semiclassical solution valid for $s \ll a_{1L}$:

$$\left(\frac{k^{(-)}}{k_L(s)}\right)^{1/2} T_L \exp\left\{ -i\int_{c_{2L}}^{\infty}[k_L(s)-k^{(+)}]ds + ik^{(+)}c_{2L} - i\frac{\pi}{4} + i2\delta_L^{(+)}\right\}$$

$$\times\left[A_r \exp\left\{ i\int_{s}^{a_{1L}} k_L(s')ds' - i\frac{\pi}{4}\right\} + A_i \exp\left\{ -i\int_{s}^{a_{1L}} k_L(s')ds' + i\frac{\pi}{4}\right\}\right], \qquad (5.6)$$

in which

$$A_r = e^{-\pi\varepsilon_{2L}} e^{i[\alpha_L(E)-\phi_1]}\left[1+e^{-2\pi\varepsilon_{1L}}\right]^{1/2}$$

$$+ e^{-\pi\varepsilon_{1L}} e^{-i[\alpha_L(E)-\phi_2]}\left[1+e^{-2\pi\varepsilon_{2L}}\right]^{1/2}, \qquad (5.7)$$

and

$$A_i = e^{-\pi(\varepsilon_{1L}+\varepsilon_{2L})} e^{i\alpha_L(E)}$$

$$+ e^{-i[\alpha_L(E)-(\phi_1+\phi_2)]} [1+e^{-2\pi\varepsilon_{1L}}]^{1/2} [1+e^{-2\pi\varepsilon_{2L}}]^{1/2}, \quad (5.8)$$

$\alpha_L(E)$ denotes the phase integral:

$$\alpha_L(E) = \int_{\varepsilon_{1L}}^{a_{2L}} k_L(s)ds \quad (5.9)$$

and ϕ_1 is the quantum correction function (2.15):

$$\phi_1 \equiv \phi(\varepsilon_{1L}) = \varepsilon_{1L} + \arg\Gamma^{-1}(\tfrac{1}{2}+i\varepsilon_{1L}) - \varepsilon_{1L}\ln|\varepsilon_{1L}|,$$

with

$$\varepsilon_{1L} = \frac{E - V_{nL}(b_{1L})}{\hbar\omega_{1L}^*} \quad (5.10)$$

where ω_{1L}^* is the classical frequency of oscillation in the upturned barrier; ϕ_2 and ε_{2L} are similarly defined for the second barrier. When the collision energy lies above either of the barriers in Figure (26) the appropriate classical turning points in (5.6)-(5.9) are to be replaced by b_{1L} or b_{2L}. Equation (5.6) may be written in a form that is suitable

for comparison with the boundary conditions (5.2):

$$\left(\frac{k^{(-)}}{k_L(s)}\right)^{1/2} T_L \left[A_r \exp\left\{ i\int_{-\infty}^{a_{1L}} [k_L(s)-k^{(-)}]ds + ik^{(-)}a_{1L} + ik^{(+)}c_{2L} - i\frac{\pi}{2} - i\int_{c_{2L}}^{\infty} [k_L(s)-k^{(+)}]ds + i2\delta_L^{(+)} - ik^{(-)}s \right\} \right.$$

$$\left. + A_i \exp\left\{ -i\int_{-\infty}^{a_{1L}} [k_L(s)-k^{(-)}]ds - ik^{(-)}a_{1L} + ik^{(+)}c_{2L} - i\int_{c_{2L}}^{\infty} [k_L(s)-k^{(+)}]ds + i2\delta_L^{(+)} + ik^{(+)}s \right\} \right]. \tag{5.11}$$

Comparing the incident wave of (5.11) with the incident wave of (5.2) allows T_L and $\delta_L^{(+)}$ to be determined:

$$T_L = |A_i|^{-1}, \tag{5.12}$$

$$2\delta_L^{(+)} = \int_{-\infty}^{a_{1L}} [k_L(s)-k^{(-)}]ds + \int_{c_{2L}}^{\infty} [k_L(s)-k^{(+)}]ds + k^{(-)}a_{1L} - k^{(+)}c_{2L} - \arg A_i + (L+1)\pi. \tag{5.13}$$

From equation (5.8), equation (5.12) becomes:

$$T_L = e^{\pi(\varepsilon_{1L}+\varepsilon_{2L})} \left[1 + T_1^2 T_2^2 + 2T_1T_2 \cos\{2\alpha_L(E) - (\phi_1+\phi_2)\} \right]^{-1/2}, \tag{5.14}$$

where

$$T_1 \equiv T(\varepsilon_{1L}) = \left[1 + e^{2\pi\varepsilon_{1L}}\right]^{1/2},$$

$$T_2 \equiv T(\varepsilon_{2L}) = \left[1 + e^{2\pi\varepsilon_{2L}}\right]^{1/2}.$$

Use of the identity:

$$\tan^{-1}\left[\frac{a\sin(\alpha-\phi)-\sin\alpha}{a\cos(\alpha-\phi)+\cos\alpha}\right] = -\frac{\phi}{2}+\tan^{-1}\left[\frac{a-1}{a+1}\tan(\alpha-\tfrac{\phi}{2})\right], \quad (5.15)$$

allows $\delta_L^{(+)}$ to be written:

$$2\delta_L^{(+)} = \int_{-\infty}^{a_{1L}}[k_L(s)-k^{(-)}]ds + \int_{c_{2L}}^{\infty}[k_L(s)-k^{(+)}]ds + k^{(-)}a_{1L}-k^{(+)}c_{2L}-\tfrac{1}{2}(\phi_1+\phi_2)+(L+1)\pi$$

$$+\tan^{-1}\left[\frac{T_1T_2-1}{T_1T_2+1}\tan\{\alpha_L(E)-\tfrac{1}{2}(\phi_1+\phi_2)\}\right]. \quad (5.16)$$

In a similar manner comparing the reflected wave in (5.11) with the reflected wave of (5.2) allows the identifications:

$$R_L = T_L|Ar|,$$

$$= [1-T_L^2]^{1/2}, \quad (5.17)$$

and for the elastic phase shift:

$$2\delta_L^{(-)} = \int_{-\infty}^{a_{1L}}[k_L(s)-k^{(-)}]ds - \int_{c_{2L}}^{\infty}[k_L(s)-k^{(+)}]ds + k^{(-)}a_{1L}+k^{(+)}c_{2L}-\frac{\pi}{2}+2\delta_L^{(+)}+\arg Ar,$$

which from equations (5.7) and (5.16) and the identity (5.15) becomes:

$$2\delta_L^{(-)} = 2\int_{-\infty}^{a_{1L}} [k_L(s) - k^{(-)}]\,ds + 2k^{(-)}a_{1L} - \phi_1 + (L+\tfrac{1}{2})\pi$$

$$+ \tan^{-1}\left[\frac{T_1T_2-1}{T_1T_2+1}\tan\left\{\alpha_L(E) - \tfrac{1}{2}(\phi_1+\phi_2)\right\}\right] + \tan^{-1}\left[\frac{T_1/T_2-1}{T_1/T_2+1}\tan\left\{\alpha_L(E) - \tfrac{1}{2}(\phi_1+\phi_2)\right\}\right]. \quad (5.18)$$

The important results of this Section are equation (5.14) for the transmission coefficient (and hence equation (5.17) for the reflection coefficient), equation (5.16) for the reactive phase shift and equation (5.18) for the elastic phase shift. All these formulae contain the quantum correction functions ϕ_1 and ϕ_2. It is clear from the discussion in the previous Chapters that their presence exactly cancels the orbiting singularities contained in the phase integrals.

When $E \gg V_{nL}(b_{1L})$ and $E \gg V_{nL}(b_{2L})$ equation (5.14) shows that the transmission coefficient rapidly approaches the classical value of unity. If $\varepsilon_{1L} \gg 0$ then T_L equals $[1 + \exp(-2\pi\varepsilon_{2L})]^{-\frac{1}{2}}$ and likewise

for $\varepsilon_{2L} \gg 0$, $T_L = [1 + \exp(-2\pi\varepsilon_{1L})]^{-\frac{1}{2}}$; these expressions are just those for the transmission coefficient through a single barrier. For energies in the region $E < V_{nL}(b_{1L})$ and $E < V_{nL}(b_{2L})$, equation (5.14) shows that the transmission coefficient passes through a series of maxima which become increasingly sharp as the energy drops below the barrier maxima. A typical maximum value of equation (5.14) is given by:

$$T_L^{max} = \frac{e^{\pi(\varepsilon_{1L} + \varepsilon_{2L})}}{T_1 T_2 - 1},$$

when the condition:

$$\alpha_L(\varepsilon_{qL}) = (q + \tfrac{1}{2})\pi + \tfrac{1}{2}(\phi_1 + \phi_2), \quad q = 0, 1, 2, \ldots \qquad (5.19)$$

holds. It is shown in the next Section that the Bohr-Sommerfeld quantization condition (5.19) determines the resonance energies of the quasi-stationary states. The condition for maximum transmission is thus that the incident energy is in resonance with one of the quasi-stationary energy levels in the dip.

Comparing the reactive phase shift of equation (5.16) with the corresponding result for the two turning point problem of Chapter (4) (equation (4.40)), it is clear that the presence of the dip is accounted for by the arctangent term in (5.16). For $\xi_{1L} \gg 0$ so that $T_1 \to \infty$, the last term becomes $\alpha_L(E) - \frac{1}{2}\phi_2$ (recall that $\phi_1(\phi_2) \to 0$ for $\xi_{1L}(\xi_{2L}) \to \pm\infty$) and the phase shift is:

$$2\delta_L^{(+)} = \int_{-\infty}^{a_{1L}} [k_L(s) - k^{(-)}]\,ds + \int_{c_{1L}}^{\infty} [k_L(s) - k^{(+)}]\,ds + k^{(-)}a_{1L} - k^{(+)}c_{1L} + \alpha_L(E) - \phi_2 + (L+1)\pi. \tag{5.20}$$

Equation (5.20) is the same as that derived for a single barrier, that is the influence of the well on the scattering has become negligible. When $T_2 \to \infty$ an equation similar to equation (5.20) holds but with ϕ_1 replacing ϕ_2. When $T_1 \to 1$ and $T_2 \to 1$, that is for collision energies below the barrier maxima, the factor $(T_1T_2 - 1)/(T_1T_2 + 1)$ is small and the contribution from the arctangent is constant unless the resonance condition (5.19) holds in which case $\delta_L^{(+)}$ rapidly increases by $\pi/2$ on passing through a resonance.

The limiting behaviour of $\delta_L^{(-)}$ can be discussed in a similar manner. If $T_1 \to \infty$ the last two terms

of equation (5.18) give a contribution $2[\alpha_L(E)-\frac{1}{2}\phi_2]$ to the phase shift, which becomes equivalent to that for a single barrier (in this case the second barrier in Figure (26)). When $T_2 \to \infty$ the last two terms of the phase shift are of opposite sign and cancel leaving the phase shift for a single barrier (this time the first barrier in the Figure). The behaviour of equation (5.18) for $T_1 \to 1$ is similar to that for $T_2 \to \infty$. When $T_2 \to 1$, the last two terms become equal and the phase shift reduces to:

$$2\delta_L^{(+)} = 2\int_{-\infty}^{a_{1L}} [k_L(s)-k^{(+)}]ds + 2k^{(+)}a_{1L} - \phi_1 + (L+\tfrac{1}{2})\pi \qquad (5.21)$$

$$+ 2\tan^{-1}\left[\frac{T_1-1}{T_1+1}\tan[\alpha_L(E)-\tfrac{1}{2}\phi_1]\right].$$

Equation (5.21) is just the expression for the phase shift deduced for orbiting collisions in Chapter (3) (equations (3.17)-(3.19)). When $T_1 = T_2$ as is the case for a symmetrical potential, the last term vanishes identically. Notice that the sign of the last term differs according to $T_1/T_2 > 1$ or

$T_1/T_2 < 1$.

In deriving equations (5.6) and (5.11), it has been assumed that the classically accessible range $c_{1L} \leqslant s \leqslant a_{2L}$ within the dip is sufficiently large for the semiclassical approximation to hold there. For energies near the minimum in $V_{nL}(s)$ this condition must break down since this range then tends to zero. A complete treatment of this problem would then employ parabolic connection formulae for a well to derive the form of T_L, R_L, $\delta_L^{(+)}$, $\delta_L^{(-)}$. However from a practical standpoint the previous treatment may be considered valid for the lowest energies of interest unless the potential is markedly anharmonic in the region of the dip. For energies above one or both barrier maxima, it follows from the discussion of Chapter (2) that the range in which the semiclassical solutions may be used decreases as the energy increases, but as T_L, R_L, $\delta_L^{(+)}$, $\delta_L^{(-)}$ rapidly approach their values in the absence of a dip, equations (5.6) and (5.11) may be considered valid in this region also. It may happen however that the dip in the potential barrier is so slight that the present method of regarding the four-turning-point problem as a composite of two two-

turning-point regions is invalid and another approach is then required.

5.3 COMPLEX ENERGY FORMALISM

Since the potential walls surrounding the dip are not infinitely high and wide, the system may tunnel through the barriers and disintegrate. Complex energy techniques similar to those developed in Chapter (3) may therefore be used to characterize the quasi-stationary states.

In the first case consider the boundary condition that solutions of equation (5.1) represent outgoing waves only at $s = \pm\infty$. This boundary condition is realized by setting the amplitude of the incoming wave of equation (5.11) to zero (that is $A_i = 0$) so that only the reflected and transmitted components remain. This operation leads to the Bohr-Sommerfeld quantization condition:

$$\int_{c_{1L}}^{a_{1L}} k_L(s)\,ds = (q+\tfrac{1}{2})\pi + \tfrac{1}{2}(\phi_1+\phi_2) - \tfrac{i}{2}\ln T_1 T_2 , \qquad (5.22)$$

with $q = 0,1,2,\ldots$. Physically the most interesting case is when the quasi-stationary states possess small widths compared with their separation. The imaginary term on the right hand side of equation

(5.22) is then small in magnitude. Following the development of Chapter (3), equation (5.22) may be characterized in terms of the complex energy:

$$E = E_{qL} - i\Gamma_{qL}/2 \quad , \quad \Gamma_{qL} > 0, \qquad (5.23)$$

with the physical interpretation that the system decays according to the exponential law $\exp(-\Gamma_{qL}t/\hbar)$. Inserting equation (5.23) into the left hand side of equation (5.22) and expanding to first order in Γ_{qL} gives:

$$\int_{c_{1L}}^{a_{2L}} k_L(s)\,ds \approx \frac{1}{\hbar}\int_{c_{1L}}^{a_{2L}} [2(E_{qL} - V_{nL}(s))]^{1/2}\,ds - \frac{i\Gamma_{qL}\pi}{2\hbar\omega_{qL}}, \qquad (5.24)$$

where ω_{qL} is the classical angular frequency of oscillation in the well:

$$\omega_{qL} = \pi \Big/ \int_{c_{1L}}^{a_{2L}} [2(E_{qL} - V_{nL}(s))]^{-1/2}\,ds .$$

If the minimum is quadratic in s then $\alpha_L(s)$ may be integrated directly in which case (5.24) is exact. Comparing the real and imaginary parts of (5.22) and (5.24) gives:

$$\frac{1}{\hbar}\int_{C_{1L}}^{a_{2L}}\left[2(E_{qL}-V_{nL}(s))\right]^{1/2}ds = (q+\tfrac{1}{2})\pi + \tfrac{1}{2}(\phi_{1q}+\phi_{2q}), \qquad (5.25)$$

$$\Gamma_{qL} = \frac{\hbar\omega_{qL}}{\pi}\ln T_{1q}T_{2q}, \qquad (5.26)$$

and the subscript q on ϕ and T indicates that E has been replaced by E_{qL} since terms arising from the imaginary part of E on the right hand side of equation (5.22) may be neglected to this order of approximation. Comparing equation (5.25) with equation (5.19) shows that the condition for maximum transmission is that the incident energy is in exact resonance with one of the energy levels in the dip.

Considering now the case where the incident energy is near to a resonance:

$$E = E_{qL} + \delta E,$$

where E_{qL} and δE are both real and following the derivation of equation (5.24):

$$\int_{c_{1L}}^{a_{2L}} k_L(s)\,ds \approx \frac{1}{\hbar}\int_{c_{1L}}^{a_{2L}} [2(E_{qL} - V_{nL}(s))]^{1/2}\,ds + \frac{(\delta E)\pi}{\hbar\omega_{qL}} \qquad (5.27)$$

Equation (5.27) together with equations (5.25) and (5.26) may be used to reduce the transmission coefficient (5.14) and the reactive phase shift (5.16) to Breit-Wigner form. For example from equation (5.27) the transmission coefficient becomes:

$$T_L = e^{\pi(\varepsilon_{1qL} + \varepsilon_{2qL})}\left[(T_{1q}T_{2q} - 1)^2 + 4T_{1q}T_{2q}\{(\delta E)\pi/\hbar\omega_{qL}\}^2\right]^{-1/2}, \qquad (5.28)$$

which from equation (5.26) and the result:

$$\ln T_{1q}T_{2q} \approx (T_{1q}T_{2q} - 1)/\sqrt{T_{1q}T_{2q}},$$

allows equation (5.28) to be written:

$$T_L^2 = \frac{1}{X_{qL}} \cdot \frac{(\Gamma_{qL}/2)^2}{(\Gamma_{qL}/2)^2 + (E_{qL} - E)^2}, \qquad (5.29)$$

where

$$X_{qL} = \frac{(T_{1q}T_{2q} - 1)^2}{e^{2\pi(\varepsilon_{1qL} + \varepsilon_{2qL})}}.$$

$X_{qL} \gtrless 1$ is a measure of the asymmetry of the potential. It becomes unity for a symmetrical potential where $\varepsilon_{1qL} = \varepsilon_{2qL}$. From equations (5.29) and (4.31) the reaction cross section is given by:

$$\sigma^{(+)} = \frac{\pi}{k^{(+)2}} \sum_{L} \frac{2L+1}{X_{qL}} \frac{(\Gamma_{qL}/2)^2}{(\Gamma_{qL}/2)^2 + (\epsilon_{qL} - \epsilon)^2} . \qquad (5.30)$$

Equation (5.30) is an equation of the Breit-Wigner type and clearly illustrates the resonance behaviour of the reaction cross section.

An important quantity that is related to the reaction cross section is the rate constant.[32] Assuming an initial Boltzmann distribution of states Child[24] showed that the high and low temperature behaviour of the rate constant followed an Arrhenius temperature dependence. This observation may be related to more formal results. At high temperatures, where tunnelling may be neglected, the calculations described in reference (24) form a concrete example of a vibrationally adiabatic derivation of transition state theory.[31-33] Eu and Ross[83], using Wigner's R matrix theory, have shown that a sufficient condition for the derivation of transition state theory is the existence of a collision complex whose energy levels

possess small widths compared with their separation. This is clearly the case for resonance tunnelling reactions at low temperatures.

In a similar manner to that described above the reactive phase shift may be reduced to the Breit-Wigner form:

$$\delta_L^{(+)} = \delta_L^{(0)} + \tfrac{1}{2}\tan^{-1}\left[\frac{\Gamma_{qL}}{2(E_{qL}-E)}\right], \qquad (5.31)$$

where Γ_{qL} is given by equation (5.26) and $\delta_L^{(0)}$ is the non-resonant contribution to the phase shift in equation (5.16).

It is also clear that the first arctangent term in the elastic phase shift (5.18) may also be reduced to the Breit-Wigner form of equation (5.31). The second arctangent term may also be reduced to a Breit-Wigner form by applying a 'forward moving waves' only boundary condition to solutions of equation (5.1). Setting $A_r = 0$ in equation (5.11) leads to the quantization condition:

$$\int_{c_{1L}}^{a_{2L}} K_L(s)\,ds = (q+\tfrac{1}{2})\pi + \tfrac{1}{2}(\phi_1+\phi_2) + \tfrac{i}{2}\ln\frac{T_1}{T_2}. \qquad (5.32)$$

Restricting attention to the case when the imaginary term in equation (5.32) is small and introducing the complex energy:

$$E = E_{qL} + i\gamma_{qL}/2 , \tag{5.33}$$

into the left hand side of (5.32), expanding to first order in γ_{qL} and comparing real and imaginary parts gives:

$$\frac{1}{\hbar}\int_{c_{1L}}^{a_{2L}} [2(E_{qL} - V_{nL}(s))]^{1/2}\, ds = (q+\tfrac{1}{2})\pi + \tfrac{1}{2}(\phi_{1q}+\phi_{2q}) , \tag{5.34}$$

$$\gamma_{qL} = \frac{\hbar\omega_{qL}}{\pi} \ln \frac{T_{1q}}{T_{2q}} . \tag{5.35}$$

Equation (5.34) for the resonance energies is equal to that previously derived, equation (5.25). Equation (5.35) for the width γ_{qL} shows that γ_{qL} may be positive, negative or zero depending on the magnitude of T_{1q} relative to that of T_{2q}. A complex energy with an imaginary part possessing such properties has not been considered before. The behaviour of γ_{qL} may be rationalized as follows. This complex energy arises from the boundary condition that there is only an incident wave and

a transmitted wave. The time dependence of the system $\exp(\gamma_{qL}t/\hbar)$ therefore provides a measure of the flux of particles through the first barrier and the loss of particles through the second barrier. When the barriers have the same dimensions the flux of particles through the first barrier equals that through the second barrier, $T_{1q} = T_{2q}$ and from equation (5.35) $\gamma_{qL} = 0$. When the second barrier is larger than the first one, more particles will tunnel through the first barrier than will leak through the second barrier and the net effect will be an increase with time in the number of particles in the well, $T_{1q} > T_{2q}$ and $\gamma_{qL} > 0$. Likewise if the first barrier is larger than the second one $T_{1q} < T_{2q}$ and $\gamma_{qL} < 0$.

Returning to the real energy case it may be shown that following the lines of the derivation of equations (5.29) and (5.31), the elastic phase shift may be reduced to the Breit-Wigner form:

$$\delta_L^{(-)} = \delta_L^{(0)} + \tfrac{1}{2}\tan^{-1}\frac{\Gamma_{qL}}{2(E_{qL}-E)} + \tfrac{1}{2}\tan^{-1}\frac{\gamma_{qL}}{2(E_{qL}-E)}.$$

It may be noticed that as $T_{2q} \to 1$, Γ_{qL} and γ_{qL} become equal and equivalent to the width derived in the case of orbiting collisions, equation (3.40).

CHAPTER SIX: REACTIVE MOLECULAR COLLISIONS - TWO DIMENSIONAL MODEL

6.1 INTRODUCTION

In the preceding two Chapters a model system for the reactive molecular collision:

$$A + BC = AB + C,$$

was developed in which the three atoms are constrained to move along a straight line but with the whole system free to rotate in three dimensions. The effect of the initial BC rotations on the reaction was therefore ignored. This Chapter describes a model system in which the BC rotations are taken into account but with the following restrictions: firstly in order to simplify the discussion of angular momenta, the atoms are constrained to move in a plane and secondly B is taken to have an infinite mass so that the same coordinates may be used on both sides of the reaction. The coordinate system is shown in Figure (27).

Child[27] has shown how this model may be used to calculate reaction cross sections and here the relevant theory is developed for differential cross sections. The theory follows similar lines to that described in Chapter (4). Natural collision coordinates s and v are introduced to replace r_A and r_C of

Figure 27

The coordinate system for the two dimensional model of reactive molecular collisions.

C
rC
x
θC
θA
y
B
rA
A

Figure (27) and an adiabatic separation of variables is used to reduce the problem to the solution of three one dimensional Schrödinger equations. These correspond with motion along the reaction coordinate s, the purely vibrational motion of the atoms, and the internal rotational motion of the atoms. The internal rotation reduces to the free rotation of the BC or AB molecules at the beginning or end of the reaction respectively and for those reactions in which the initial BC rotation is quenched as the reaction proceeds, with the bending vibration of the ABC complex at $s \approx 0$. Alternatively the rotational motion of BC may remain essentially free in the transition state region.

In the way the theory is developed, the wavefunction for the internal rotational motion satisfies a differential equation with non-periodic boundary conditions. A detailed analysis is made of this equation with the aid of Floquet's theorem.[84] Semiclassical expressions for the internal energy levels are derived using the parabolic connection formulae of Chapter (2).

A partial wave analysis of the reactive and elastic scattering amplitudes allows the respective cross sections to be determined. It is shown that

for free internal rotational motion in the transition state region each partial wave has the same angular part,which gives rise to an isotropic reactive differential cross section,but this is not (in general) the case for reactions which proceed via a preferred configuration,where each partial wave has a different angular part.

The theory described in this Chapter is developed in such a way as to bring out the connection with two dimensional elastic scattering from a central potential. An account of two dimensional elastic scattering is given in Appendix (B).

6.2 HAMILTONIAN AND BOUNDARY CONDITIONS

The classical kinetic energy T for the system shown in Figure (27) is given by:

$$2T = \dot{q}_A^2 + \dot{q}_C^2 + q_A^2\dot{\theta}_A^2 + q_C^2\dot{\theta}_C^2 , \qquad (6.1)$$

where q_A and q_C denote the mass weighted coordinates:

$$q_A = m_A^{\frac{1}{2}} r_A,$$

$$q_C = m_C^{\frac{1}{2}} r_C,$$

and m_A and m_C are the masses of A and C respectively. The total angular momentum of the system is:

$$q_A^2\dot{\theta}_A + q_C^2\dot{\theta}_C,$$

$$= I\omega,$$

where I is the total moment of inertia of the system:

$$I = q_A^2 + q_C^2,$$

and ω is defined by:

$$\omega = [q_A^2\theta_A + q_C^2\theta_C]/I . \qquad (6.2)$$

In terms of ω and the angle χ defined by:

$$\chi = \theta_A - \theta_C , \qquad (6.3)$$

the kinetic energy expression (6.1) may be written:

$$2T = \dot{q}_A^2 + \dot{q}_C^2 + I\dot{\omega}^2 + I^*\dot{\chi}^2, \qquad (6.4)$$

where I^* is a reduced moment of inertia:

$$I^* = q_A^2 q_C^2 / I .$$

Since the potential energy U of the system is of the form:

$$U = U(q_A, q_C, \chi),$$

ω is the ignorable coordinate associated with the conservation of total angular momentum. However for the immediate development of the theory, the form (6.1) is more convenient than (6.4) since the quantum mechanical boundary conditions are more simply written in terms of $q_A, q_C, \theta_A, \theta_C$ than q_A, q_C, ω, χ.

Introducing the conjugate momentum $p_\alpha = \partial T / \partial \dot{\alpha}$ allows (6.1) to be written:

$$2T = p_{q_A}^2 + p_{q_C}^2 + \frac{1}{q_A^2} p_{\theta_A}^2 + \frac{1}{q_C^2} p_{\theta_C}^2 . \qquad (6.5)$$

From equation (6.5) the corresponding quantum mechanical hamiltonian may be written down by means of equation (4.9). The choice of volume element is

$q_A q_C dq_A dq_C d\theta_A d\theta_C$, that is the mass weighted two dimensional space. The hamiltonian is:

$$\mathcal{H} = -\frac{\hbar^2}{2}\left\{ \frac{1}{q_A}\frac{\partial}{\partial q_A} q_A \frac{\partial}{\partial q_A} + \frac{1}{q_C}\frac{\partial}{\partial q_C} q_C \frac{\partial}{\partial q_C} + \frac{1}{q_A^2}\frac{\partial^2}{\partial \theta_A^2} + \frac{1}{q_C^2}\frac{\partial^2}{\partial \theta_C^2} \right\} + U(q_A, q_C, \theta_A - \theta_C), \tag{6.6}$$

and the Schrödinger equation:

$$\mathcal{H}\Psi = E\Psi .$$

The boundary condition satisfied by Ψ is:

$$\left.\begin{aligned} \Psi \underset{q_A \to \infty}{\sim} & e^{ik^{(-)} q_A \cos\theta_A} q_C^{-1/2} \xi_n(q_C) e^{ij^{(-)}\theta_C} + \sum_{k^{(-)}, j^{(-)}, n} \frac{e^{ik^{(-)} q_A}}{\sqrt{q_A}} \cdot q_C^{-1/2} \xi_n(q_C) e^{ij^{(-)}\theta_C} f^{(-)}(\theta_A), \\ \underset{q_C \to \infty}{\sim} & \sum_{k^{(+)}, j^{(+)}, n} \frac{e^{ik^{(+)} q_C}}{\sqrt{q_C}} q_A^{-1/2} \xi_n(q_A) e^{ij^{(+)}\theta_A} f^{(+)}(\theta_C) . \end{aligned}\right\} \tag{6.7}$$

The first term in (6.7) represents the motion of A by a plane wave moving in the positive x direction with BC in the rotational state $j^{(-)}$ (with eigenfunction $\exp(ij^{(-)}\theta_C)$, $j^{(-)} = 0, \pm 1, \pm 2, \ldots$) and vibrational state n (with eigenfunction $q_C^{-\frac{1}{2}}\xi_n(q_C)$, $n = 0, 1, 2, \ldots$). The second term corresponds with elastic and non-reactive inelastic scattering and the third term corresponds with reactive scattering.

$f^{(-)}(\theta_A)$ and $f^{(+)}(\theta_C)$ are the corresponding scattering amplitudes and $k^{(-)}$ and $k^{(+)}$ the respective mass reduced wave numbers. As in Chapter (4), the notation used in the boundary condition (6.7) anticipates the further development of the theory where it will be shown that it is only necessary to consider an initial elastic channel and a final reactive channel.

The hamiltonian (6.6) may be simplified by the substitution:

$$\psi = (q_A q_C)^{1/2} \Phi , \tag{6.8}$$

with the result:

$$H = -\frac{\hbar^2}{2}\left\{ \frac{\partial^2}{\partial q_A^2} + \frac{\partial^2}{\partial q_C^2} + \frac{1}{q_A^2}\frac{\partial^2}{\partial \theta_A^2} + \frac{1}{q_C^2}\frac{\partial^2}{\partial \theta_C^2} \right\} + V(q_A, q_C, \theta_A - \theta_C), \tag{6.9}$$

where

$$V(q_A, q_C, \theta_A - \theta_C) = U(q_A, q_C, \theta_A - \theta_C) - \hbar^2/2I^* .$$

The Schrödinger equation is:

$$H\psi = E\psi ,$$

and from (6.7) and (6.8) the boundary condition obeyed by ψ is:

$$\left.\begin{aligned}\psi \underset{q_A\to\infty}{\sim} & \; q_1^{-1/2} e^{ik^{(-)}q_A\cos\theta_A}\xi_n(q_C)e^{ij^{(-)}\theta_C} + \sum_{k^{(-)},j^{(-)},n} e^{ik^{(-)}q_A}\xi_n(q_C)e^{ij^{(-)}\theta_C}f^{(-)}(\theta_A), \\ \underset{q_C\to\infty}{\sim} & \sum_{k^{(+)},j^{(+)},n} e^{ik^{(+)}q_C}\xi_n(q_A)e^{ij^{(+)}\theta_A}f^{(+)}(\theta_C).\end{aligned}\right\} \quad (6.10)$$

Natural collision coordinates s and v are now introduced to replace q_A and q_C, as discussed in Chapter (4):

$$\left.\begin{aligned} s &= -q_A\cos\alpha + q_C\sin\alpha, \\ v &= q_A\sin\alpha + q_C\cos\alpha, \end{aligned}\right\} \quad (6.11)$$

where the angle α is shown in Figure (6). In the present case where B has an infinite mass, the angle of skewing $\gamma = 90^{\circ}$. Substituting (6.11) into (6.9) and with neglect of the curvature terms, the hamiltonian becomes:

$$H = -\frac{\hbar^2}{2}\left\{\frac{\partial^2}{\partial s^2} + \frac{\partial^2}{\partial v^2} + \frac{1}{q_1^2}\frac{\partial^2}{\partial\theta_1^2} + \frac{1}{q_C^2}\frac{\partial^2}{\partial\theta_C^2}\right\} + V(s, v, \theta_A - \theta_C), \quad (6.12)$$

and the boundary condition (6.10) becomes:

$$\left.\begin{aligned}\psi \underset{s\to-\infty}{\sim} & \sqrt{-s}\, e^{-ik^{(+)}s\cos\theta_A} \xi_n(v) e^{ij^{(+)}\theta_C} + \sum_{k^{(+)},j^{(+)},n} e^{-ik^{(+)}s} \xi_n(v) e^{ij^{(+)}\theta_C} f^{(+)}(\theta_A), \\ & \\ \underset{s\to+\infty}{\sim} & \sum_{k^{(+)},j^{(+)},n} e^{ik^{(+)}s} \xi_n(v) e^{ij^{(+)}\theta_A} f^{(+)}(\theta_C),\end{aligned}\right\} \quad (6.13)$$

Although the boundary conditions are simply written in terms of s, v, θ_A, θ_C these latter two coordinates are not convenient for the further development of the theory because they do not take advantage of the conservation of angular momentum. To this end, the coordinates ω and χ defined by equaticns (6.2) and (6.3) are introduced to replace θ_A and θ_C. The hamiltonian becomes:

$$H = -\frac{\hbar^2}{2}\left\{\frac{\partial^2}{\partial s^2} + \frac{\partial^2}{\partial v^2} + \frac{1}{I}\frac{\partial^2}{\partial \omega^2} + \frac{1}{I^*}\frac{\partial^2}{\partial \chi^2}\right\} + V(s, v, \chi), \quad (6.14)$$

By separation of variables in equation (6.14), every solution may be written as the partial wave sum:

$$\psi(s, v, \chi, \omega) = \sum_{L=-\infty}^{\infty} A_L \Psi_L(s, v, \chi) e^{iL\omega}, \quad (6.15)$$

where L is the total angular momentum quantum number and A_L is a constant to be chosen so that the boundary condition (6.13) is satisfied.

As an example of the partial wave expansion (6.15) consider the initial asymptotic limit in the boundary condition (6.13). From Appendix (B) the asymptotic form of the two dimensional plane wave partial wave expansion is:

$$\sqrt{-s}\, e^{-ik^{(-)}s\cos\theta_A} \sim \frac{1}{\sqrt{2\pi i k^{(-)}}} \sum_{\ell^{(-)}=-\infty}^{\infty} e^{i\ell^{(-)}\theta_A}\left[e^{-ik^{(-)}s} + e^{ik^{(-)}s + i(\ell^{(-)}+1)\pi}\right],$$

where $\ell^{(-)}$ is the initial orbital angular momentum quantum number. The first term in (6.13) may therefore be written:

$$\frac{\xi_n(v)}{\sqrt{2\pi i k^{(-)}}} \sum_{L=-\infty}^{\infty} e^{-i[j^{(-)}-g_L]\chi}\left[e^{-ik^{(-)}s} + e^{ik^{(-)}s + i(L-j^{(-)}+1)\pi}\right] e^{iL\omega}, \qquad (6.16)$$

where the summation over $\ell^{(-)}$ has been changed to one over L:

$$L = \ell^{(-)} + j^{(-)},$$

and g_L denotes the quantity:

$$g_L = \frac{Lq^2}{I}.$$

Operating on the partial wave expansion (6.15) by the hamiltonian (6.14) gives an equation obeyed by $\psi_L(s,v,\chi)$:

$$\left\{-\frac{\hbar^2}{2}\left[\frac{\partial^2}{\partial s^2}+\frac{\partial^2}{\partial v^2}+\frac{1}{I^*}\frac{\partial^2}{\partial \chi^2}\right]+\frac{L^2\hbar^2}{2I}+V(s,v,\chi)-E\right\}\psi_L(s,v,\chi)=0. \quad (6.17)$$

In the next section it is shown how, with the aid of an adiabatic separation of variables, $\psi_L(s,v,\chi)$ may be written as the product:

$$\psi_L(s,v,\chi) = S_{Lnj\epsilon}(s)\,\xi_{Ln}(s;v)\,f_{Lj\epsilon}(s;\chi), \quad (6.18)$$

where $S_{Lnj\epsilon}(s)$ is the wavefunction for motion along the reaction coordinate, $\xi_{Ln}(s;v)$ is the wavefunction for the internal vibrational motion of the atoms and $f_{Lj\epsilon}(s;\chi)$ is the wavefunction for the internal rotational motion of the atoms. From the asymptotic representations of the wavefunctions in the product (6.18), the scattering amplitudes may be determined.

6.3 ADIABATIC SEPARATION OF VARIABLES

This Section shows how an adiabatic separation of variables reduces equation (6.17) to three one dimensional Schrödinger equations in the variables s, v, and χ.

Following the development of Chapter (4) internal wavefunctions $\phi_{Lt}(s;v,\chi)$ are defined by:

$$\left[-\frac{\hbar^2}{2}\frac{\partial^2}{\partial v^2} - \frac{\hbar^2}{2I^*}\frac{\partial^2}{\partial \chi^2} + \frac{L^2\hbar^2}{2I} + V(s,v,\chi)\right]\phi_{Lt} = V_{Lt}(s)\,\phi_{Lt}, \qquad (6.19)$$

where $V_{Lt}(s)$ is the internal energy of the system. Since the $\phi_{Lt}(s;v,\chi)$ form a complete set at each s, $\psi_L(s,v,\chi)$ may be expanded in the form:

$$\psi_L(s;v,\chi) = \sum_t S_{Lt}(s)\,\phi_{Lt}(s;v,\chi),$$

whence the $S_{Lt}(s)$ satisfy:

$$\left[-\frac{\hbar^2}{2}\frac{d^2}{ds^2} + V_{Lt}(s) - E\right]S_{Lt}(s) = \sum_{t'} C_{Ltt'}(s)\,S_{Lt}(s), \qquad (6.20)$$

where

$$C_{Ltt'}(s) = \frac{\hbar^2}{2}\iint \phi^*_{Lt}\frac{\partial^2}{\partial s^2}\phi_{Lt'}\,dv\,d\chi + \hbar^2\iint \phi^*_{Lt}\frac{\partial}{\partial s}\phi_{Lt'}\,dv\,d\chi\,\frac{\partial}{\partial s}, \qquad (6.21)$$

Neglect of the coupling terms (6.21) means that the system always stays in the same internal state (since this approximation neglects rotational transitions it is expected to be rather poor in practice) and equation (6.20) simplifies to:

$$\left[-\frac{\hbar^2}{2}\frac{d^2}{ds^2} + V_{Lt}(s) - \epsilon\right] s_{Lt}(s) = 0. \tag{6.22}$$

The boundary conditions satisfied by equation (6.22) are taken in the form:

$$\left.\begin{aligned} s_{Lt}(s) &\underset{s\to-\infty}{\sim} e^{ik^{(-)}s + i(L-j^{(-)}+\frac{1}{2})\pi} + R_L e^{2i\delta_L^{(-)}} e^{-ik^{(-)}s}, \\ &\underset{s\to+\infty}{\sim} \left(\frac{k^{(-)}}{k^{(+)}}\right)^{1/2} T_L e^{2i\delta_L^{(+)}} e^{ik^{(+)}s}, \end{aligned}\right\} \tag{6.23}$$

where the first term represents an incoming wave (with phase determined by equation (6.16)) and the second and third terms represent elastically and reactively scattered waves. Semiclassical methods for the determination of the phase shifts $\delta_L^{(+)}$ and $\delta_L^{(-)}$ and the reflection and transmission coefficients R_L and T_L for various choices of profile for

$V_{Lt}(s)$ have been described in Chapters (4) and (5).

In order to solve equation (6.19) for the internal motion it is assumed that at a given value of s:

$$V(s,v,\chi) = V(s,v) + V(s,\chi),$$

that is vibration-rotation interactions have been neglected. In this case equation (6.19) separates into an equation for the internal vibrations and one for the internal rotations:

$$\phi_{Lt}(s;v,\chi) = \xi_{Ln}(s;v) f_{Lj\epsilon l}(s;\chi), \tag{6.24}$$

$$V_{Lt}(s) = V_{Ln}(s) + V_{Lj\epsilon l}(s). \tag{6.25}$$

The Schrödinger equation for the internal vibrations is:

$$\left[-\frac{\hbar^2}{2}\frac{\partial^2}{\partial v^2} + \frac{L^2\hbar^2}{2I} + V(s,v)\right]\xi_{Ln}(s;v) = V_{Ln}(s)\xi_{Ln}(s;v), \tag{6.26}$$

and that for the internal rotations:

$$\left[\frac{-\hbar^2}{2I_e}\frac{\partial^2}{\partial\chi^2} + V(s,\chi)\right] f_{Lj\epsilon l}(s;\chi) = V_{Lj\epsilon l}(s) f_{Lj\epsilon l}(s;\chi), \tag{6.27}$$

and I_e^* indicates that I^* has been replaced by its equilibrium value at $v = v_e$.

An approximate solution of equation (6.26) is obtained by replacing I with I_e and assuming that $V(s,v)$ is a quadratic function in $v - v_e$, so that $\zeta_{Ln}(s;v)$ is a harmonic oscillator function and the internal energy $V_{Ln}(s)$ is:

$$V_{Ln}(s) = \frac{L^2\hbar^2}{2I_e} + (n+\tfrac{1}{2})\hbar\omega \qquad n = 0, 1, 2, \cdots \qquad (6.28)$$

where ω is the classical vibration frequency.

Equation (6.25) shows that the barrier to reaction along the reaction coordinate has four contributions (1) the variation of the original potential surface along the reaction coordinate, (2) the centrifugal barrier associated with the conservation of angular momentum, (3) the change in internal vibrational energy for a given vibrational state. Contributions (2) and (3) are explicitly illustrated by equation (6.28), (4) the change in the internal rotational energy for a given rotational state as the reaction proceeds.

Contributions (1)-(3) were found previously in Chapters (4) and (5). The internal rotational energy is obtained from equation (6.27). The solution

of this equation is more difficult than that for the internal vibrational states and is considered in the next Section.

6.4 INTERNAL ROTATIONAL STATES

From the previous Section the equation to be solved is:

$$\left[-\frac{\hbar^2}{2I_e^*} \frac{d^2}{d\chi^2} + V(s,\chi) \right] f_{Lj\omega}(s;\chi) = V_{Lj\omega}(s) f_{Lj\omega}(s;\chi), \qquad (6.29)$$

where the potential $V(s,\chi)$ is periodic in χ. For a system in which the ABC complex forms a linear preferred configuration ($\chi = \pi$) for example, a Fourier analysis of $V(s,\chi)$ gives for the first two terms:

$$V(s,\chi) = \frac{H(s)}{2}(1 + \cos\chi) . \qquad (6.30)$$

Typically H(s) takes its maximum value for $s \approx 0$ and tends to zero as $s \to \pm\infty$.

Consider now the boundary condition obeyed by $f_{Lj\omega}(s;\chi)$. The coordinates ω and χ were chosen in such a way so as to avoid a cross term between them in the kinetic energy (6.4). The coupling still exists however and is apparent in the boundary conditions. In the theory of hindered rotations this approach forms part of the 'internal axis method'.[85,86]

Since $V(s,\chi)$ is periodic in χ Floquet's theorem states that a particular solution of equation (6.29) will have the form:[84]

$$f_{Lj+1}(s;\chi) = e^{i\sigma\chi}P(\chi), \tag{6.31}$$

where $P(\chi)$ is periodic in χ and σ is a real constant (the characteristic exponent). σ may be found by considering the total angular part of the wavefunction $u(\theta_A,\theta_C)$ where:

$$U(\theta_A,\theta_C) = f_{Lj+1}(s;\chi)\,e^{iL\omega}. \tag{6.32}$$

Making the changes:

$$\theta_A \rightarrow \theta_A + 2\pi n_1,$$

$$\theta_C \rightarrow \theta_C + 2\pi n_2,$$

where n_1 and n_2 are integers, it is clear that since the physical situation is unchanged, the total angular part of the wavefunction is also unchanged.

$$u(\theta_A,\theta_C) = u(\theta_A+2\pi n_1,\theta_C+2\pi n_2), \tag{6.33}$$

Substituting equations (6.31) and (6.32) into equation (6.33) it follows that:

$$\frac{L}{I}(n_1 q_A^2 + n_2 q_C^2) + \sigma(n_1-n_2) = n, \tag{6.34}$$

where n is an integer. Equation (6.34) therefore determines σ :

$$\sigma = \frac{n - n_1 L}{n_1 - n_2} + g_L , \tag{6.35}$$

where $g_L = Lq_C^2/I$ is the quantity introduced previously. Since n_1 and n_2 (and n) are arbitrary, a convenient choice is that which makes the first term on the right hand side of equation (6.35) zero so that $\sigma = g_L$ and equation (6.31) gives:

$$f_{Lj\Theta l}(s;\chi) = e^{ig_L\chi} P(\chi) . \tag{6.36}$$

For an increase in χ of 2π equation (6.36) shows that the boundary condition obeyed by $f_{Lj\Theta l}(s,\chi)$ takes the form:

$$f_{Lj\Theta l}(s;\chi+2\pi) = e^{2\pi i g_L} f_{Lj\Theta l}(s;\chi) , \tag{6.37}$$

$$= e^{-2\pi i h_L} f_{Lj\Theta l}(s;\chi) , \tag{6.38}$$

where $h_L = Lq_A^2/I$. Notice also that $g_L + h_L = L$.

Solutions of equation (6.29) may be obtained in the limiting cases of $H(s) \to 0$ and $H(s) \to \infty$.

In the first instance suppose $H(s) = 0$; this is the case of free internal rotation. Equation (6.29)

becomes:

$$\frac{d^2f}{d\chi^2} = -c^2 f, \tag{6.39}$$

where

$$c = \left[\frac{2I_e^* V_{Lj^{(-)}(S)}}{\hbar^2}\right]^{1/2}.$$

The solutions of equation (6.39) are:

$$f = e^{\pm ic\chi}. \tag{6.40}$$

It is also evident that

$$P(\chi) = e^{-ij^{(-)}\chi},$$

where $j^{(-)}$ is an integer, so that from equation (6.36):

$$f_{Lj^{(-)}(S;\chi)} = e^{-i[j^{(-)}-g_L]J\chi}. \tag{6.41}$$

Comparing with equation (6.40) gives:

$$\pm c = -j^{(-)} + g_L,$$

from which:

$$V_{Lj^{(-)}(S)} = \frac{[j^{(-)}-g_L]^2 J^2 \hbar^2}{2I_e^*}. \tag{6.42}$$

At the beginning of the reaction $g_L = 0$ and equation (6.42) gives the energy of rotation of the BC molecule. All levels are two fold degenerate except $j^{(+)} = 0$ (the degeneracy corresponds with the two possible directions of rotation). As g_L increases in value however this degeneracy is removed until at certain values of g_L, equation (6.42) shows that the energy levels cross each other in pairs.[27,87] This happens when $j_1 + j_2 = 2g_L$ and since j_1 and j_2 are integers, the crossings occur for g_L having integer values (when j_1 and j_2 have the same parity) or half integer values (when j_1 and j_2 have opposite parity).

Equations (6.41) and (6.42) are in a form suitable for the reactants side of the collision since $g_L \to 0$ as $s \to -\infty$. On the products side of the reaction, the solution of equation (6.29) in the free rotation case may be likewise written:

$$f_{Lj^{(+)}}(s;\chi) = e^{i[j^{(+)} - h_L]\chi}, \qquad (6.43)$$

and the energy is:

$$W_{Lj^{(+)}}(s) = \frac{[j^{(+)} - h_L]^2 \hbar^2}{2I_e^*},$$

where $j^{(+)}$ is the final rotational angular momentum

quantum number of AB, which is related to L by:

$$L = \ell^{(+)} + j^{(+)},$$

where $\ell^{(+)}$ is the final orbital angular momentum quantum number of C.

When there is free rotation throughout the course of the reaction, the wavefunctions (6.41) and (6.43) are equivalent so that:

$$-j^{(-)} + g_L = j^{(+)} - h_L,$$

from which:

$$\left.\begin{aligned} j^{(+)} &= \ell^{(-)} \\ \ell^{(+)} &= j^{(-)} \end{aligned}\right\} \qquad (6.44)$$

that is the initial orbital angular momentum of A becomes the final rotational angular momentum of AB and the initial rotational angular momentum of BC becomes the final orbital angular momentum of C. However if the initially free rotational motion of BC at $s = -\infty$ becomes quenched at $s \approx 0$, the above simple correlation no longer holds.

The second limiting case for which solutions of equation (6.29) may be obtained is when the internal energy is much less than the barrier height. The

motion takes place within such a small range of χ that the exponential in equation (6.36) will be practically constant. $P(\chi)$ on the other hand will be rapidly varying in this region. The internal wavefunction may therefore be written:

$$f_{Lj\theta}(s;\chi) = e^{ig_L\chi_e} X_q(\chi-\chi_e), \qquad (6.45)$$

where χ_e is the equilibrium value of χ and $X_q(\chi-\chi_e)$ is a harmonic oscillator wavefunction for example. This may be seen for the potential (6.30) for example by expanding the cosine up to powers of χ^2 around the point $\chi_e = \pi$. Equation (6.45) provides the connection with the fixed orientation model described in Chapter (4). The exponential factor in equation (6.45) may be removed by measuring θ_c from the preferred configuration, so that $\chi_e = 0$.

When $V(s,\chi)$ does not take one of the limiting forms described above, exact solutions of equation (6.29) will in general require numerical methods. Approximate expressions for the energy levels may however be obtained semiclassically by means of the parabolic connection formulae derived in Chapter (2). The m fold barrier problem has been treated by Miller[41] . His results are incomplete

however because they do not include the quantum correction function $\phi(\varepsilon)$. The necessary extension is given below. Child has explicitly considered the one and two barrier cases.[27,87] The use of matrix notation leads to an elegant solution.[41]

Figure (28) illustrates the symmetrical three barrier case and for definiteness this example is considered in the first instance.

In region I, the wavefunction may be written:

$$f_I(x) = \frac{c_1}{\sqrt{k(x)}} \exp\left\{ -i\int_{x}^{x_1} k(x')dx' \right\} + \frac{c_2}{\sqrt{k(x)}} \exp\left\{ i\int_{x}^{x_1} k(x')dx' \right\}, \qquad (6.46)$$

and in region II:

$$f_{II}(x) = \frac{c_4}{\sqrt{k(x)}} \exp\left\{ -i\int_{x_2}^{x} k(x')dx' \right\} + \frac{c_3}{\sqrt{k(x)}} \exp\left\{ i\int_{x_2}^{x} k(x')dx' \right\}, \qquad (6.47)$$

where in equations (6.46) and (6.47):

$$k(x) = \left\{ \frac{2I_e^*}{\hbar^2} \left[V_{ij\ldots}(s) - V(s,x) \right] \right\}^{1/2}.$$

From Chapter (2), the connection between the coefficients c_1, c_2 and c_3, c_4 is:

$$\begin{pmatrix} c_3 \\ c_4 \end{pmatrix} = D \begin{pmatrix} c_1 \\ c_2 \end{pmatrix}, \qquad (6.48)$$

Figure 28

The barrier to internal rotation in the symmetrical three fold case.

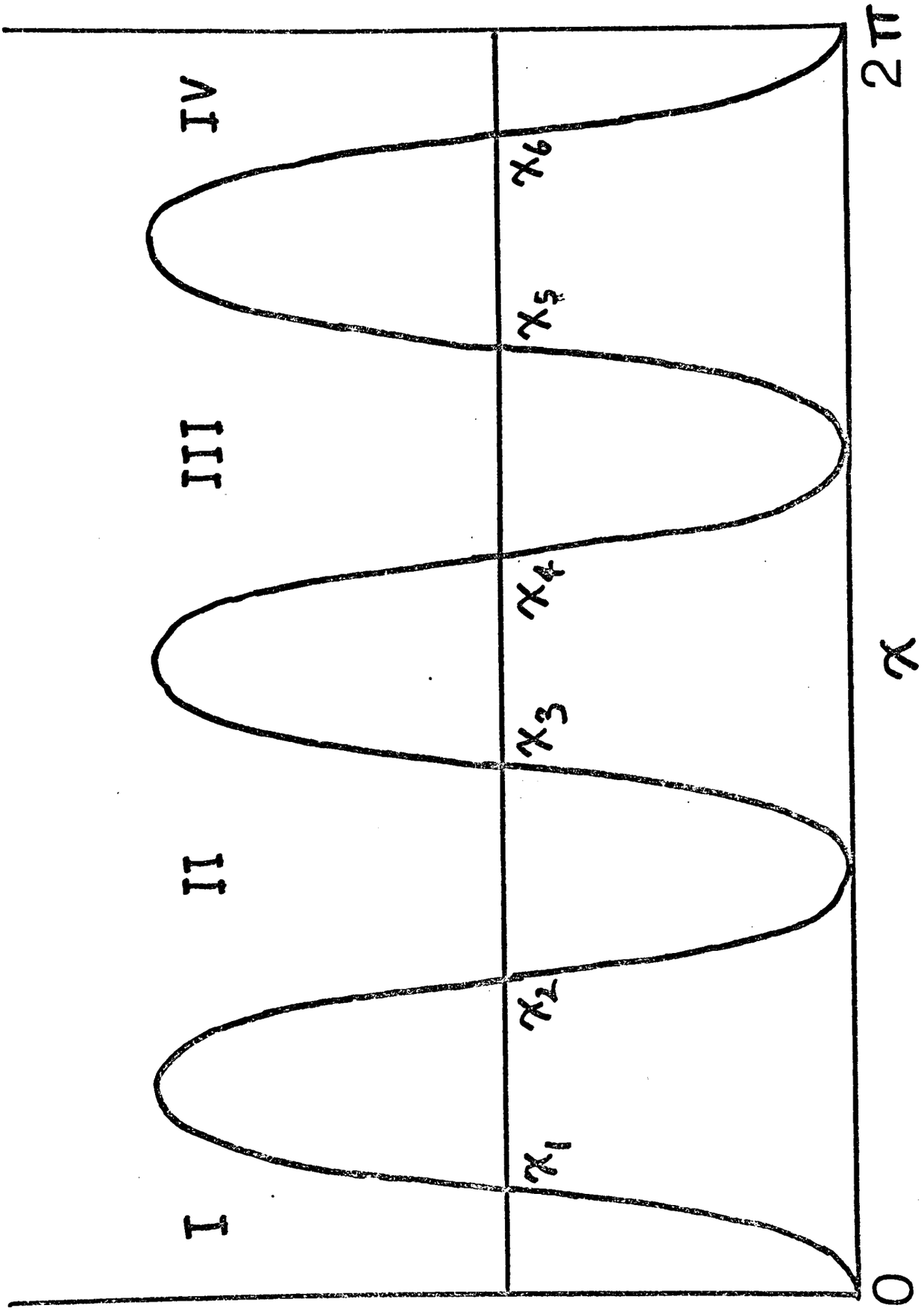
IV
III
II
I
α_6
α_5
α_4
α_3
α_2
α_1
2π
0
α

where

$$D = \begin{pmatrix} \left[1+e^{-2\pi\varepsilon}\right]^{1/2} e^{-i\phi} & -ie^{-\pi\varepsilon} \\ ie^{-\pi\varepsilon} & \left[1+e^{-2\pi\varepsilon}\right]^{1/2} e^{i\phi} \end{pmatrix}, \qquad (6.49)$$

and ε is the reduced energy displacement variable introduced in Chapter (2). In region IV the wavefunction is:

$$f_{IV}(x) = \frac{c_8}{\sqrt{k(x)}} \exp\left\{-i\int_{x_b}^{x} k(x')dx'\right\} + \frac{c_7}{\sqrt{k(x)}} \exp\left\{i\int_{x_1}^{x} k(x')dx'\right\}, \qquad (6.50)$$

and repeated use of the connections (6.48) and (6.49) allows c_7, c_8 to be related to c_1, c_2.

$$\begin{pmatrix} c_7 \\ c_8 \end{pmatrix} = D\,B\,D\,B\,D \begin{pmatrix} c_1 \\ c_2 \end{pmatrix}, \qquad (6.51)$$

where

$$B = \begin{pmatrix} e^{i\alpha} & 0 \\ 0 & e^{-i\alpha} \end{pmatrix},$$

where α is the usual phase integral across the well. The boundary condition (6.37) is taken in the form:

$$f_{L,j(L)}(s;2\pi) = e^{2\pi i g_L} f_{L,j(L)}(s;0). \qquad (6.52)$$

Using equations (6.46) and (6.50), the boundary condition (6.52) is equivalent to:

$$\begin{pmatrix} c_3 \\ c_4 \end{pmatrix} = e^{i2\pi g_L} B^{-1} \begin{pmatrix} c_1 \\ c_2 \end{pmatrix}. \qquad (6.53)$$

Equating equations (6.51) and (6.53) gives:

$$\left(DBDBD - e^{2\pi i g_L} B^{-1} \right) \begin{pmatrix} c_1 \\ c_2 \end{pmatrix} = 0.$$

This has non-trivial values for c_1 and c_2 only if:

$$\det\left(DBDBD - e^{2\pi i g_L} B^{-1} \right) = 0,$$

or equivalently (since $\det(B) \neq 0$):

$$\det\left((DB)^3 - e^{2\pi i g_L} \right) = 0.$$

This is the result for a three fold potential barrier. It is clear that the result for an m fold barrier is:

$$\det\left((DB)^m - e^{2\pi i g_L} \right) = 0, \qquad (6.54)$$

or if the potential barriers and wells are not all the same:

$$\det\left((DB)_1 (DB)_2 \cdots (DB)_m - e^{2\pi i g_L} \right) = 0,$$

with a different ε_i, α_i for each barrier and well.

Since det(D) = det(B) = 1, equation (6.54) is equivalent to:

$$Tr\,(DB)^m = 2\cos(2\pi g_L). \tag{6.55}$$

A trace is invariant under a similarity transformation:

$$Tr\,(DB)^m = Tr\,(UDBU^{-1})^m,$$

and if U is chosen so that $UDBU^{-1}$ is diagonal then the diagonal elements of $UDBU^{-1}$ are the eigenvalues of DB. In this way it is found that:

$$Tr\,(DB)^m = 2\cos(m\theta), \tag{6.56}$$

where

$$\cos\theta = (1+e^{-2\pi\varepsilon})^{1/2}\cos(\alpha-\phi(\varepsilon)).$$

From equations (6.55) and (6.56), the quantization condition for the internal rotational energy levels is:

$$\cos[\alpha-\phi(\varepsilon)] = [1+e^{-2\pi\varepsilon}]^{-1/2}\cos\left[\tfrac{2\pi}{m}(j^{(-)}-g_L)\right],$$

where $j^{(-)} = 0, \pm1, \pm2, \ldots$ and for the alternative boundary condition (6.38), the quantization condition is:

$$\cos[\alpha-\phi(\varepsilon)] = [1+e^{-2\pi\varepsilon}]^{-1/2}\cos\left[\tfrac{2\pi}{m}(j^{(+)}-h_L)\right],$$

where $j^{(+)} = 0, \pm1, \pm2, \ldots$.

When the height of the barrier tends to zero so that $\varepsilon \to \infty$ the above quantization conditions yield the free rotation results previously derived (for example equation (6.42)). As the height of the barriers increase on the other hand so that $\varepsilon \to -\infty$ then the usual Bohr-Sommerfeld quantization condition for a well is obtained.

6.5 SCATTERING AMPLITUDES

In Section (6.3), it has been shown how an adiabatic separation of variables allows the partial wave expansion of the total wavefunction to be written:

$$\psi(s,v,\chi,w) = \sum_L A_L S_{Lnj^{(\epsilon)}}(s)\, \xi_{Ln}(s;v) f_{Lj^{(\epsilon)}}(s;\chi) e^{iLw}. \qquad (6.57)$$

Inserting the initial asymptotic limit for $S_{Lnj^{(\epsilon)}}(s)$ equation (6.23), and for $f_{Lj^{(\epsilon)}}(s;\chi)$ equation (6.41), into equation (6.57) and comparing with equation (6.16) allows A_L to be determined, namely:

$$A_L = \frac{1}{\sqrt{2\pi i k^{(\epsilon)}}}.$$

In a similar manner, if the asymptotic limits for $S_{Lnj^{(\epsilon)}}(s)$ and $f_{Lj^{(\epsilon)}}(s;\chi)$ for the elastically and reactively scattered waves are substituted into equation (6.57), comparison with the boundary condition (6.13) and equation (6.16) allows the elastic and reactive scattering amplitudes to be determined. The results are:

$$f^{(\epsilon)}(\theta_A) = \frac{1}{\sqrt{2\pi i k^{(\epsilon)}}} \sum_L e^{-ij^{(\epsilon)}\theta_c} e^{-i(j^{(\epsilon)}-g_L)\chi} \left[R_L e^{2i\delta_L^{(\epsilon)}} - 1\right] e^{iLw},$$

$$f^{(+)}(\theta_c) = \frac{1}{\sqrt{2\pi i k^{(+)}}} \sum_L e^{-ij^{(+)}\theta_A} e^{i(j^{(+)}-h_L)\chi} T_L e^{2i\bar{\delta}_L^{(+)}} e^{iL\omega},$$

or reverting back to the angles θ_A and θ_C from ω and χ in the above equations:

$$f^{(-)}(\theta_A) = \frac{1}{\sqrt{2\pi i k^{(-)}}} \sum_L e^{i(L-j^{(-)})\theta_A} \left[R_L e^{2i\delta_L^{(-)}} - 1 \right], \tag{6.58}$$

$$f^{(+)}(\theta_c) = \frac{1}{\sqrt{2\pi i k^{(+)}}} \sum_L e^{i(L-j^{(+)})\theta_c} T_L e^{2i\delta_L^{(+)}}. \tag{6.59}$$

and the differential cross sections are obtained from equations (6.58) and (6.59) by:

$$I^{(-)}(\theta_A) = |f^{(-)}(\theta_A)|^2,$$

$$I^{(+)}(\theta_c) = \frac{k^{(+)}}{k^{(-)}} |f^{(+)}(\theta_c)|^2. \tag{6.60}$$

The elastic scattering amplitude may be further approximated by the semiclassical procedure described in Chapter (4) and Appendix (B).

The treatment accorded the reactive scattering amplitude depends on how the final rotational angular momentum correlates with the initial rotational angular momentum. For the free rotation

case described in Section (6.4) $j^{(+)} = l^{(-)}$ and equation (6.59) becomes:

$$f^{(+)}(\theta_c) = \frac{e^{ij^{(-)}\theta_c}}{\sqrt{2\pi i k^{(+)}}} \sum_L T_L e^{2i\delta_L^{(+)}}.$$

Each partial wave therefore has the same angular part so that the reactive differential cross section (6.60) is:

$$I^{(+)}(\theta_c) = \frac{1}{2\pi k^{(-)}} \left| \sum_L T_L e^{2i\delta_L^{(+)}} \right|^2, \qquad (6.61)$$

that is the differential cross section is isotropic.

On the other hand suppose the initial rotational angular momentum is quenched in the transition state region in such a way that $j^{(+)} = j^{(-)} + c$, where c is a constant (for example c = 0 for a symmetric reaction). Equation (6.59) gives:

$$f^{(+)}(\theta_c) = \frac{e^{-i[j^{(-)}+c]\theta_c}}{\sqrt{2\pi i k^{(+)}}} \sum_L T_L e^{iL\theta_c} e^{2i\delta_L^{(+)}}. \qquad (6.62)$$

In this case each partial wave possesses a different angular part and the standard semiclassical approximations may be applied to equation (6.62) (Chapter (4) and Appendix (B)). The cross section resulting from equation (6.62) will in general be

anisotropic.

The effect of the rotational state of BC on the reactive differential cross section may therefore be described as follows. At low $j^{(-)}$ values the rotational motion of BC will (typically) be quenched as the system enters the transition state and these rotational states will (in general) give rise to an anisotropic contribution to the differential cross section. At high $j^{(-)}$ values however, free rotation in the transition state region will prevail and these states will give an isotropic contribution to the cross section. There will also be an intermediate range of $j^{(-)}$ values in which a transition from anisotropic to isotropic behaviour takes place.

APPENDIX A: NUMERICAL ASPECTS

A.1 INTRODUCTION

This Appendix describes various numerical aspects of the work considered in the remainder of this thesis. All the calculations were programmed in ALGOL on the Physical Chemistry Laboratory's Elliott 903 computer.

A.2 THE INTEGRAL $\int_{-\infty}^{\infty} \exp[i(x^4 + ax)]dx$

The integral:

$$C(a) = \int_{-\infty}^{\infty} \exp[i(x^4+ax)]dx, \qquad (A.1)$$

was encountered in Chapter (4) in connection with the semiclassical description of the cubic rainbow effect. The properties of the integral (A.1) are described in this Section together with its numerical evaluation.

An important property apparent from the definition (A.1) is that C(a) is even in a:

$$C(a) = C(-a).$$

A series expansion, which is used to evaluate C(a), may be obtained as follows. By writing C(a) in the form:

$$C(a) = Dc(a) + Dc(-a) + i[Ds(a) + Ds(-a)], \qquad (A.2)$$

where

$$Dc(a) = \int_0^{\infty} \cos(x^4+ax)dx,$$

$$Ds(a) = \int_0^{\infty} \sin(x^4+ax)dx,$$

reduces C(a) to known integrals. Applying the expansions:[88]

$$\int_0^{\infty} \cos(ax^p + bx^q)\,dx = \frac{1}{p}\sum_{k=0}^{\infty} \frac{(-b)^k}{k!}\, a^{-\left(\frac{kq+1}{p}\right)} \Gamma\left(\frac{kq+1}{p}\right) \cos\left[\frac{k(q-p)+1}{2p}\pi\right],$$

$$\int_0^{\infty} \sin(ax^p + bx^q)\,dx = \frac{1}{p}\sum_{k=0}^{\infty} \frac{(-b)^k}{k!}\, a^{-\left(\frac{kq+1}{p}\right)} \Gamma\left(\frac{kq+1}{p}\right) \sin\left[\frac{k(q-p)+1}{2p}\pi\right],$$

to Dc(a) and Ds(a) gives:

$$Dc(a) = \frac{1}{4}\sum_{k=0}^{\infty} \frac{(-a)^k}{k!}\, \Gamma\left(\frac{k+1}{4}\right) \cos\left[\frac{1-3k}{8}\pi\right], \qquad (A.3)$$

$$= 0.8374 - 0.3133a - 0.0526a^2 + 0.0417a^3 - \ldots,$$

$$Ds(a) = \frac{1}{4}\sum_{k=0}^{\infty} \frac{(-a)^k}{k!}\, \Gamma\left(\frac{k+1}{4}\right) \sin\left[\frac{1-3k}{8}\pi\right], \qquad (A.4)$$

$$= 0.3469 + 0.3133a - 0.1415a^2 - 0.0087a^4 - \ldots.$$

C(a) was evaluated by means of equation (A.2) and summation of the series (A.3) and (A.4). The maximum number of terms the computer could handle was $k \approx 20$ which allowed a determination of C(a) to three significant figures for $0 \lesssim a \lesssim 6$. The gamma functions

were calculated by using the recurrence formula $\Gamma(z+1) = z\Gamma(z)$ to express each gamma function in terms of $\Gamma(z+1)$ with $0 \leqslant z \leqslant 1$ and using a polynomial approximation for the latter.[89] Graphs of Re C(a), Im C(a) and $|C(a)|$ are shown in Figures (29)-(31).

Writing C(-a) in the form:

$$C(-a) = a^{1/3}\int_{-\infty}^{\infty} \exp\left[i a^{4/3}(x^4 - x)\right] dx,$$

allows C(-a) to be evaluated for large values of a by the method of stationary phase.[38] There is only one stationary point in the integrand, namely when $x = 4^{-\frac{1}{3}}$ from which the asymptotic behaviour of C(-a) is found to be:

$$C(-a) \sim \left(\frac{16^{1/3}\pi}{6}\right)^{1/2} \frac{1}{a^{1/3}} \exp\left[i\left(\frac{\pi}{4} - \frac{3}{4^{4/3}} a^{4/3}\right)\right]. \qquad (A.5)$$

The asymptotic behaviour of Re C(a), Im C(a) and $|C(a)|$ according to equation (A.5) is also shown in Figures (29)-(31). The graphs indicate that equation (A.5) may be used with confidence to evaluate C(a) for $a \gtrsim 6$. The plot for $|C(a)|$ illustrates the quantum mechanical rounding off

Figure 29

The solid line represents the function Re C(a), whilst the dashed line is its asymptotic representation.

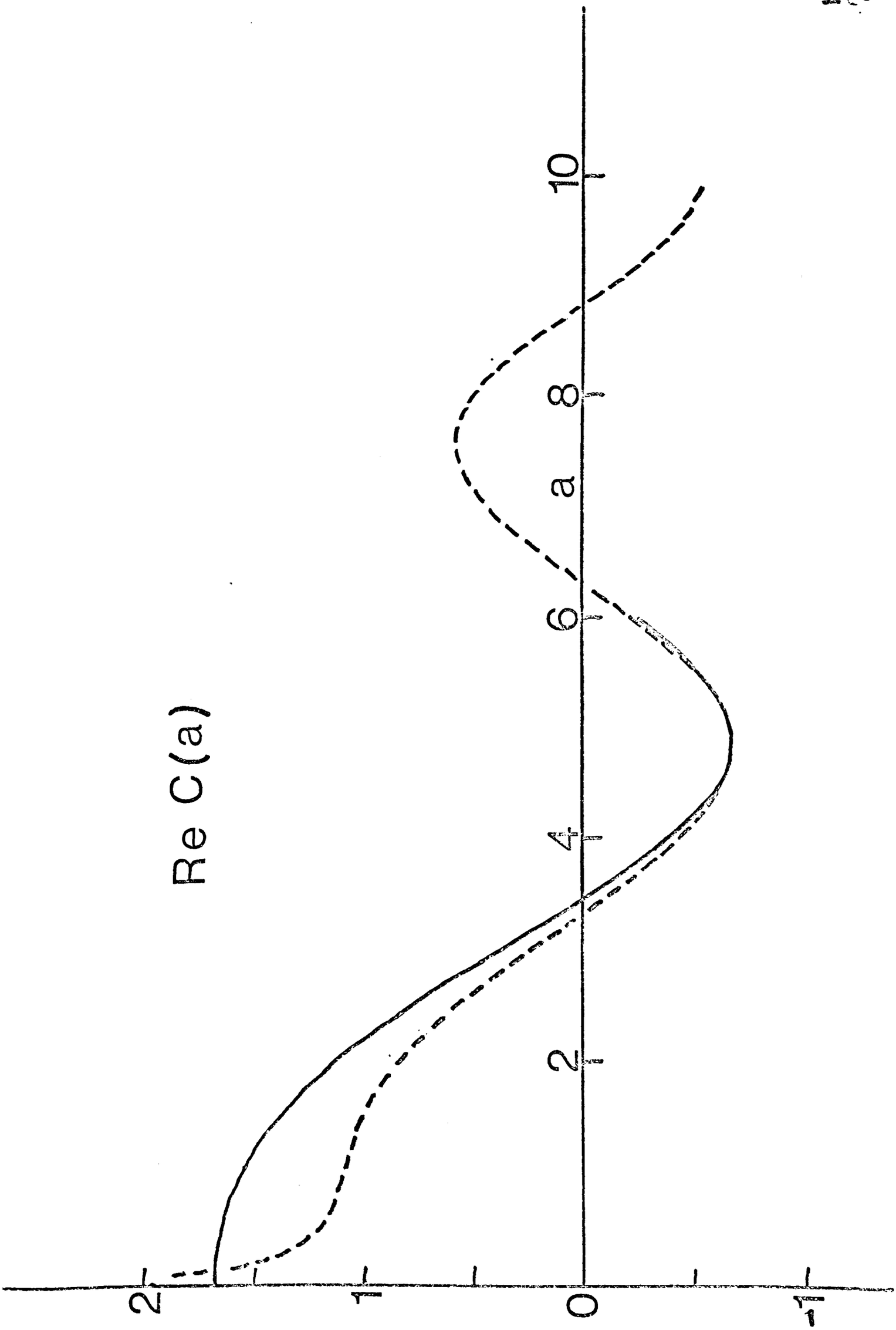
Re C(a)
a
2
4
6
8
10
2
1
0
1

Figure 30

The solid line represents the function Im C(a), whilst the dashed line is its asymptotic representation.

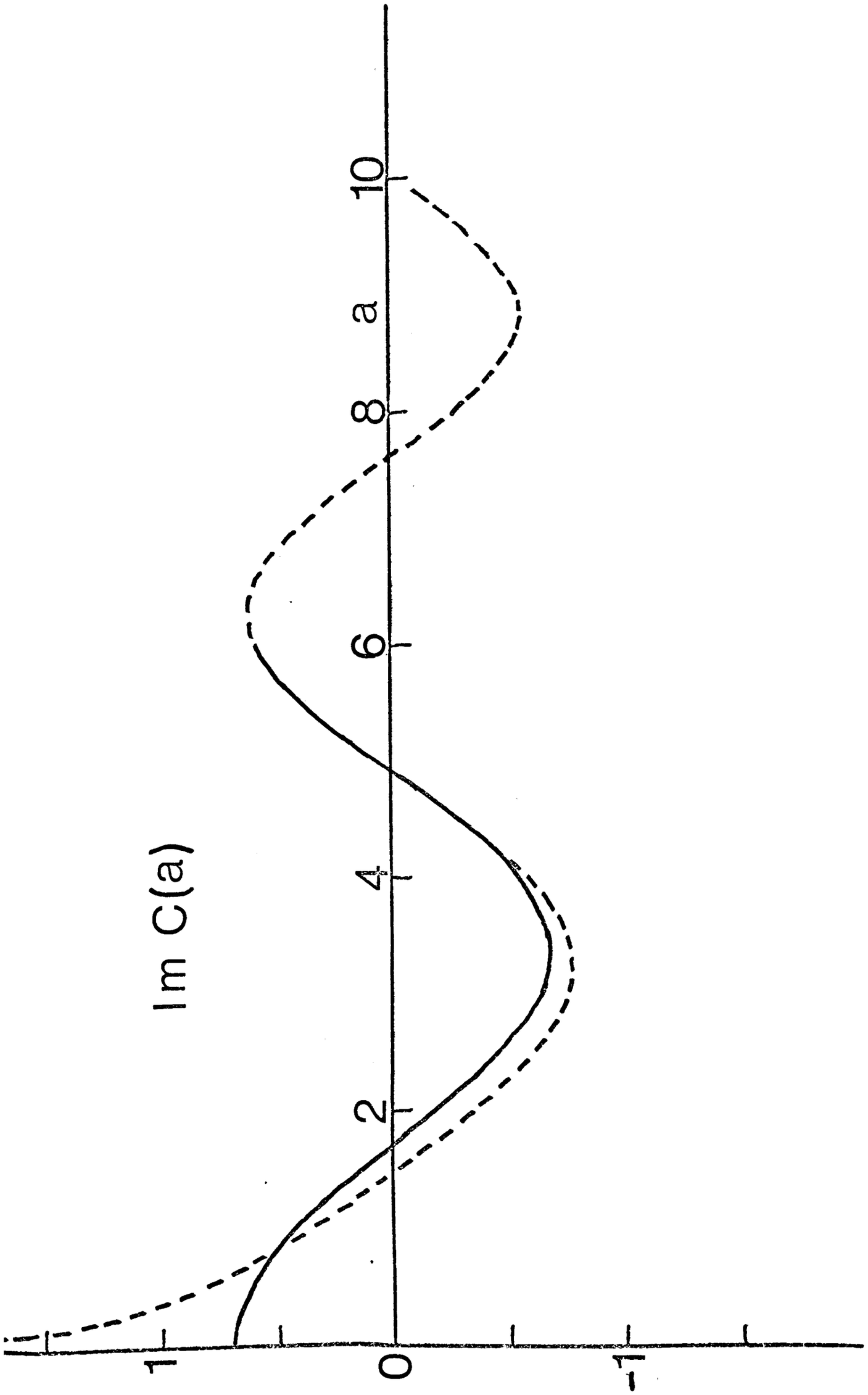
Im C(a)
10
a
8
6
4
2
0
-1
1

Figure 31

The solid line represents the function $|C(a)|$, whilst the dashed line is its asymptotic representation.

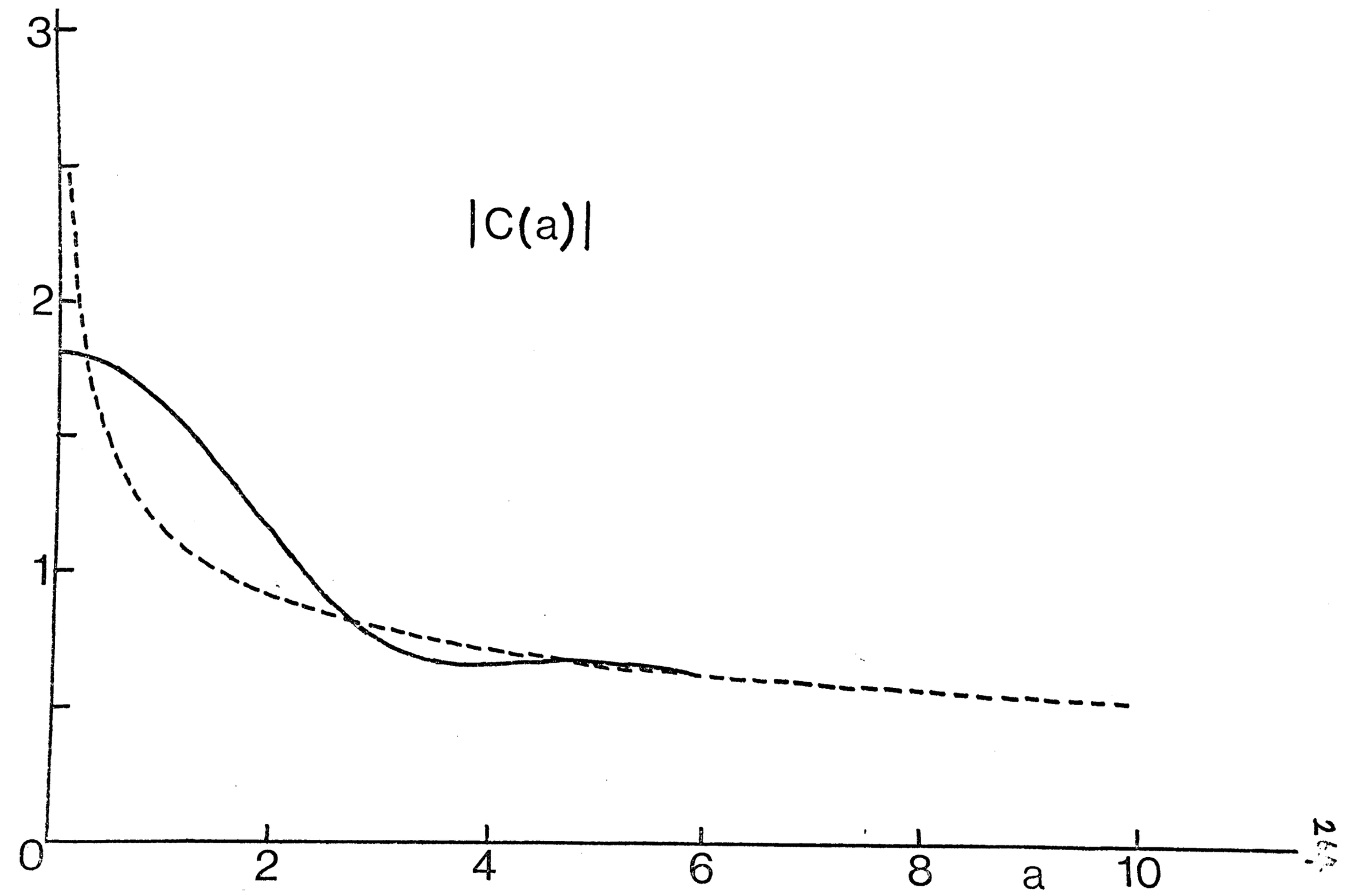
|C(a)|
3
2
1
0
2
4
6
8
a
10

of the classical mechanical infinity discussed in Chapter (4). Note also that the asymptotic form for $|C(a)|$ is monotonic whereas $|C(a)|$ possesses a minimum at $a \approx 3.9$ and a maximum at $a \approx 4.7$. The oscillation is however a weak one. This result is of interest in connection with supernumerary cubic rainbows.

A.3 PHASE SHIFT EVALUATION

Kennedy and Smith[79] have made a systematic investigation of methods for evaluating phase shifts within the semiclassical approximation. They have recommended a modified Clenshaw-Curtis integration procedure which has the advantage of being efficient and accurate and for which it is straightforward to obtain reliable error estimates. However the formulae given by Kennedy and Smith become inefficient for small values of the turning point and break down altogether if the turning point is zero. Other computational methods for semiclassical phase shifts suffer the same disadvantage. A scaled version of the Clenshaw-Curtis method which avoids this difficulty is described below.

In the Clenshaw-Curtis method the interval of integration is first changed to (-1,1) by a linear change of variable so that the integral takes the form:

$$I = \int_{-1}^{1} F(t)\,dt .$$

The integral is expanded in a Chebyshev polynomial series and integrated term by term. However this is equivalent to a quadrature of the form:

$$I_N = \sum_{s=0}^{N} h_s^{(N)} F\left(\cos \frac{\pi s}{N}\right), \qquad (A.6)$$

where the weights $h_s^{(N)}$ are defined by:[90]

$$h_s^{(N)} = \frac{2(-1)^s}{N^2-1} + \frac{4}{N} \sin \frac{s\pi}{N} \sum_{r=1}^{N/2} \frac{\sin\left[(2r-1)s\pi/N\right]}{2r-1}, \quad 1 \leqslant s \leqslant N-1,$$

$$h_s^{(N)} = \frac{1}{N^2-1}, \quad s = 0, N.$$

An estimate of the error is given by:[79]

$$\varepsilon_N = \frac{1}{N} \max\left(|a_N|, |a_{N-2}|, |I_N - I_{N/2}|\right),$$

for $N \geqslant 4$, where

$$|a_N| = \frac{2}{N} \left| \sum_{s=0}^{N}{}'' (-1)^s F\left(\cos \frac{\pi s}{N}\right) \right|, \qquad (A.7)$$

$$|a_{N-2}| = \frac{2}{N} \left| \sum_{s=0}^{N}{}'' (-1)^s \cos\left(\frac{2\pi s}{N}\right) F\left(\cos \frac{\pi s}{N}\right) \right|, \qquad (A.8)$$

and $\sum''$ means that the first and last terms in the summation are halved. Comparing equations (A.7) and (A.8) with equation (A.6) shows that reliable

error estimates may be obtained with little extra work.

From Chapter (4), the phase shift may be written in the form:

$$\bar{\delta} = k \lim_{R\to\infty} \left\{ \int_{r_L}^{R} F_L(r)\,dr - \int_{b}^{R} \left(1 - \frac{b^2}{r^2}\right)^{1/2} dr \right\}, \qquad (A.9)$$

where

$$F_L(r) = \left\{ 1 - \frac{2}{\hbar^2}\frac{V(r)}{k^2} - \frac{[L(L+1)+1]}{k^2(r^2+\sigma_c^2)} \right\}^{1/2},$$

$$b = (L+\tfrac{1}{2})/k .$$

r_L is the zero of the integrand or the top of the barrier when $F_L(r)$ does not possess a real zero.

Before the quadrature (A.6) can be applied the singularities in the integrands of equation (A.9) must be removed. For all cases considered in this thesis $b \geqslant r_L$ and following Kennedy and Smith, equation (A.9) may be transformed to:

$$\delta = k(r_L+\alpha)\int_0^{r_0} F_L(r_1)\frac{\sin\theta}{\cos^2\theta}\,d\theta + kb\int_0^{\pi/2}[F_L(r_2)-\sin\theta]\frac{\sin\theta}{\cos^2\theta}\,d\theta, \qquad (A.10)$$

where

$$r_1 = \frac{r_L+\alpha}{\cos\theta} - \alpha \quad , \quad r_0 = \cos^{-1}\left(\frac{r_L+\alpha}{b+\alpha}\right) \quad , \quad r_2 = \frac{b}{\cos\theta} \quad ,$$

in which α is a scaling factor. Changing the limits in equation (A.10) to (-1,1) and applying the Clenshaw-Curtis formula (A.6) leads to:

$$\delta \approx \frac{k(r_L+\alpha)r_0}{2} \sum_{s=0}^{N-1} h_s^{(N)} F_L(r_3) \frac{\sin\theta_1}{\cos^2\theta_1}$$

$$+ \frac{kb\pi}{4} \sum_{s=1}^{N-1} h_s^{(N)} \left[F_L(b/\cos\theta_2) - \sin\theta_2\right] \frac{\sin\theta_2}{\cos^2\theta_2} \quad . \qquad \text{(A.11)}$$

In equation (A.11):

$$\theta_1 = \frac{r_0}{2}\left(1 + \cos\frac{\pi s}{N}\right) \quad , \quad \theta_2 = \frac{\pi}{4}\left(1 + \cos\frac{\pi s}{N}\right)$$

$$r_0 = \cos^{-1}\left(\frac{r_L+\alpha}{b+\alpha}\right) \quad , \quad r_3 = \frac{r_L+\alpha}{\cos\theta_1} - \alpha \quad .$$

In the computer programme the weights $h_s^{(N)}$ were computed initially and stored for N = 2,4,8,.... . The phase shift was then computed until the error ε_N was less than the permitted error ε . In practice ε was set equal to 0.01 which gives four figure

accuracy for $\delta \geq 10$. For this error it was found that 32 terms were required for small L values (occasionally 64 terms were required) and this reduced to 8 terms for large L values. The computational procedure described above was found to be well suited for this problem. There was no obvious case where the error estimation ε_N failed. A satisfactory choice for the scaling parameter was found to be $\alpha = 5$. The convergence for $r_L \neq 0$ was not affected. The turning points r_L were found by the Newton-Ralphson method.[91]

The computer programme was checked by calculating phase shifts for the lorentzian potential of Chapter (4) and comparing these with the exact results in terms of elliptic integrals.

A.4 DEFLECTION FUNCTION EVALUATION

In Chapter (4) it was shown that the deflection function Θ is related to the phase shift via the semiclassical equivalence relationship:

$$\Theta = 2\frac{\partial\delta}{\partial L}, \tag{A.12}$$

With δ given by equation (A.9), equation (A.12) gives:

$$\Theta = \pi - \frac{2(L+\frac{1}{2})}{k}\int_{r_L}^{\infty}\frac{dr}{(r^2+v_e^2)F_L(r)}, \tag{A.13}$$

Smith[92] has also made a study of methods available for the numerical evaluation of integrals similar to (A.13), and has recommended the use of Gauss-Mehler quadratures. As in the case of the phase shift, Smith's procedure needs scaling to allow for the possibility of r_L being zero (or what is the same thing $v_e \neq 0$).

In the Gauss-Mehler quadrature method the integral to be evaluated is written in the form:

$$I = \int_{-1}^{1}\frac{f(v)dv}{(1-v^2)^{1/2}}, \tag{A.14}$$

and this is approximated by:

$$I_N = \frac{\pi}{N} \sum_{j=1}^{N} f\left(\cos \frac{2j-1}{2N}\pi\right),$$

Unlike the Clenshaw-Curtis method there is no reliable error estimate that is also easy to use in practice. Denoting the integral in equation (A.13) by I:

$$I = \int_{r_L}^{\infty} \frac{dr}{(r^2+v_2^2)\, F_L(r)} ;$$

by change of variable this may be written:

$$I = \frac{r_L+\alpha}{2} \cdot \int_{-1}^{1} \frac{dy}{x^2(r^2+v_2^2)\, F_L(r)} ,$$

where

$$x = \tfrac{1}{2}(1+y) , \qquad r = \frac{r_L+\alpha}{x} - \alpha ,$$

in which α is the scaling factor. From equation (A.14) the expression for the deflection function becomes:

$$\textcircled{H} \approx \pi - \frac{(L+\frac{1}{2})}{k}(r_L+\alpha)\frac{\pi}{N}\sum_{j=1}^{N} f\left(\cos\frac{2j-1}{2N}\pi\right), \qquad (A.15)$$

with

$$f(y) = \frac{\sqrt{1-y^2}}{\pi^2 (r^2+v_\infty^2) F_L(r)} .$$

The choice $\alpha = 10$ was found to be satisfactory. The difference $I_N - I_{N/2}$ was used as an estimate of the error ε_N. The summation in equation (A.15) was computed until $\varepsilon_N < \varepsilon$ with $\varepsilon = 0.001$. However $I_N - I_{N/2}$ is not a reliable error estimate. Several examples were found where this condition failed. To guard against this possibility all values of ⓗ requiring $N < 16$ were recomputed using a smaller error estimate until $N \geqslant 16$.

The deflection function programme was checked by comparison with the exact results for the lorentzian potential of Chapter (4).

APPENDIX B: TWO DIMENSIONAL ELASTIC SCATTERING

B.1 INTRODUCTION

This Appendix presents a discussion of two dimensional elastic scattering from a central potential as there does not appear to be an account available in the literature. In particular the partial wave expansion of the wavefunction is considered together with the semiclassical approximation for the phase shift and the correspondence with two dimensional scattering of classical particles. The results of this Appendix are used in Chapter (6).

B.2 PARTIAL WAVE ANALYSIS

As in the three dimensional case, the two dimensional partial wave analysis proceeds by analogy with the scattering of sound waves.[93] In polar coordinates the two dimensional Schrödinger equation is:

$$\left\{ \frac{1}{r}\frac{\partial}{\partial r} r \frac{\partial}{\partial r} + \frac{1}{r^2}\frac{\partial^2}{\partial \phi^2} + \frac{2\mu}{\hbar^2}\left[E - V(r)\right] \right\} \psi(r,\phi) = 0. \qquad \text{(B.1)}$$

The boundary condition on $\psi(r,\phi)$ is that at large distances it represents an incoming plane wave and an outgoing scattered one:

$$\psi(r,\phi) \sim e^{ikr\cos\phi} + f(\phi)\frac{e^{ikr}}{\sqrt{r}}, \qquad \text{(B.2)}$$

in which $f(\phi)$ is the scattering amplitude. $f(\phi)$ is related to the differential cross section $I(k,\phi)$ and total cross section $\sigma(k)$ by:

$$I(k,\phi) = |f(\phi)|^2,$$

$$\sigma(k) = \int_0^{2\pi} I(k,\phi)\, d\phi .$$

By separation of variables every solution of equation (B.1) may be written as sums of products of the form $R_m(r)\exp(im\phi)/r^{\frac{1}{2}}$ with $m = -\infty,\ldots,-1,0,1,\ldots,+\infty$, and where $R_m(r)$ satisfies:

$$\frac{d^2R_m(r)}{dr^2} + \left[\frac{2\mu}{\hbar^2}\{E - V(r)\} - \frac{(m^2-\frac{1}{4})}{r^2}\right]R_m(r) = 0, \qquad (B.3)$$

Equation (B.3) is equivalent to the three dimensional radial equation if the substitution $m \to \ell + \frac{1}{2}$ is made (see equation (3.4)). The boundary conditions satisfied by $R_m(r)$ are:

$$\left.\begin{aligned} R_m(0) &= 0, \\ R_m(r) &\sim \cos\left[kr - \tfrac{\pi}{2}(m+\tfrac{1}{2}) + \delta_m\right], \end{aligned}\right\} \qquad (B.4)$$

where δ_m is the (real) phase shift and the reference phase is that determined by the free particle solution (that is $V(r) = 0$) given below. Using the two dimensional partial wave expansion of a plane wave:[93]

$$e^{ikr\cos\phi} = \sum_{m=-\infty}^{\infty} e^{im\pi/2} e^{im\phi} J_m(kr),$$

$$\sim \left(\frac{2}{\pi kr}\right)^{1/2} \sum_m e^{im\pi/2} e^{im\phi} \cos\left[kr - \tfrac{\pi}{2}(m+\tfrac{1}{2})\right].$$

it is not difficult to deduce that the partial wave expansion of $\psi(r,\phi)$ satisfying the boundary conditions (B.2) and (B.4) is:

$$\psi(r,\phi) = \left(\frac{2}{\pi k r}\right)^{1/2} \sum_m e^{im\pi/2} e^{i\delta_m} R_m(r) e^{im\phi},$$

and that the scattering amplitude is:

$$f(\phi) = \frac{1}{\sqrt{2\pi i k}} \sum_m e^{im\phi} \left[e^{2i\delta_m} - 1\right]. \qquad \text{(B.5)}$$

The total cross section takes the simple form:

$$\sigma(k) = \frac{4}{k} \sum_m \sin^2 \delta_m .$$

B.3 SEMICLASSICAL PHASE SHIFT

The semiclassical formalism cannot be applied directly to equation (B.3) because of the rapid variation of V(r) near r = 0. This difficulty is overcome by using the Langer transformation to map $[0, \infty)$ onto $(-\infty, +\infty)$.[37] The substitutions:

$$r = e^{x}$$

$$R_m = e^{x/2} U_m$$

gives an equation for U_m:

$$\frac{d^2 U_m(x)}{dx^2} + \left[\frac{2\mu}{\hbar^2} \{ E - V(e^x) \} e^{2x} - m^2 \right] U_m(x) = 0, \qquad \text{(B.6)}$$

to which the semiclassical approximation can be applied. The semiclassical solution of equation (B.6) in terms of the original variables is:

$$R_m(r) = \left[\frac{2\mu}{\hbar^2} \{ E - V(r) \} - \frac{m^2}{r^2} \right]^{-1/4} \sin \left[\int_{r_m}^{r} \left[\frac{2\mu}{\hbar^2} \{ E - V(r) \} - \frac{m^2}{r^2} \right]^{1/2} dr + \frac{\pi}{4} \right], \qquad \text{(B.7)}$$

where r_m is the zero of the integrand. The reference phase is that given by equation (B.7) with V(r) = 0, so that the phase shift δ_m is:

$$\delta_m = \lim_{R\to\infty}\left\{ \int_{r_m}^{R}\left[\frac{2\mu}{\hbar^2}\{E-V(r)\} - \frac{m^2}{r^2}\right]^{1/2} dr - \int_{m/k}^{R}\left[k^2 - \frac{m^2}{r^2}\right]^{1/2} dr \right\}$$

$$= \lim_{R\to\infty}\left\{ \int_{r_m}^{R}\left[\frac{2\mu}{\hbar^2}\{E-V(r)\} - \frac{m^2}{r^2}\right]^{1/2} dr - kR \right\} + \frac{\pi m}{2} . \qquad (B.8)$$

This is analogous to the three dimensional phase shift if the substitution $\ell+\frac{1}{2}\to m$ is made.

B.4 QUANTUM - CLASSICAL CORRESPONDENCE

The correspondence between the quantum cross section and the classical cross section for two dimensional collisions is outlined below. By excluding $\phi = 0$, the second summation in equation (B.5) may be dropped leaving:

$$f(\phi) = \frac{1}{\sqrt{2\pi i k}} \sum_{m=0}^{\infty}{}' e^{2i\delta_m} \left[e^{im\phi} + e^{-im\phi} \right], \qquad (B.9)$$

where $\sum'$ denotes a factor of $\frac{1}{2}$ when m = 0. This result follows by noting that[93]:

$$\sum_{m=-J}^{J} e^{im\phi} = \frac{\sin\left[(J+\tfrac{1}{2})\phi\right]}{\sin\left(\frac{\phi}{2}\right)}, \quad \phi \neq 0,$$

and

$$\lim_{J\to\infty} \frac{\sin\left[(J+\tfrac{1}{2})\phi\right]}{\sin\left(\frac{\phi}{2}\right)} = 0, \quad \phi \neq 0.$$

Replacing the summation by an integration over m gives for the scattering amplitude:

$$f(\phi) = \frac{1}{\sqrt{2\pi i k}} \int_0^{\infty} dm \left[e^{iA_+(m)} + e^{iA_-(m)} \right], \qquad (B.10)$$

where

$$A_{\pm}(m) = 2\delta_m \pm m\phi .$$

Since the terms in the integrand are oscillating rapidly, it is appropriate to use the method of stationary phase. The stationary point of the first term yields $2\partial\delta_m/\partial m = -\phi$ and that of the second term yields $2\partial\delta_m/\partial m = \phi$. Thus in terms of the deflection function Φ there results the semiclassical equivalence relation:

$$2\frac{\partial\delta_m}{\partial m} = \Phi . \qquad \text{(B.11)}$$

From equation (B.8), equation (B.11) becomes:

$$\Phi = \pi - 2\int_{r_m}^{\infty} \frac{m\hbar}{r^2\{2\mu[E-V(r)]-m^2\hbar^2/r^2\}^{1/2}}\,dr . \qquad \text{(B.12)}$$

If the correspondence $m\hbar = J$ is made then equation (B.12) is just the classical expression for the deflection function.

Returning to the expression for the scattering amplitude, equation (B.10), and supposing that only the first term contains a point of stationary phase, standard theory gives:[38]

$$f(\phi) = e^{iA_+(m)} \left[k \left| \frac{\partial^2 A_+(m)}{\partial m^2} \right| \right]^{-1/2} . \qquad (B.13)$$

If $\partial^2 A_+(m)/\partial m^2 < 0$ then the right hand side of equation (B.13) is to be multiplied by $\exp(-i\pi/2)$. Making use of the equivalence $m = bk$ where b is the impact parameter gives for the differential cross section:

$$I(k,\phi) = 1 \Big/ \left| \frac{d\Phi}{db} \right|_{\Phi = \phi} ,$$

which is the classical result. Notice that there is no effect analogous to the glory in two dimensional scattering. The above derivation has assumed a monotonic variation of Φ with b. When this is not the case, the development of the three dimensional theory may be applied.

REFERENCES

1. J.O. Hirschfelder and W.J. Meath,1967, Adv. Chem. Phys.,12,3.
2. H. Pauly and J.P. Toennies,1965, Adv. Atm. Mol. Phys., 1,201.
3. R.B. Bernstein,1966, Adv. Chem. Phys.,10,75.
4. R.B. Bernstein and J.T. Muckerman,1967, Adv. Chem. Phys.,12,389.
5. A.S. Davydov,1965, Quantum Mechanics, (Pergamon), Chap. 3.
6. K.W. Ford,D.L. Hill, M. Wakano and J.A. Wheeler, 1959, Ann.Phys.,7,239.
7. I. Amdur and J.E. Jordan,1966,Adv.Chem.Phys., 10,29.
8. T.Y. Wu and T. Ohmura,1962,Quantum Theory of Scattering, (Prentice-Hall),Chap.1, Sect.A.
9. E.H. Taylor and S. Datz,1955,J.Chem.Phys.,23,1711.
10. D.R. Herschbach,1966,Adv.Chem.Phys.,10,319.
11. J.P. Toennies,1968, in Chemische Elementarprozesse, (Springer-Verlag),Ed. H. Hartmann, p.157.
12. J.P. Toennies,1968,Ber.Bunsen.Phys.Chem.,72,927.
13. K.R. Wilson and D.R. Herschbach,1968,J.Chem.Phys., 49,2676.
14. W.B. Miller,S.A. Safron and D.R. Herschbach,1967, Disc.Faraday Soc.,44,108.

15. M.Karplus,1968, in Structural Chemistry and Molecular Biology, (Freeman),Ed. A.Rich and N. Davidson.

16. M.Karplus,R.N. Porter and R.D. Sharma,1965,J.Chem. Phys.,43,3259.

17. M Karplus,1967,Disc. Faraday Soc.,44,76.

18. E.M. Mortensen,1968,J.Chem.Phys.,49,3526.

19. E.M. Mortensen,1968,J.Chem.Phys.,48,4029.

20. R.A. Marcus,1966,J.Chem.Phys.,45,2138.

21. R.A. Marcus,1966,J.Chem.Phys.,45,2630.

22. R.A. Marcus,1967,J.Chem.Phys.,46,959.

23. J.C.Light,1967,Disc.Faraday Soc.,44,14.

24. M.S. Child,1967,Mol.Phys.,12,401.

25. D.J. Diestler and V.McKoy,1968,J.Chem.Phys.,48,2951.

26. K.T. Tang,B,Kleinman and M.Karplus,1969,J.Chem. Phys.,50,1119.

27. M.S. Child,1966,Proc.Roy.Soc.,292A,272.

28. R.A. Marcus,1966,J.Chem.Phys.,45,4493.

29. R.A. Marcus,1966,J.Chem.Phys.,45,4500.

30. R.A. Marcus,1968,J.Chem.Phys.,49,2610.

31. J.O. Hirschfelder and E.P. Wigner,1939,J.Chem. Phys.,7,616.

32. M.A.Eliason and J.O. Hirschfelder,1959,J.Chem. Phys.,30,1426.

33. L.Hofacker,1963,Z.Naturforsch.,18A,607.

34. J.N.L. Connor,1968,Mol.Phys.,15,37.

35. J.N.L. Connor,1968,Mol.Phys.,15,621.

36. J.N.L. Connor,1969,Mol.Phys.,16,525.

37. R.E. Langer,1937,Phys.Rev.,51,669.

38. C.F. Carrier,M.Krook and C.E.Pearson,1966, Functions of a Complex Variable,(McGraw-Hill),Chap.6.

39. J.Heading,1962,An Introduction to Phase Integral Methods,(Methuen).

40. N.Fröman and P.O. Fröman,1965,JWKB Approximation, (North-Holland).

41. W.H. Miller,1968,J.Chem.Phys.,48,1651.

43. M.Abramovitz and I.A.Stegun,1965,Handbook of Mathematical Functions,(Dover),Chap.19.

44. R.P. Bell,1959,Trans.Faraday Soc.,55,1.

45. E.C. Kemble,1958,The Fundamental Principles of Quantum Mechanics,(Dover),p.109.

46. A.Erdelyi et al,1953,Higher Transcendental Functions, (McGraw-Hill),Vol.1,p.48.

47. L.D. Landau and E.M.Lifshitz,1965,Quantum Mechanics, 2nd.Edition,(Pergamon),pp.472-475.

48. J.O. Hirschfelder,C.F.Curtiss and R.B.Bird,1964, The Molecular Theory of Gases and Liquids,(Wiley), p.553.

49. E.F. Greene,A.L.Moursund and J.Ross,1966,Adv.Chem. Phys.,10,135.

42. J.C.P. Miller, 1955, Tables of Weber Parabolic Cylinder Functions, (H.M.S.O.).

50. C.F. Giese,1966,Adv.Chem.Phys.,10,247.

51. R.M. Eisberg and C.E. Porter,1961,Rev.Mod.Phys., 33,190.

52. K.W. Ford and J.A. Wheeler,1959,Ann.Phys.,7,287.

53. R.B. Bernstein,1966,Phys.Rev.Lett.,16,385.

54. E.E. Nikitin,1968,Chemische Elementarprozesse, (Springer-Verlag),Ed.H.Hartmann,p.43.

55. M.S. Child,1969,Mol.Phys.,16,313.

56. R.E.Roberts,1968,University of Wisconsin Theoretical Chemistry Institute Report,No.WIS-TCI-306.

57. R.E. Roberts,R.B. Bernstein and C.F. Curtiss, 1968,Chem.Phys.Lett.,2,366.

58. R.J. Munn,E.A. Mason and F.J. Smith,1964,J.Chem.Phys., 41,3978.

59. R.B. Bernstein,C.F. Curtiss,S.Iman-Rahjoe and H.T. Wood,1966,J.Chem.Phys.,44,4072.

60. A.E. Glassgold and S.A. Lebedeff,1964,Ann.Phys., 28,181.

61. R.R.Herm,1967,J.Chem.Phys.,47,4290.

62. G.V.Dubrovsky,1964,Optika.Specktrosk.,17,771, (English translation: Optics.Spectrosc.N.Y.,17,416).

63. P.M. Livingston,1966,J.Chem.Phys.,45,601.

64. R.A.Buckingham and A.Dalgarno,1952,Proc.Roy.Soc., 213A,506.

65. M.V. Berry,1966,Proc.Phys.Soc.,88,285.

66. E.Gal and J.W. Fox,1967,Proc.Phys.Soc.,86,55.

67. C.F.Curtiss and H.S. Powers,1964,J.Chem.Phys., 40,2145.

68. C.F. Curtiss,1965,J.Chem.Phys.,42,2267.

69. J.A. Barker and C.H.J. Johnson,1965,J.Chem.Phys. 42,2263.

70. J.Reuss and S.Stolte,1969,Physica,42,111.

71. W.C.Stwalley,A.Niehaus and D.R. Herschbach,1967, Abstracts of Papers of Vth ICPEAC,(Nauka),p.639.

72. S.Glasstone,K.J.Laidler and H.Eyring,1941, Theory of rate processes, (McGraw-Hill),Chap.3.

73. E.B. Wilson,J.C.Decius and P.C.Cross,1955, Molecular Vibrations,(McGraw-Hill) p.281.

74. L.D.Landau and E.M.Lifshitz,1965,Quantum Mechanics, 2nd. Edition,(Pergamon)pp.541-544.

75. K.W. Ford and J.A. Wheeler,1959,Ann.Phys.,7,259.

76. G.Kwei and D.R.Herschbach,1963,University of California Lawrence Radiation Laboratory Report, No. UCRL 11178.

77. G.Kwei and D.R. Herschbach,1964,Atomic Collision Processes,(North-Holland),Ed.M.R.C.McDowell,p.972.

78. E.Jahnke and F.Emde,1945,Tables of Functions,(Dover) Chap.V.

79. M.Kennedy and F.J. Smith,1967,Mol.Phys.,13,443.

80. M.Abramovitz and I.A. Stegun,1965,Handbook of Mathematical Functions,(Dover),Item 23.3.6.

81. R.D. Present,1958,Kinetic Theory of Gases, (McGraw-Hill),p.151.

82. R.J.Munn and F.J. Smith,1966,Mol.Phys.,10,163.

83. B.C.Eu and J.Ross,1966,J.Chem.Phys.,44,2467.

84. M.Abramovitz and I.A.Stegun,1965,Handbook of Mathematical Functions,(Dover),Section 20.3.

85. C.C.Lin and J.D.Swalen,1959,Rev.Mod.Phys.,31,841.

86. J.E.Wollrab,1967,Rotational Spectra and Rotational Structure, (Academic Press),Chap.6.

87. M.S. Child,1967,Disc. Faraday Soc.44,68.

88. I.S.Gradshteyn and I.M.Ryzhik,1965,Tables of Integrals, Series and Products,4th Edition,(Academic Press), translated by A.Jeffrey,Item 3.713.

89. M.Abramovitz and I.A. Stegun,1965,Handbook of Mathematical Functions,(Dover),Item 6.1.36.

90. H.O'Hara and F.J.Smith,1968,Computer J.,11,213.

91. J.Hawgood,1965,Numerical Methods in ALGOL,(McGraw-Hill), Chap.6.

92. F.J. Smith,1964,Physica,30,497.

93. P.M. Morse and H.Feshbach,1953,Methods of Theoretical Physics,(McGraw-Hill),Section 11.2.